African Journal of Biotechnology

Volume 15 Number 40, 5 October 2016
ISSN 1684-5315

ABOUT AJB

The African Journal of Biotechnology (AJB) (ISSN 1684-5315) is published weekly (one volume per year) by Academic Journals.

African Journal of Biotechnology (AJB), a new broad-based journal, is an open access journal that was founded on two key tenets: To publish the most exciting research in all areas of applied biochemistry, industrial microbiology, molecular biology, genomics and proteomics, food and agricultural technologies, and metabolic engineering. Secondly, to provide the most rapid turn-around time possible for reviewing and publishing, and to disseminate the articles freely for teaching and reference purposes. All articles published in AJB are peer-reviewed.

Contact Us

Editorial Office: ajb@academicjournals.org

Help Desk: helpdesk@academicjournals.org

Website: http://www.academicjournals.org/journal/AJB

Submit manuscript online http://ms.academicjournals.me/

African Journal of Biotechnology

Table of Content: Volume 15 Number 40 5 October. 2016

ARTICLES

In vitro **regeneration of disease free enset [*Ensete ventricosum* (Welw) Cheesman] planting materials from bacterial wilt diseased plants using shoot tip culture** 2192
Genene Gezahegn and Firew Mekbib

Unraveling possible association between quantitative trait loci (QTL) for partial resistance and nonhost resistance in food barley (*Hordeum vulgaris* L.) 2202
Dido A. A., Yeo F. K. S. and Niks R. E.

Screening of spontaneous castor bean accesses for genetic improvement programs 2209
Rener Luciano de Souza Ferraz, Jane Lima Batista, Marcelo de Andrade Barbosa, Ivomberg Dourado Magalhães, Alberto Soares de Melo and Antonio Sergio Ferraudo

Assessment of the genetic diversity of Kenyan coconut germplasm using simple sequence repeat (SSR) markers 2215
Maurice E. Oyoo, Najya Muhammed, Kimani N. Cyrus and Simon M. Githiri

Evaluation of various pesticides-degrading pure bacterial cultures isolated from pesticide-contaminated soils in Ecuador 2224
Pérez Mónica, Rueda O. Darwin, Bangeppagari Manjunatha, Johana J. Zúñiga, Ríos Diego, Rueda B. Bryan, Sikandar I. Mulla and Naga R. Maddela

Use of response surface methodology to optimize the drying conditions of a bioactive ingredient derived from the African opaque sorghum beer 2234
I. B. Chabi, A. P. P. Kayodé, B. P. Agbobatinkpo, A. Adénilé, O. A. Mamadou, G. Vieira-Dalodé, L. Baba-Moussa and J. T. C. Codjia

Enzymatic regulation of organic acid metabolism in an alkali-tolerant halophyte *Chloris virgata* during response to salt and alkali stresses 2243
Huan Wang, Bing Bai, Ziyu Bai, Lijun Shi, Jinlin Ye, Siwen Fan, Huahua Xu and Decheng Shi

Comparison of four nonlinear growth models for effective exploration of growth characteristics of turbot *Scophthalmus maximus* fish strain 2251
Xin'an Wang and Aijun Ma

Genetic determinants of antifungal resistance in *Candida* species 2259
Danielly Beraldo dos Santos Silva, Alexéia Barufatti Grisolia and Kelly Mari Pires de Oliveira

African Journal of Biotechnology

Table of Content: Volume 15 Number 40 5 October. 2016

ARTICLES

Phylogenetic relationships of the genus *Quercus* L. (Fageceae) from three different sections 2265
Yılmaz Aykut

Antioxidant assessment on promethazinr HCl decomposition using RP-HPLC assay method 2272
Rasha Saad, Heyam Saad Ali, Babiker M. A. Elhaj and Mai Al Ajaji

academicJournals

Vol. 15(40), pp. 2192-2201, 5 October, 2016
DOI: 10.5897/AJB2016.15213
Article Number: 689DE0460810
ISSN 1684-5315

http://www.academicjournals.org/AJB

African Journal of Biotechnology

Full Length Research Paper

In vitro regeneration of disease free enset [*Ensete ventricosum* (Welw) Cheesman] planting materials from bacterial wilt diseased plants using shoot tip culture

Genene Gezahegn[1]* and Firew Mekbib[2]

[1]Biotechnology University of Gonder, Ethiopia.
[2]Plant breeder and Molecular Genetist, Haramaya University, Ethiopia.

Received 6 January, 2016; Accepted 1 June, 2016

Enset is an important food crop produced in Ethiopia with great role in food security. The demand of the crop is increasing throughout the country. However, the production as a whole is decreasing due to devastation by enset bacterial wilt. The studies were conducted to develop the procedure for obtaining multiple disease free plantlets from infected enset plants. Shoot tip explants from infected suckers of three clones Arkiya, Digomerza and Mazia were cultured on MS media supplemented with different combinations of benzylaminopurine (BAP) and naphthaleneacetic acid (NAA) each with concentration of 0, 1.5, 3, 4.5 and 6 mg/L with 0, 0.5, 1, 1.5 and 2 mg/L, respectively. The effect of growth regulators on shoot growth parameters was examined. The minimum days (11.66) for multiple shoot induction were recorded for Mazia on media with 4.5 mg/L BAP and 1.5 m/L NAA. The maximum number of shoots (23.0) was also obtained for Mazia on the same hormone combination as for days of induction. Whereas, the maximum shoot length (8.1 cm) was recorded for Digomerza on media with 3 and 1 mg/L NAA. Similarly, for root induction and growth MS media with different concentrations of indulebutyric acid (IBA; 0, 0.5, 1, 1.5 and 2 mg/L) were evaluated. The minimum days (10.5) to root induction was observed for Mazia on media with 1.5 mg/L IBA and the maximum root number (3.8) was recorded at 2 mg/L IBA. In the efficiency of shoot tip culture for Xanthomonas pathogen elimination, sample suspension was prepared from shoots regenerated from diseased suckers and transferred on semi-selective yeast peptone sucrose agar (YPSA) medium. The result of colony observation indicated that many microbes are living in enset saprophytically as mixed colony growth was observed within 24 h after sample culturing. Pathogenesity test on clean suckers of susceptible clone showed that the colonies grown were due to endophytic microbes since none of the colonies were capable to develop disease symptoms as sample of the pathogen strain.

Key words: *Ensete ventricosum*, benzylaminopurine (BAP), indulebutyric acid (IBA), naphthaleneacetic acid (NAA), shoot tip, *Xanthomonas*, yeast peptone sucrose agar (YPSA).

INTRODUCTION

Enset (*Ensete ventricosum* (Welw.) Cheesman) is a diploid (2n=18) herbaceous perennial edible species of the separate genus of the banana family, thus named ‘false banana’ (Cheesman ,1947). Enset is the vernacular name used in the Amharic language in Ethiopia for Ensete ventiricosm whose fruit is not edible and one of the indigenous root crops widely cultivated for its food and fiber values (Taye, 1996). Variation within the

species to altitude, soil and climate has allowed widespread cultivation in the mid to highlands of Southern and South-Western part of the country. It is estimated that a quarter or more than 20 million of Ethiopia's population depends on enset as staple and co-staple food source, for fiber, animal forage, construction materials and medicines (Zerihun et al., 2014) and and the area of enset production in Ethiopia is estimated to be over 321,362.43 hectares (CSA, 2013). The average yield of kocho (non-dehydrated fermented product from the mixture of decorticated pseudo stem, pulverized trunk and corm) of superior food and fiber yielding cultivars such as Digomerza gave yield over 43 ton per hectare bases per year (Atnafua and Endale, 2008). Fresh enset parts are used as fodder for domestic animals during dry season and some enset clones are reported to have medicinal value to human beings and domestic animals (Temesgen et al., 2014). Enset is also well known to conserve soil and enrich plant nutrients through its dropped foliage, dried leaf sheath and petioles of enset are used for wrapping materials and other utensils (Endale and Mulugeta, 1994).

Due to limited research attention given to enset crop, its production system is still traditional and tiresome. Different management practices starting from propagation to harvesting and processing demand high labor. Various diseases and insect pests of enset also have been reported. Some of these are: leaf damaging fungal diseases, corm rot, sheath rot and dead heartleaf rot of enset with unknown causal agents and root knot, root lesion and black leaf streak nematode diseases. There are also viral diseases of enset known as mosaic and chlorotic leaf streak diseases. Insects damaging enset leaves such as Jassid fly, spider mites, mealy bugs and wild animals such as porcupine, mol rat and wild pigs have been reported (Brandt et al., 1997). However, based on the distribution and the damage incurred on enset production, enset bacterial wilt disease caused by *Xanthomonas campestris* pv. *musacearum* is known to be the most threatening and important problem to enset production system.

The disease was first reported and described by Dagnachew and Bradbury (1968) that attributed it to *Xanthomonas musacearum* (Eshetu, 1981). It was widely distributed in many enset growing regions of the country and affects the crop at all developmental stages and the results obtained from recent bacterial wilt disease assessment made in some enset fields in Southern Nations, Nationalities, and Peoples Region (SNNPR) showed losses of up to 100% under severe damage (Awassa Agricultural Research center, 2008). Natural epidemics of the disease were also observed in banana fields at different enset growing areas. Even though the disease is widely distributed and important, there are limited research efforts directed to manage the disease using cultural practices and enset clonal screening against bacterial wilt which were hindered due to knowledge gap from farmers and tedious destructive work to farmers to remove all infected plants from field in which sometimes the whole farm is infected. There is no clone still that can resist the pathogen after artificial inoculation by different researchers with conflicting reports for the same clones interaction to the pathogen strains which have variations on pathogenicity as well as biochemical reactions (Kidist, 2003; Gizachew, 2008).

Attempts by recombinant DNA technology to develop genetically improved enset clones with resistant gene are absent due to lack of detailed genetic information (Morpurgo et al., 1993). Different researchers have tried to develop protocols for micro propagation of clean planting materials to distribute for end users, which indicated that there is a possibility to produce large amount of *in vitro* plantlets with further work needed in the basic physiology of the crop to verify efficient micro propagation protocol (Mulugeta and Tesfaye, 2010). Recently, shoot tip/meristem culture has the potential to eliminate viral, fungal and bacterial diseases from plants. In the closely related crop, banana, tissue culture effectively eliminates weevils and nematodes, bacterial diseases such as the Banana *Xanthomonas* wilt (BXW) and fungal diseases like *Fusarium* wilt and Sigatoka (Kabir et al., 2008). Tissue culture has been also shown to bring down the cost of controlling foliar diseases by half. However, there is no information either for the possibility of generating disease free suckers from infected enset plant explants.

Therefore, the objective of this study was to optimize *in vitro* protocol for enset bacterial wilt free planting materials production and finally test for pathogen absence using different diagnostic techniques.

MATERIALS AND METHODS

Experimental materials

Three month old suckers of three clones of enset were collected from Areka station and maintained under greenhouse conditions until they resume growth. After one month these suckers were inoculated by Hagereselam strain of *Xanthomonas* and later used as explants source for culture initiation.

Explants surface sterilization and culture initiation

Explants with 2 cm were collected from sucker corms (Figure 1) and

*Corresponding author. E-mail: genuaetu2005@gmail.com or genenegezhegn@yahoo.com. Tel: +251913818867 or +251465520503. Fax: +251465520502.

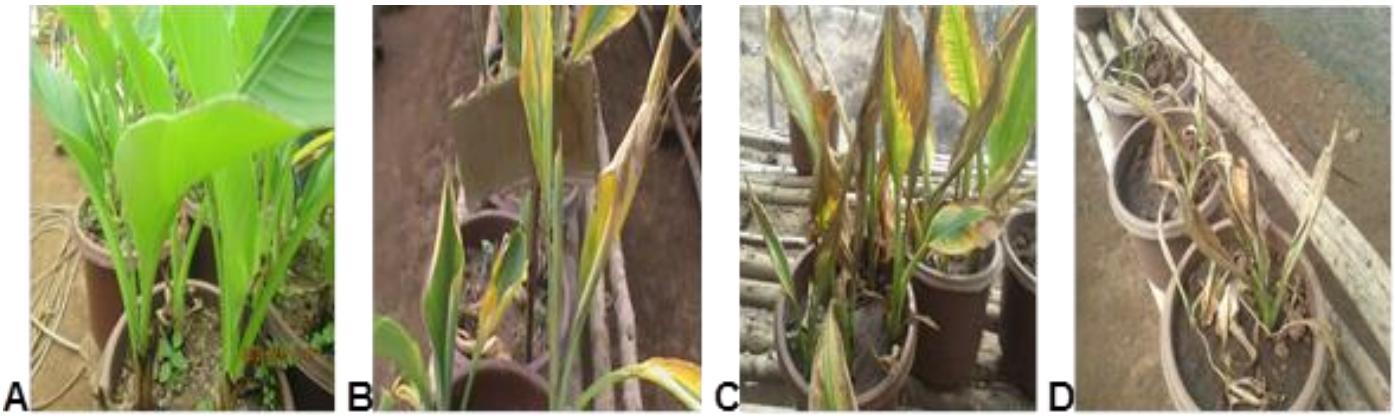

Figure 1. Mother plants used as explants source: A. Clean suckers of Enset before artificial inoculation, B. Diseased Mazia suckers, C. Diseased Digomerza suckers, D. Diseased Arkiya suckers.

thoroughly washed with detergent and sterile distilled water (SDW). Then, the explants were treated with 70% of ethanol for 5 min followed by double sterilization with 40% of gion berekina (2% NaOCl) for 10 and 20 min accompanied by 4x rinse with SDW between each treatment. Finally, the size of the explants was trimmed to appropriate size (1 cm) and inoculated to initiation medium as per treatments.

Shoot induction and multiplication

Surface sterilized explants were cultured in jars containing 40 ml of shoot initiation MS medium (Murashige and Skoog, 1962) with 3% of sucrose, 0.6% of agar and 0.3% of activated charcoal (AC). MS media supplemented with different combinations of benzylaminopurine (BAP) and naphthaleneacetic acid (NAA) as per treatmet. All treatments were maintained in dark condition for fifteen days at initiation stage to enhance explants establishment by reducing blackening of explants due to phenolic exudation and preventing formation of other growth inhibitors in the media as recommended by Pierik and Steegmans (1975). Sub-culturing of initiated cultures for multiplication was done after one month in multiplication medium supplemented with different combinations of growth regulators as in shoot initiation. Multiplication stages were maintained in controlled growth room set at average of 27 ± 2°C temperature, 60 to 70% of relative humidity (RH) and 40 µmol/m^2s of light intensity under 14/10 h light and dark period. While sub-culturing the middle growing shoot tip was carefully excised together with the lower corm base part and transferred to multiplication medium supplemented with different concentration and combination of growth regulators. After one month of incubation in growth room, shoots with length of 1.5 cm and more were carefully separated from the explants and transferred to regeneration media. However, explants with smaller shoot buds that cannot grow independently but potentially grow to shoots were transferred to the same multiplication media to get more shoots in the second sub-culture.

Root induction

Elongated individual shoots with leaves were carefully separated from explants and cultured in 250 ml jars containing 40 ml of rooting MS media supplemented with 0, 0.5, 1, 1.5 and 2 mg/L of indole butyric acid (IBA). Similar to multiplication stages, cultures were maintained in controlled growth room.

Diagnostic techniques to test pathogen elimination

Bacterial sample preparation

Sample suspension was prepared from well regenerated *in vitro* plantlets leaf and leaf sheath section at which *Xanthomonas* was believed highly available. The sample plantlets were taken from growth medium by forceps and the lower corm part with roots was cut down and the upper part was placed in sterile distilled water. The sample shoots were then crashed carefully in order to make bacterial cell suspension if available within plant tissue in 1 ml of distilled water. The suspension sample was then serially diluted five times by 1:9 ratio of sample and distilled water, respectively.

Semi-selective medium preparation

Semi-selective culture media yeast peptone sucrose agar (YPSA) for the pathogen was prepared from 5 g/L of yeast extract, 10 g of peptone, 10 g/L of sucrose and 15 g/L of bacteriological type agar for 1 L media as in the case it was prepared for initial inoculums preparation by dissolving the mixture of media components together on hot plate with magnetic stirrer. The media solution was autoclaved in pressure cooker for 25 min under 1.2 kgms^2/m^2 and 121°C. Finally, 20 ml of the hot media was dispensed to sterile Petri dishes and stored in refrigerator at 15°C for two days.

Plant extract sample inoculation to semi-selective media and colony observation

All petri dishes were labeled according to sample code and replicated twice. The suspension sample was then stricked on the media by loop. The loop was sterilized in the intervals of samples stricking. For negative and positive control two petri dishes for SDW and two petri dishes for bacterial sample, respectively, were used. Then petri dishes with samples were sealed by plaster and taken to incubator set at temperature of 27°C. After incubating overnight, cultures were checked for any colony growth on the media including the controls.

Pathogenesity test

Pure colonies were taken by sterile loop from mixed colonies grown on semi-selective media and sample suspension was prepared by

serial dilution technique to 10^8 cfu/ml. The suspension was then inoculated to healthy growing suckers of Arkiya which has shown high susceptibility to check that the grown colonies are of *Xanthomonas* pathogen or not. Artificially, inoculated plants were observed for disease symptom development in seven days interval up to 35 days.

Acclimatization

After four weeks of transferring shoots to rooting medium, well regenerated plantlets with shoots, roots and leaves were gently removed from the culture jars and the roots were washed in tap water to remove traces of agar. The plantlets then were transplanted into dark plastic pots filled with sterile soil mix of 1:1 red ash and sandy loam soil under green house. The pots in which plants were planted for acclimatization were finally covered with white polyethylene bags and red cheesecloth to maintain high humidity for fifteen days.

Data recording

Data for explants response to treatments such as number of explants contaminated on initiation mean number of days to shoot and root induction, mean number of shoots, number of leaves and roots per plant, shoot and root length and fresh and dry weight of shoot and root were recorded.

Data analysis

The experiment was designed in CRD and laid in factorial arrangement with three replications for all treatments. Data recorded for all responses were subjected to analysis of variance (ANOVA) and significant differences among treatments were determined by Fisher's Least Significance Difference test (LSD) using SAS software (JMP version 9.2) for the differentiation of the effect of treatment, genotype and treatment-genotype interaction.

RESULTS AND DISCUSSION

Surface sterilization of explants

Initial surface sterilization experiment was effective when 2 cm shoot tip explants were treated with 70% ethanol for 5 min followed by double sterilization with 40% of gion berekina (2% chlorox) first for 10 and then 20 min. This treatment resulted in 95% contamination free explants and very less (2%) dead explants for all the clones until 10 days of inoculation in MS media. Later when explants started to develop single shoot let bacterial colonies started to develop under the explants in both pathogen inoculated and healthy mother plant sourced explants which led to loss of many cultures. Combination of two antibiotics, namely ampicilin and gentamicine with the concentration of 30 mg and 10 mg, respectively, per 100 ml of distilled water was used for decontamination by immersing surface sterilized explants for 2 h before transferring to initiation media. Similarly, Birmeta et al. (2004) reported that microbial contamination, in particular by apparently endophytic microbes that are resistant to antimicrobial agents was encountered during micro propagation work of enset.

Effect of BAP and NAA concentration on shoot induction and growth of enset clone explants

Days to single shoot initiation

Remarkable variation was observed for days required for shoot initiation among the three clones and 5 levels of hormones (BAP with NAA) combinations. The minimum days required for shoot initiation (5.25 days) was noted in Arkiya at 6 mg/L BAP and 2 mg/L NAA in combination, Digomerza (5.50 days) on the same hormone combination as in Arkiya and for Mazia (5.50 days) on media with 4.5 and 1.5 mg/L of BAP and NAA (Table 1). Whereas, the maximum days required for single shoot initiation for Mazia (9.00) and (8.67) were recorded on hormone free and media supplemented with 1.5 mg/L BAP and 0.5 NAA, respectively, followed by Digomerza (8.33) and Arkiya (8.25) on hormone free MS media (Table 1). Mulugeta et al. (2005) reported that, single shoot initiation observed after two weeks when enset shoot tip explants cultured on MS media gelled with 11 g/L of agar and supplemented with 2.5 mg/L BAP alone. The most probable reasons for this early initiation in the present experiment were the low amount of solidifying agent used that can reduce nutrient uptake by explants if in large amount since the media become very compact and the combined the effect of BAP and NAA.

Days to multiple shoot induction

Considerable variation was observed in days to multiple shoot induction among clones cultured on different concentration of growth hormones. The minimum days to multiple shoot induction was recorded for Mazia clone (11.66 days) cultured on media with 4.5 mg/L BAP and 1.5 mg/L NAA followed by 12.67 days for the same clone explants cultured on 6 and 2 mg/L supplemented MS media. On the other hand, the maximum days to multiple shoot induction was noted more for Arkiya (25.33) and Digomerza (23.33) followed by 23 days for Mazia explants cultured on hormone free MS media (Table 1). So far there is no report on enset for mean days to multiple shoot induction *in vitro* after sub-culturing initiated explants in multiplication media. Hirimburegama and Gamage (1996) conducted experiment to develop micro propagation protocol for ten cultivars of close related species banana. They have reported that different cultivars of banana shoot tips cultured for shoot proliferation has induced multiple shoots at different times after inoculation to MS medium supplemented with BAP and IAA at different level which agreed to the present finding.

Number of micro-shoots per explants

Mazia was the best performing clone in terms of shoot numbers (23.00) proliferated per explants on media with

Table 1. Effect of plant growth regulators (BAP and NA) combination on different clones for shoot induction and growth parameters of the three clones.

Hormone combination		Clone	Days to single shoot initiation	Days to multiple shoot induction	Number of shoots	Shoot length (cm)	Shoot fresh weight(g)	Shoot dry weight (g)
BAP (mg/L)	NAA (mg/L)							
0	0	Mazia	9.00^{a}	23.00^{b}	1.33^{g}	0.65^{f}	0.08^{g}	0.02^{g}
0	0	Digomerza	8.33^{b}	23.33^{ab}	1.67^{fg}	0.69^{f}	0.07^{g}	0.023^{g}
0	0	Arkiya	8.25^{b}	25.33^{a}	2.33^{fg}	0.61^{f}	0.08^{g}	0.020^{g}
1.5	0.5	Mazia	8.67^{ab}	18.66^{c}	2.67^{fg}	4.53^{c}	0.17^{e}	0.07^{f}
1.5	0.5	Digomerza	6.67^{c}	17.00^{cd}	3.33^{f}	2.83^{d}	0.16^{e}	0.09^{ef}
1.5	0.5	Arkiya	6.67^{c}	14.00^{efg}	1.66^{fg}	3.17^{d}	0.17^{e}	0.11^{de}
3	1	Mazia	6.00^{ed}	15.67^{de}	19.00^{b}	7.33^{a}	0.45^{cd}	0.098^{ef}
3	1	Digomerza	5.50^{ef}	15.00^{def}	15.00^{d}	8.06^{a}	0.46^{cd}	0.15^{cd}
3	1	Arkiya	5.75^{ed}	15.67^{de}	5.33^{e}	4.66^{bc}	0.48^{bc}	0.16^{c}
4.5	1.5	Mazia	5.50^{ef}	11.66^{h}	23.00^{a}	7.46^{a}	0.55^{b}	0.20^{b}
4.5	1.5	Digomerza	6.25^{dc}	14.33^{efg}	16.33^{c}	7.36^{a}	0.81^{a}	0.22^{b}
4.5	1.5	Arkiya	6.17^{dc}	13.33^{fgh}	7.00^{e}	5.40^{b}	0.41^{d}	0.28^{a}
6	2	Mazia	6.08^{ed}	12.67^{gh}	17.00^{c}	2.53^{d}	0.14^{ef}	0.11^{de}
6	2	Digomerza	5.50^{ef}	15.33^{def}	20.33^{b}	2.73^{d}	0.16^{e}	0.13^{cd}
6	2	Arkiya	5.25^{f}	14.00^{efg}	15.67^{c}	1.50^{e}	0.18^{e}	0.103^{ef}
LSD (5%)			0.59	2.03	1.89	0.75	0.07	0.033
CV (%)			5.41	7.35	11.23	11.44	13.76	16.86

Means with the same letter in the same column are non-significant at 5% significance level. LSD: Least Significant Difference; CV: coefficient of variation.

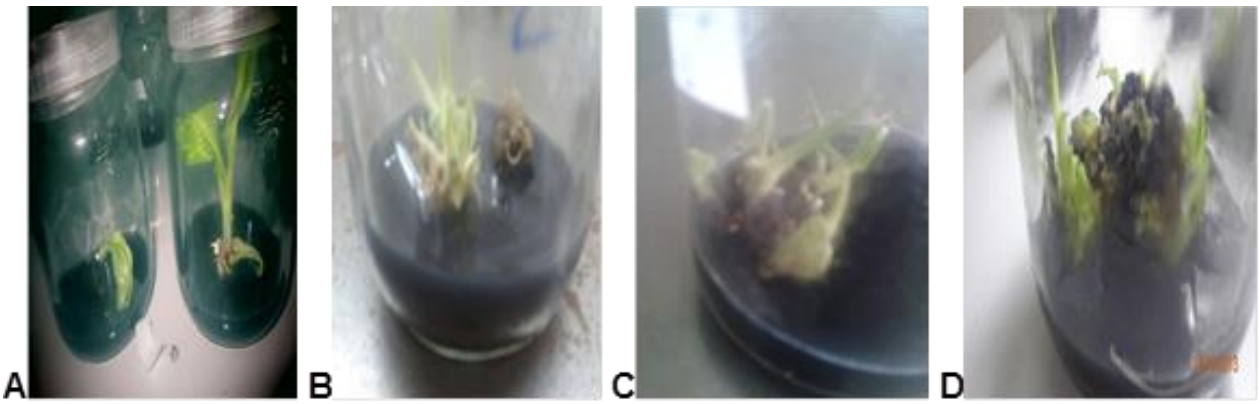

Figure 2. Shoot induction and growth at 4.5 mg/L BAP and 1.5 mg/L NAA. A. Initiated Mazia explants, B. Multiple shoots from Arkiya explants, C. Multiple shoots from Digomerza explants and D. Multiple shoots from Mazia explants.

4.5 mg/L BAP and 1.5 mg/L NAA followed by Digomerza (20.33) on media containing 6 mg/L BAP and 2 mg/L NAA. On the other hand, Arkiya has responded poorly for number of micro-shoots to all combinations of BAP and NAA as compared to the other two clones Whereas, explants cultured on hormone free media has produced the smallest number of shoots for the three clone explants (Table 1 and Figure 2). Earlier, a procedure for micro propagation of enset has been reported by Negash et al. (2000), but only 2 to 3 shoots were produced from a single explant. Similarily, Mulugeta et al. (2005) obtained 3.7 shoots and 3.5 shoot buds per single shoot after splitting the explants in two and culturing them separately. In spite of the limited response of the crop *in vitro,* Birmeta and Welander (2004) reported about 75 shoot buds that can potentially grow to shoots per explants in one sub-culture through meristem wounding of initiated explants. However, the regeneration capability of the protocol she had developed was reported later has draw back (Mulugeta and Tesfaye, 2010). The result of

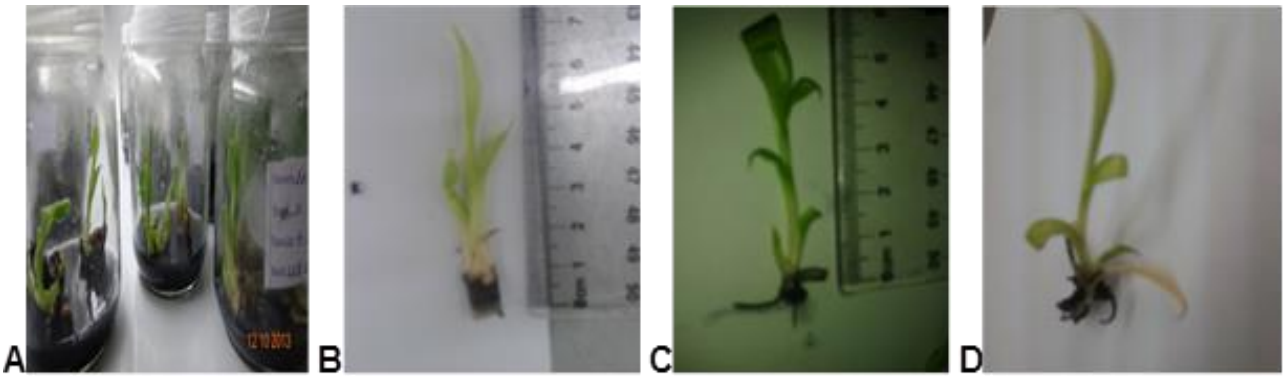

Figure 3. Shoot length and leaf number per shoots at 4.5 mg/L BAP and 1.5 mg/L NAA in MS media. A. Shoots of Mazia on elongation, B. Shoots of Digomerza, C. Shoots from Mazia explants, D. Shoots from Arkiya.

the present experiment showed that the maximum mean number of shoots obtained was 23 for Mazia clone on media with 4.5 mg/L BAP and 1.5 mg/L NAA in one sub-culture that can be transferred to regeneration media directly and more than 30 buds that can potentially grow to shoots in second sub-culturing to the same multiplication medium.

Shoot length per plantlet

Remarkable variation was observed for length of shoots among clones and in different hormone combination. The maximum shoot length was recorded for Digomerza (8.06 cm) on media with hormone combination of 3 mg/L BAP and 1 mg/L NAA followed by 7.46 and 7.36 cm for Mazia and Digomerza, respectively, on media supplemented with 4.5 mg/L BAP and 1.5 mg/L NAA (Table 1 and Figure 3A to D). Whereas, the lowest shoot length (1.5 to 2.73 cm) was recorded for all the three clone shoots developed on media with 6 mg/L BAP and 2 mg/L NAA followed by shoots from hormone free MS media (Table 1 and Figure 3). In the current study, the appropriate concentration of BAP and NAA that resulted in maximum shoot length is 3 and 1 mg/L, respectively, for all the three clones. Because further increase up to 4.5 mg/LBAP and 1.5 mg/L of NAA did have any significant effect and has reduced shoot length for all the three clone explants, indicating the upper limit in concentration (Table 1).

Leaf number per shoots

Among the three clones tested the highest mean number of leaves (2.80) per plantlets was recorded for Mazia clone followed by 2.66 for Digomerza clone. Whereas, the lowest number of leaves (2.06) were recorded for Arkiya (Table 2). The maximum leaf number (4.11) was recorded for explants cultured on MS media supplemented with 4.5 and 1.5 mg/L BAP and NAA hormone combination followed by 3.77 leaves per shoot on 3 and 1 mg/L NAA supplemented media (Table 2). Whereas, the lowest mean leaf number was recorded for explants cultured on hormone free MS media (1.00) that looks like leaf primordial rather than normal leaf with stunted growth (Table 2 and Figure 3). In comparative study for effect of explants source on plant regeneration, Mulugeta et al. (2005) have reported that three to four leaf per shoot for *in vitro* source explants and two to three leaves for shoots regenerated from greenhouse source explants. In the present study, the experimental material was from green house grown suckers that were artificially inoculated by bacterial wilt pathogen, but the result was in agreement with that of number of leaves recorded for shoots grown from *in vitro* source explants.

Table 2. Effects of hormones and clones on number of leaves per shoot.

Means of hormone treatments combination main effect		
BAP (mg/L)	**NAA (mg/L)**	**Leaf number**
0	0	1.00[c]
1.5	0.5	1.89b
3	1	3.77[a]
4.5	1.5	4.11[a]
6	2	1.77[b]
LSD (5%)		0.48

Clones main effect	
Clones	**Leaf number**
Mazia	2.80[a]
Digomerza	2.66[a]
Arkiya	2.06[b]
LSD (5%)	0.36
CV (%)	13.03

Means with the same letter in the same column are non-significant at 5% significance level. CV: Coefficient of variation; LSD: least significant difference.

Table 3. Effect of IBA on root induction and growth related parameters of Mazia, Digomerza and Arkiya clone shoots proliferated.

IBA (mg/L)	Clone	Days to root induction	Mean length of roots	Root fresh weight/plant (g)	Root dry weight/plant (g)
0	Mazia	15.33^{ab}	2.50^{i}	0.019^{h}	0.007^{j}
0	Digomerza	16.50^{a}	4.33^{de}	0.018^{h}	0.006^{j}
0	Arkiya	15.33^{ab}	3.26^{h}	0.018^{h}	0.004^{j}
0.5	Mazia	14.66^{bc}	5.03^{b}	0.034^{g}	0.011^{i}
0.5	Digomerza	14.00^{bced}	5.96^{a}	0.035^{g}	0.014^{h}
0.5	Arkiya	12.83^{def}	4.32^{de}	0.037^{g}	0.015^{h}
1	Mazia	13.50^{cde}	4.60^{cd}	0.044f	0.020^{g}
1	Digomerza	14.17^{bcd}	4.96^{b}	0.043^{f}	0.023^{f}
1	Arkiya	12.66^{ef}	4.46^{de}	0.050^{e}	0.03^{e}
1.5	Mazia	10.50^{g}	4.16^{e}	0.053^{de}	0.033^{cd}
1.5	Digomerza	11.83^{fg}	4.90^{bc}	0.055^{cd}	0.036^{b}
1.5	Arkiya	13.33^{cde}	3.63^{fg}	0.061^{b}	0.032^{d}
2	Mazia	14.00^{be}	3.76^{f}	0.074^{a}	0.038^{a}
2	Digomerza	12.83^{def}	4.80^{bc}	0.064^{b}	0.035^{b}
2	Arkiya	13.66^{cde}	3.43^{gh}	0.057^{c}	0.034^{bc}
LSD (5%)		1.37	0.17	0.0039	0.0019
CV (%)		5.99	2.40	5.26	4.89

Means with same letter in a column are non-significant at 5% significance level. LSD: Least significant difference; CV: coefficient of variation.

Effect of IBA concentration on root induction and growth in explants of the three enset clones

Number of days to root induction

The minimum number of days to root induction was recorded for Mazia (10.50 days) and Digomerza (11.83 days) for shoots cultured on media supplemented with 1.5 mg/L of IBA followed by Arkiya (12.66 days) on media with 1 mg/L IBA and Digomerza (12.83 days) on media containing 2 mg/L of IBA. Whereas, the maximum mean days to root induction was recorded on control hormone free media for all clone roots (Table 3). Negash et al. (2000) reported that root formation occurred in less than two weeks after transfer to root induction medium supplemented with 5 µM IBA, 1 µM IAA and 1 µM BAP in combination for all three enset clones on which they have conducted their experiment which is in agreement with the present finding.

Number of roots induced per shoots

The maximum root number (3.77) was recorded on MS media supplemented with 2 mg/L of IBA followed by 3.11 on media with 1.5 mg/L of IBA (Table 2). Whereas, the lowest mean number (1.44) of roots per shoot was recorded for roots induced on hormone free MS media. Experiment on clonal propagation of wild type *Enset superbum* (Roxb.) Cheesman conducted by Mathew and Philipe (1996) recorded 6 to 7 adventitious roots per shoots transferred to half strength MS media supplemented with 3 mg/L IBA and 0.5 mg/L BAP after one month of incubation in growth room. The result of the present experiment revealed smaller number of roots per shoot which might be due species difference and high concentration of IBA they have used.

Table 4. Main effect of hormone concentration on number of roots per shoot.

Mean of hormone treatment main effect	
IBA	**Number of roots/shoot**
0	1.44^{d}
0.5	2.55^{c}
1	3.55^{ab}
1.5	3.11^{b}
2	3.77^{a}
LSD (5%)	0.51
CV (%)	15.51

LSD: Least significant difference.

Length of roots induced per shoots

The maximum mean root length was obtained from shoots cultured on media with the lowest concentration of IBA (0.5 mg/L) for Digomerza (5.96 cm) followed by Mazia (5.03 cm) cultured on the same IBA concentration and 4.96, 4.90 and 4.80 cm for Digomerza shoots transferred to media with 1, 1.5 and 2 mg/L of IBA, respectively, with no significance difference (Table 4 and Figure 4A to D). On the contrary, the lowest root length

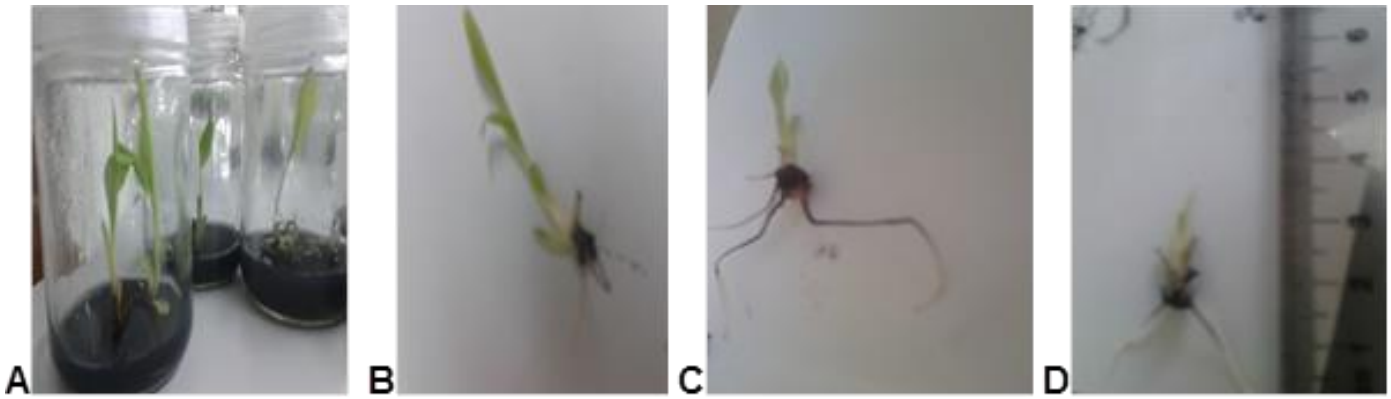

Figure 1. Plantlets in rooting MS media with 1mg/l IBA. A. Regenerated plantlets of Mazia. B. Mazia shoots with roots, C. Roots of Digomerza clone, D. Roots of Arkiya clone.

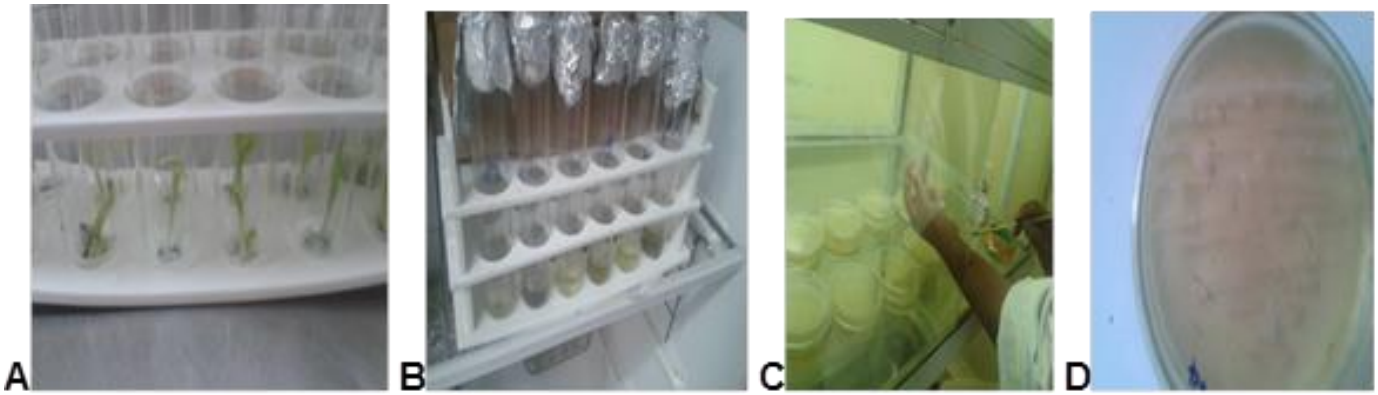

Figure 2. Procedures followed for pathogen testing. A. Shoots of the three clones for suspension sample preparation, B. suspension sample prepared from the shoots, C. Inoculation of samples to YPSA media under laminar hood. D. Mixed colony grown on YPSA.

(2.50 cm) was recorded for Mazia on hormone free media followed by Arkiya (3.20 cm) on the hormone free media after four weeks of culturing (Table 3). Digomerza has responded better for root length as compared to the two clones whereas, Arkiya responded poorly. The optimum level of IBA concentration seems to be 1 mg/l for all the three clones and the trend of root length for clones on media with different levels of IBA except the control was not significant (Table 3). Munguatosha et al. (2013) on their study for the effect of auxin and cytokinin on plant regeneration of the closely related Musacea family banana genotypes reported that there were increasing trend of root length with increasing concentration of IBA up to 2 mg/L which is not in conformity with this study due to species difference.

Plantlets cleaned from *Xanthomonas* pathogen by shoot tip culture technique

The result of plant extract sample culture on YPSA showed that mixed bacterial and fungal colonies on the media within 18 to 24 h of incubation under 27°C temperature set incubator (Figure 5).

The colony growth was in different manner than positive control sample culture of *Xanthomonas compestris* pv. musacearum in which bacterial colony was grown after 48 h. Colony growth was also evident on media inoculated by suspension sample prepared from control sample plantlets regenerated from non-inoculated suckers of the three clones. There was no any microbial colony growth on the control petri dishes with sterile distilled water stricked on media even after four days of inoculation. The colony growth pattern in this study is different from that of previous report by Eshetu (1981) in that it was very faster and mixed colonies together with fungus in the present experiment than in previous report that distinct colonies appear after 48 h incubation at 25 to 28°C on YPSA medium.

Birmeta et al. (2004) in their genetic variability and biotechnological studies for the conservation and improvement of *Ensete ventricosum* reported that

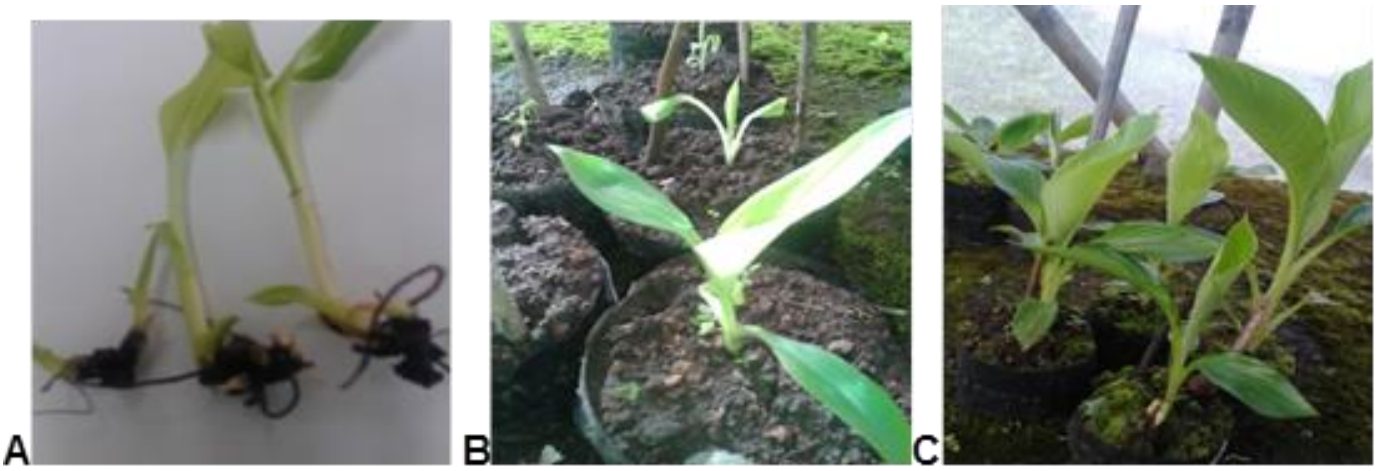

Figure 3. Plantlets acclimatized to soil mix of red ash and loam soil. A. Plantlets ready for acclimatization, B. Acclimatized plantlets after 15 days. C. Acclimatized plantlets current status.

microorganisms that influence the micro propagation efficiency are also associated with field-grown enset. The microbes recorded were regarded as endophytic since they were not prevented by standard surface sterilization procedures or by addition of antimicrobial compounds in the medium. Similarly, in this study microbial colony growth was observed on YPSA media from sample suspension prepared from healthy *in vitro* growing plantlets including shoots regenerated from control clean plantlets not artificially inoculated with pathogen. To confirm weather the bacterial colonies were *Xanthomonas* pathogen or not, pathogenecity test was done on healthy growing suckers of the most susceptible clone three months Arkiya suckers. Any of the plants inoculated did not show disease symptom. In addition to different colony, growth pattern and pathogenecity test result of plantlets *in vitro* and in acclimatization are growing healthy which indicates that 100% of the plantlets regenerated from diseased mother plants were cleaned from *Xanthomonas compestris* pv. *musacearum.*

Acclimatization

Among the plantlets acclimatized in pots filled with sterile soil mix, 90% survival was recorded for Digomerza plantlets (Figure 6B) and 80% for both Arkiya and Mazia after 15 days of acclimatization. Whereas, 60% survival was recorded for Digomerza plantlets acclimatized to soil mix without sterilization followed by 50% for Mazia. Soil sterilization has high effect on survival of plantlets and Digomerza clone has high performance in terms of survival in acclimatization even in non sterile acclimatization media. Rajani (2006) reported 80% survival rate of ginger *in vitro* plantlets acclimatized to solar sterilized peat soil mix after 15 days of acclimatization which is in agreement with the present finding. Dawit (2009) also reported an average (70%) survival rate for cassava *in vitro* regenerated plantlets acclimatized under screen house to a sterile soil mixture of red soil, compost and sand in the ratio of 1:1:2 respectively.

In conclusion, the protocol developed for *in vitro* regeneration of disease free plantlets of enset for three clones is efficient and new in its type. Where surface sterilizing explants with 70% of ethanol for 5 min followed by 2% of chlorox for 10 and 20 min were found as optimum. MS media with 4.5 mg/L BAP and 1.5 mg/L NAA in combination is sufficient for shoot induction and growth, whereas, 1 mg/L IBA is obtained to be optimum for root induction and growth.

Conflict of Interests

The authors have not declared any conflict of interests.

REFERENCES

Atnafua B, Endale T (2008). Food production and nutritional value of Enset. Proceedings of Enset National workshop, 9-14 August 2010, Wolkite, Ethiopia.

Awassa Agricultural Research Center, (2008). *Progress Report*, plant protection Research Division. Awassa, Ethiopia.

Birmeta G, Welander M (2004). Efficient micro propagation of *Ensete ventricosum* applying meristem wounding: a three step protocol. Plant Cell Rep. 23:277-283.

Birmeta G, Passoth V, Roos S, Welander M (2004). Identification of bacteria and yeasts from in vitro and surface sterilizedfield samples of ensete ventricosum by rDNA analysis. Biotechnol. Lett. 26:1867-1872.

Brandt SA, Spring A, Hiebsch C, McCabe ST, Endale T, Mulugeta D, Gizachew W/M, Gebre Y, Shigeta M, Shiferaw T (1997). The 'Tree Against Hunger'. Enset-based Agricultural Systems in Ethiopia. American Association for the Advancement of Science. P 56.

Central Statistics Ageency (CSA). 2013. Report on Area and Crop Production forecast for Major Crops Dec., 2013. Addis Ababa, Ethiopia.

Cheesman EE (1947). Classification of the Banana. The genus *Ensete horan.* Imperial college of tropical agriculture. Trinidad, Kew Bulletin 2**:**97-116.

Dagnachew Y, Bradbury JF (1968). Bacterial wilt of Enset (*Ensete ventricosum*) incited by Xanthomonas campestris sp. Phytopathology 59:111-112.

Dawit B (2009). Micropropagation of Selected Cassava Varieties (*Manihot esculenta* Crantz) from Meristem Culture. Msc Thesis, Addis Ababa University, Ethiopia. 54 p.

Endale, T. and Mulugeta, D. 1994. Improvement studies on enset and sweet potato. In: Proceedings of the second national horticultural workshop of Ethiopia. Herath, E. and Desalegn, L. (Eds.), 1-3 December 1992. IAR, Addis Ababa, Ethiopia pp. 63-64.

Eshetu W (1981). The role of *Poecilocarda nigrinervis*, *Pentanolia nigronervosa* and *Plantococcus ficus* in the transmission of enset wilt pathogen Xanthomonas musacearum sp. in Wolaita, Ethiopia. In. Ethiopia (Tsedeke Abate, Clifton Hiebsch and Steve Brandt). Proceedings of the first international workshop on Enset. Dec 13-21 1993. IAR, Addis Ababa, Ethiopia. pp. 188-203.

Gizachew W (2000). Variation in isolates of enset pathogen (*Xanthomonas campestris* Pv. *musacearum*) and reaction on enset clones (*Ensete ventricosum* (Welw) Cheesman) to this disease. MSc. Thesis. Alemaya university, Ethiopia. 61 p.

Hirimburegama K, Gamage N (1996). In *Vitro* Multiplication of Local Cultivars of Banana *(Musa* Spp.) Through Shoot-Tip Culture. Department of Botany, University of Colombo. 20 p.

Kidist B (2003). Characterization of Xanthomonas campestris PV. Musacearum isolates: causal agent of Enset Bacterial wilt disease. Msc Thesis, Addis Ababa University, Ethiopia. 100 p.

Morpurgo R, Afza R, Novak FJ (1993). Biotechnology and Enset Achievements and prospective. In. Enset sustainable Agriculture in Ethiopia proceedings 1996, Ethiopia, Addis Abeba. pp. 256-272.

Mulugeta D, Tesfaye D (2010). Research Experiences on Enset Biotechnology in Ethiopia. Proceedings of Enset National workshop, 19-20 August 2010, Wolkite, Ethiopia. pp. 38-45.

Mulugeta D, Van Staden J, Bornman CH (2005). The type of explants plays a determining role in the micro propagation of Ensete Ventricosium. S. Afr. J. Bot. 71(2):154-159.

Munguatosha N, Emerald M, Patrick N (2013). The Effects of Auxins and Cytokinin on Growth and Development of (Musa sp.) Var. "Yangambi" Explants in Tissue Culture. Am. J. Plant Sci. 4:2174-2180.

Murashige T, Skoog F (1962). A revised medium for rapid growth and bioassays with tobacco tissue cultures. Physiol. Plant. 15:219-223.

Negash A, Putie K, Schaart J, Visser B, Krens F (2000). *In vitro* regeneration and micropropagation of enset from south-western Ethiopia. Plant Cell Tissue Organ Cult. 62:153-158.

Rajani CH (2006). Micro propagation of ginger (*Zingiber officinale Rosc*.). Msc thesis University of Agricultural Sciences, Dharwad, India. 43 p.

Shiragi MH, Baque MA, Nasiruddin KM (2008). Eradication of Banana Bunchy Top Virus (Bbtv) Andbanana Mosaic Virus (Bmv) From Infected Plant Of Banana Cv. Amritasagar Through Meristem Culture. South Pac. Stud. 29(1):17-41.

Taye, B (1996). An Over view of enset research and the future technological needs for enhancing its production and utilization. *Proceedings of the First international workshop on Enset*. Dec 13-21 1993. IAR, Addis Ababa, Ethiopia. pp. 1-14.

Temesgen M, Bizuayehu T, Marcello C, Mario E (2014). Indigenous knowledge, use and on-farm management of enset (*Ensete ventricosum* (Welw.) Cheesman) diversity in Wolaita, Southern Ethiopia. J. Ethnobiol. Ethnomed. 10(1):1.

Zerihun Y, Hussein M, Mulugeta D, Temesgen A, Guy B (2013). Enset (Ensete ventricosum) clone selection by farmers and their cultural practices in southern Ethiopia. Genet. Resour. Crop Evol. 61(3):1-16.

academicJournals

Vol. 15(40), pp. 2202-2208, 5 October, 2016
DOI: 10.5897/AJB2016.15278
Article Number: C3A068A60815
ISSN 1684-5315

http://www.academicjournals.org/AJB

African Journal of Biotechnology

Full Length Research Paper

Unraveling possible association between quantitative trait loci (QTL) for partial resistance and nonhost resistance in food barley (*Hordeum vulgaris* L.)

Dido A. A.[1]*, Yeo F. K. S.[2] and Niks R. E.[2]

[1]Oromia Agricultural Research Institute, Sinana Agricultural Research Center, P.O.Box 208, Bale-Robe, Ethiopia.
[2]Department of Plant Breeding, Graduate school for Experimental Plant Sciences, Wageningen University, Droevendaalsesteeg 1, 6708 PB Wageningen, The Netherlands.

Received 15 February, 2016; Accepted 25 August, 2016

Many quantitative trait loci (QTLs) in different barley populations were discovered for resistance to *Puccinia hordei* and heterologous rust species. Partial resistance (host basal resistance) and nonhost resistance (nonhost basal resistance) in barley to leaf rusts are based on prehaustorial mechanism of resistance which is associated with papillae formation. They are mainly governed by genes with relatively small, quantitative effects, located on QTL. The genes for host basal resistance seem to play similar roles in basal resistance as those governing nonhost basal resistances. From different studies it was observed that these two resistance types are based on shared principles. Four and two quantitative trait loci-near isogenic lines (QTL-NILs), respectively, were developed for basal resistance and nonhost resistance QTLs using SusPtrit as recurrent parent. SusPtrit is a research line which is exceptionally susceptible to leaf rusts for which normally barley is a nonhost. They were infected with one homologous (*P. hordei* isolate 1.2.1) and three heterologous (*Puccinia* triticina isolate 'Flamingo', *P. hordei*-murini and *P. hordei*-secalini) leaf rusts in three replications at seedling stage to evaluate whether relatively large-effect QTLs show specificity in their reaction to homologous and heterologous rust isolates. The result showed that, the QTLs for host basal resistance and the QTL for nonhost basal resistance have a significant ($P<0.05$) effect on both homologous and heterologous rusts. Also, higher positive ($P<0.05$, $r = 0.98$) correlation was observed between different macroscopic and microscopic parameters measured indicating that there is a possible association between partial resistance quantitative trait loci and nonhost resistance quantitative trait loci. These give an indication that indeed, host and nonhost basal resistance are associated.

Key words: Partial resistance, nonhost resistance, near isogenic lines, barley.

INTRODUCTION

Naturally, most plant species are resistant to most pests and pathogen species. Such form of resistance is called non-host resistance which is commonly defined as resistance expressed by the whole plant species to all genetic variants of a non-adapted pathogen species or forma species (f.sp.) and represents the most durable form of plant resistance (Lipka et al., 2010; Schulze-Lefert and Panstruga, 2011). However, partially resistant genotypes can still be infected by the pathogen and show reduced rate of infection compared to susceptible

genotypes, which is an outcome of lower rate of colonization by the fungus (Niks and Rubiales, 2002; Niks and Marcel, 2009). Many factors contribute to nonhost resistance to unadapted pathogens, including constitutive defenses and induced defenses (Uma et al., 2011; Fan and Doerner, 2012). The possibility of transferring nonhost resistance to crop plants enabled the study of its association with host resistance. There are a number of examples of successful transfer of such resistance from nonhost to host species (Wulff et al., 2011). An important question will be whether there is association between genes potentially involved in nonhost resistance and host resistance and genes involved in nonhost resistance deploying them into host plants will result in durable resistance.

As QTLs can confer certain level of resistance by their cumulative effects, the adaptation of a pathogen and breakdown of each QTL resistance-allele is more difficult than breakdown of one monogenic resistance gene (Lindhout, 2002), particularly when each QTL-gene encodes a different gene product.

Near-isogenic lines (NILs) differing with regard to disease QTLs provide valuable material for a more detailed study into the genetic basis of quantitative resistance. Thus, development of such NILs allows the evaluation of a QTL in a nearly uniform genetic background, overcoming the difficulties of identifying QTL phenotypes (Marcel et al., 2007). QTL-NILs do not only provide a better estimate for the effect of single QTL alleles, but also provide a better insight into QTL x pathogen and QTL x environment interactions. Furthermore, QTL-NILs may provide a starting point for the unraveling of functional genes underlying these loci and possibly be useful for positional cloning (van Berloo et al., 2001).

For the purpose of evaluation of a QTLs genetic basis for quantitative resistance, five QTL-near isogenic lines (QTL-NILs) were developed by introgressing four host basal resistance QTLs and a nonhost resistance QTL into SusPtrit genetic background. SusPtrit is an experimental line which not only susceptible to the homologous rust, *P. hordei*, but also exceptionally susceptible to leaf rusts for which normally barley is a nonhost. The QTL-NILs developed allow us to study the possible association between the QTLs for host basal resistance and nonhost resistance (Marcel et al., 2007).

Therefore, this study was conducted to evaluate whether relatively large-effect QTLs show association in their reaction to homologous and heterologous rust isolates, and also, to evaluate their mechanism of resistance at tissue and cell level, especially whether the resistance is based on hypersensitivity or non-hypersensitivity.

Table 1. QTL-NILs used in this study.

QTL-NILs	Donor line
Vada-Rphq2	Vada
Vada-Rphq3	Vada
L-94-Rphq2	L-94*Vada
L-94-Rphq3	L-94*Vada
Su-Rphq2	SusPtrit*Vada
Su-Rphq3	SusPtrit*Vada
Su-Rphq11	SusPtrit*Steptoe
Su-Rphq16	SusPtrit*Dom
Su-Qnh.L	SusPtrit*L94
Su-Qnh.V	SusPtrit*Vada

MATERIALS AND METHODS

All experiments were conducted in Plant Research International (PRI) laboratory and greenhouse at Wageningen University, The Netherlands.

Plant materials

Near isogenic lines (NILs) with SusPtrit genetic background (Table 1) and having resistance QTLs, *Rphq2*, *Rphq3*, *Rphq11, Rphq16* and *Rnhq* (*Rnhq-V* and *Rnhq-L*), were used for this study.

The parental lines for each respective NILs were used as a reference. In addition, L94-NILs (L94-*Rphq2* and *-Rphq3*) and Vada-NILs (Vada-*rphq2*, and *-rphq3*) were included as well. For the histology assays, host plants corresponding to the rust species under observation were added as a reference.

Inoculum

Four isolates of rust fungi were used in infection studies (Table 2). They were multiplied on their respective host species. Urediniospores were collected and dried in desiccators for 5 to 7 days before used for inoculation.

Genotyping QTL-NILs

Genotyping of each QTL-NILs was performed before sowing to confirm the introgression of donor resistant allele by using molecular markers flanking the QTL region (Table 3). For this purpose DNA of each QTL-NILs was isolated following the CTAB isolation method according to Wang et al. (1993).

Phenotyping QTL-NILs with homologous rust isolate

Seeds of QTLs-NILs were sown in 37 × 39 cm boxes in two rows along with reference lines. Depending on the availability of seeds, 1 to 2 seeds were sown for each NIL. The secondary leaves were clipped out and the fully grown primary leaves were fixed horizontally with adaxial side up in an inoculation tower and

*Corresponding author. E-mail: alloaman2001@yahoo.com.

Table 2. Rust isolates used in this study.

Pathogens	Host plant	Common name
P. hordei isolate 1.2.1	*Hordeum vulgare*	Barley leaf rust
P. hordei-murini	*H. murinum*	Wall barley leaf rust
P. hordei-secalini	*H.secalinum*	Meadow barley leaf rust
P. triticina isolate "Flamingo"	*T.aestivum*	Wheat leaf rust

Table 3. List of markers used in genotyping of QTL-NILs.

Name(s)	Chrom.	Type	Tm (°C)	RE(s)	Linked QTL	Source
besV76P5D5AR	2H	ASPCR	56	-	*Rphq2*	
k00345	2H	CAPS	56	*Sdu I*	*Rphq2*	Marcel et al., 2008
scP15M51-204	2H	SCAR	56		*Rphq2*	Marcel et al., 2007
ABG388	6H	CAPS	58	*Nla III*	*Rphq3*	Marcel et al., 2007
WBE201	6H	CAPS	58	*Mnl I*	*Rphq3*	Marcel et al., 2007
GBM1212	6H	SSR			*Rphq3*	Marcel et al., 2007
HVM14	6H	SSR			*Rphq3*	Marcel et al., 2007
GBS0512	2H	CAPS	58	*Aci I - (Hpy99 I)*	*Rphq11*	Marcel et al., 2007
TC134748	2H	CAPS	47	*ApoI = XapI*	*Rphq11*	Rice synteny
GBM1062	2H	SSR	55		*Rphq11*	Marcel et al., 2007
GBMS244	2H	SSR	55		*Rphq11*	Marcel et al., 2007
DsT-33	5H	SCAR	45	-	*Rphq16*	Marcel et al., 2007
Scsnp03275_2	5H	CAPS	65	*BglII*	*Rphq16*	Marcel et al., 2007
GMS002	5H	SSR			*Rphq16*	
MWG2031	1H	CAPS	55	*Mwo I*	*Rnhq*	Kikuchi et al, 2004
SKT1	1H	CAPS	60	*Alu I*	*Rnhq*	Kikuchi et al., 2004
WBE101	1H	CAPS	52	*HpyCH4 IV*	*Rnhq*	Marcel et al., 2007
GBM1303	1H	SSR			*Rnhq*	Marcel et al., 2007

inoculated with 3.5 g of freshly collected spores of *P. hordei* isolate 1.2.1 diluted 10 times with lycopodium spores to obtain uniform spore distribution. The inoculated boxes were placed in a humidity chamber to incubate the spores overnight for eight hours at 100% relative humidity in the dark at 18°C. After incubation, the inoculated boxes were transferred to a greenhouse compartment where the temperature is set at 14 ± 3°C with 30 to 70% relative humidity. The experiment was carried out in two replications.

The latent period (LP) was measured one week after inoculation. The LP50S was then calculated with the following formula:

$$LP50 = T1 + (T2 - T1) \times \frac{(N100-2-N1)}{(N2-N1)}$$

T1 = the time just before 50% of the pustules are mature; T2 = the time just after 50% of the pustules are mature; N1 = number of mature pustules at T_1; N2 = number of mature pustules at T_2; N100/2 = half of the total mature pustules number.

To normalize the results, the relative latency period (RLP50S) was calculated relative to the LP50S of SusPtrit which set at 100.

Phenotyping QTL-NILs with heterologous rust isolates

The QTL-NILs were grown as described above except that in this case susceptible host plants were included. Ten to twelve days after sowing, completely unfolded primary leaves were fixed horizontally with the adaxial side up, and inoculated with 10 mg of spores per box using a settling tower (Atienza et al., 2004). For each QTL-NIL and reference lines, two seedlings were inoculated of which one seedling was sampled for histological studies. The second seedling was used for macroscopic phenotyping. To avoid cross contamination of rusts, the settling tower and other tools were cleaned with 70% ethanol before and after use. Latency period (LP) was measured six days (*Phs*) and eight days (*Phm* and *P. triticina*) after inoculation. Additionally, the level of infection was quantified by estimating the following traits: Infection frequency (IF, pustules/cm^2), flecks (F, non- sporulating infection sites/cm^2), frequency of visible infection sites (VIF, IF/total amount of visible infection sites/cm^2), and TotF (total amount of visible infection sites/cm^2) by using a metal frame with 1 cm^2 window. RLP50S and Relative Infection Frequency (RIF) were calculated by setting the RLP50S and RIF of SusPtrit to 100 as stated above. Analysis of variance for both RLP50S and RIF was carried out using GenStat statistical software (11.1th edition). All genotypes were grown in one box and the experiment was carried out in two replications.

Histological evaluation of pathogenesis

Histology is the study of the microanatomy of cells and tissues of plants. It is commonly performed by examining cells and tissues under microscope. The specimen having been sectioned (cut into a

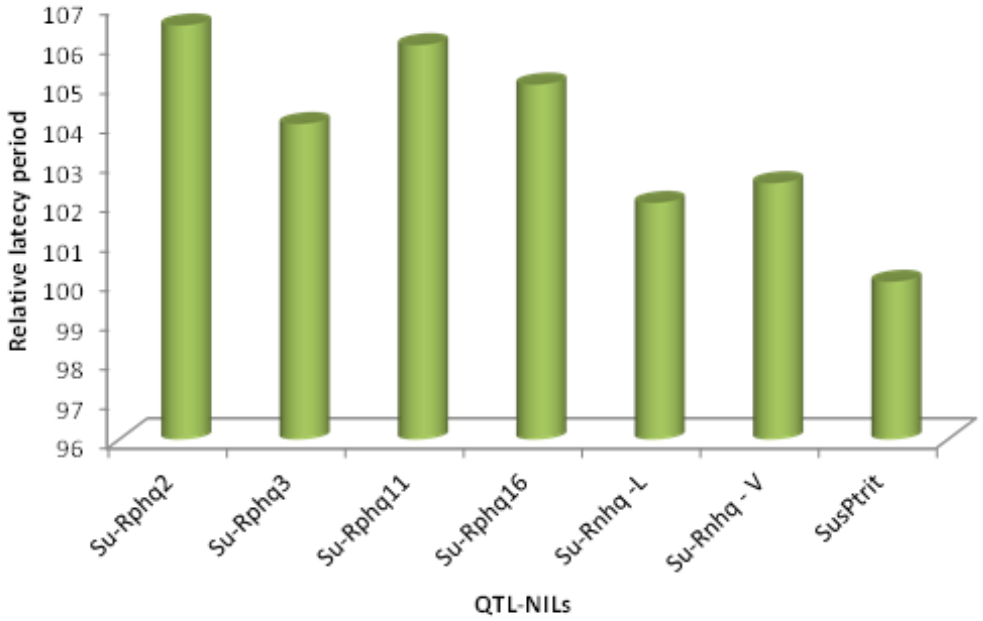

Figure 1. RLP50S of *P. hordei* isolated 1.2.1 on SusPtrit NILs and the reference lines at seedling stage (Source my own result of research data 2012).

thin cross section), stained, and mounted on a microscope slide.

Preparation of leaf samples for fluorescence microscopy

Seven days after inoculation, leaf segments of approximately 2 to 3 cm long cut out from the middle of primary leaf. These leaf segments were prepared as whole mount for fluorescence microscopy, except that Uvitex 2B (Ciba-Geigy) was used instead of Calcofluor. The leaf segments were immediately fixed and bleached by boiling for 1.5 min in a water bath in lactophenol-ethanol (1:2 v/v). After the leaves were bleached, the lactophenol-ethanol was poured off and they were washed once for 30 min in ethanol (50%) and in 0.05 N NaOH (2 g/l), respectively one after the other. The washed leaf segments were rinsed three times in water and soaked for 30 min in 0.1 M Tris/HCl buffer (pH 8.5). After 5 min of staining in a solution of 0.1% Uvitex in the same buffer, they were rinsed thoroughly for four times in water and then washed for 30 min in a solution of 25% glycerol. Finally, to prepare the slides, small drops of glycerol were added on the slide before the leaf samples were put along the longitudinal axis of the slide and the leaves samples were embedded on slide with the adaxial side facing up. Then the slide cover was carefully placed on the samples.

Observation of infection units under UV-microscope

For ease of inspection, different classes of infection units were set based on status of infection unit, where an infection unit is described as non-penetrating (NP), early aborted (EA) and established (Jafary et al., 2006). The detailed observation and scoring were done with a 10×10 and 40×10 magnification. The preparations were screened starting from one of the corners and moving horizontally along longitudinal axis of the leaves. The outmost stomata rows were excluded from observation to avoid possible border effects. Also overlapping and infection points close to air bubble were ignored. The infection hyphae were scored as "established" type (more than six haustorial mother cells) or "early aborted" type (having six or less haustorial mother cells). The data collected were analyzed using GenStat statistical software.

RESULTS AND DISCUSSION

Effects of PR and nonhost resistance QTLs towards homologous rust *P. hordei* isolate 1.2.1

QTL-NILs with PR and nonhost resistance QTLs had longer LP and RLP50S than susceptible check line, SusPtrit (Figure 1).

Against *P. hordei* isolate 1.2.1, *Rphq2*, *Rphq3, Rphq11* and *Rphq16* significantly ($P<0.05$) increase the LP observed in Su-*Rphq2*, Su-*Rphq3,* Su-*Rphq11* and Su-*Rphq16* as compared to SusPtrit. The effect of *Rphq3* in the seedling stage was smaller than that of the other three partial resistant (PR) QTLs (Figure 1). This is in agreement with the previous studies (Qi et al., 1999; Marcel et al., 2007). On the other hand, the effects of non-host QTLs (both on Su-*Rnhq-L* and Su-*Rnhq-V*) were not statistically significant. However, they have positive effect on resistance towards *P. hordei*.

SusPtrit NIL with PR QTLs had longer LP than SusPtrit, indicating that, these QTLs contributed to the effect on PR. Furthermore, it had an effect on resistance in Vada and L94 NILs (Data not shown). On the other hand, *Rnhq* QTL on Su-*Rnhq-V* had relatively more positive effect on resistance than that of Su-*Rnhq*-L. Likewise, both Su-*Rnhq-V* and Su-*Rnhq*-L had higher RLP50S than SusPtrit, indicating that *Rnhq* had an effect towards homologous rust.

Table 4. Mean relative latency period (RLP), relative infection frequency (RIF), percentage of non-penetrating (NP), early aborted (EA) and established (Est.) infection units by *P. triticina, P. hordei-murini* and *P. hordei-secalini* of tested lines.

QTL-NILs	*P. triticina* (Flamingo)					*P. hordei-murini*					*P. hordei-secalini*				
	RLP	**RIF**	**NP**	**EA**	**Est.**	**RLP**	**RIF**	**NP**	**EA**	**Est.**	**RLP**	**RIF**	**NP**	**EA**	**Est.**
Vada-*rphq2*	106.6^{ab}	6.4^{a}	24.2^{e}	69.5^{f}	4.7^{a}	103.4^{a}	9.1^{a}	15.4^{cd}	70.6^{f}	8.0^{a}	109.5^{c}	4.6^{a}	17.3^{a}	76.3^{g}	8.0^{a}
Vada-*rphq3*	117.3^{d}	7.2^{a}	24.5^{e}	66.4^{f}	9.3^{b}	103.5^{a}	11.0^{a}	16.0^{d}	73.8^{ef}	10.6^{b}	114.1^{c}	15.2^{b}	15.5^{a}	74.1^{fg}	10.4^{bc}
L94-*Rphq2*	113.9^{cd}	38.8^{b}	14.0^{bcd}	48.0^{e}	19.8^{c}	104.7^{a}	30.0^{b}	11.7^{bc}	68.9^{e}	10.0^{ab}	103.7^{ab}	42.5^{de}	12.0^{a}	70.0^{ef}	9.0^{ab}
L94-*Rphq3*	108.0^{bc}	33.4^{b}	12.0^{bc}	39^{d}	24.5^{d}	103.3^{a}	55.9^{e}	11.7^{bc}	59.6^{d}	14.3^{c}	102.7^{ab}	32.6^{c}	11.0^{a}	64.5^{de}	12.3^{cd}
Su-*Rphq2*	106.5^{ab}	37.8^{b}	16.0^{cd}	34.5^{cd}	24.5^{d}	104.5^{a}	30.3^{b}	14.7^{cd}	56.1^{cd}	14.8^{c}	104.9^{b}	31.2^{c}	14.6^{a}	63.3^{d}	12.0^{cd}
Su-*Rphq3*	106.0^{ab}	55.8^{c}	17.0^{d}	31.5^{bc}	25.8^{de}	10.9^{a}	39.7^{cd}	12.3^{bcd}	56.0^{cd}	15.9^{cd}	102.0^{ab}	29.4^{c}	12.5^{a}	56.3^{c}	14.7^{e}
Su-*Rphq11*	106.4^{ab}	57.7^{c}	16.0^{cd}	32.3^{bc}	25.9^{de}	104.2^{a}	31.2^{bc}	13.2^{bcd}	52.7^{c}	17.2^{d}	104.0^{ab}	39.1^{d}	14.5^{a}	57.0^{c}	13.9^{de}
Su-*Rphq16*	104.4^{ab}	63.0^{c}	15.0^{cd}	28.0^{b}	28.5^{e}	102.4^{a}	40.7^{d}	14.3^{cd}	45.2^{b}	20.3^{e}	102.2^{ab}	40.8^{be}	14.0^{a}	55.5^{c}	15.1^{e}
Su-*Rnhq-L*	100.6^{a}	64.2^{c}	10.0^{ab}	22.5^{a}	33.7^{f}	103.2^{a}	55.3^{e}	10.3^{ab}	37.8^{a}	26.1^{f}	102.0^{ab}	57.1^{f}	9.0^{a}	39.8^{b}	25.6^{g}
Su-*Rnhq-V*	102.6^{ab}	64.2^{c}	13.0^{bcd}	30.0^{bc}	28.3^{e}	103.0^{a}	44.5^{d}	12.2^{bcd}	38.5^{a}	24.7^{f}	102.9^{ab}	45.7^{e}	12.0^{a}	43.2^{b}	22.4^{f}
SusPtrit	100.0^{a}	100.0^{d}	7.0^{a}	21.0^{a}	36.0^{f}	100.0^{a}	100.0^{f}	7.0^{a}	34.2^{a}	29.7^{g}	100.0^{a}	100.0^{g}	11.2^{a}	26.4^{a}	30.9^{h}
Mean	**106.6**	**50.0**	**15.3**	**38.4**	**23.7**	**103.6**	**40.7**	**12.6**	**54.5**	**17.4**	**104.1**	**41.5**	**13.1**	**56.9**	**15.8**
CV (%)	**2.8**	**7.6**	**13.4**	**6.4**	**5.5**	**1.8**	**10.1**	**14.0**	**6.2**	**5.3**	**1.9**	**6.2**	**15.4**	**4.5**	**6.9**
LSD (5%)	**6.6**	**8.9**	**4.5**	**5.4**	**2.9**	**4.0**	**9.0**	**3.9**	**4.3**	**2.0**	**4.5**	**6.0**	**4.4**	**5.7**	**2.3**

Effects of PR and nonhost resistance QTLs towards heterologous rust isolates

The macroscopic observation revealed that all SusPtrit NILs had lower RIF and longer LP as compared to SusPtrit. The RIF of SusPtrit NILs with PR QTLs ranges from 38% (Su-*Rphq2*) to 63% (Su-*Rphq16*) on seedlings infected by *P. triticina*. As shown in Table 4, lower RIF were observed in lines with *Rphq2*. Nonhost resistance QTLs, showed nonhost resistance on Su-*Rnhq-V,* having 45% RLF for both *Phm* and *Phs,* while the percentage was the same with Su-*Rnhq-L* for *P. triticina*.

Concerning, microscopic observations, the distribution of infection units type based on counting of ≥50 infection units per plant revealed differences between QTL-NILs and SusPtrit for *P. triticina, Phs,* and *Phm*. These differences could be in proportion of NP, EA, formation of sporogenic tissue and colony size.

On the SusPtrit NILs it was observed that the percentage of non-penetrating (NP) infection units (this non-penetration of infection units was recognized by the absence of substomatal vesicle (SSV)) of *P. triticina* and *Phm* on average, were almost twice as high as in the susceptible line, SusPtrit. For *Phs* on the other hand, the percentage of NP infection units showed no significant differences (Table 4). Higher percentage of NP was observed in Su-*Rphq3* for *P. triticina*, while for *Phm* and *Phs* higher values were in Su-*Rphq2.* In case of nonhost SusPtrit NILs, Su-*Rnhq-V* had higher percentage of NP than that of Su-*Rnhq-L* for the three rusts species tested (Table 4).

Of the four infection unit classes studied in this experiment, it seems that EA and established infection units appeared to be the parameters with the largest contrasts between lines to see the existing variation among the NILs containing PR QTLs (*Rphq2, Rphq3, Rphq11, Rphq16*), non-host QTL (*Rnhq*-V and *Rnhq*-L) and susceptible line, SusPtrit. Thus, higher proportions of EA were observed on NILs containing *Rphq2* QTL except in Vada-*rphq3*, for all inappropriate rust species. The occurrence of large proportions of early abortion (EA) combined with host cell necrosis has been reported as a typical feature of nonhost reaction. On non-host plant, infection units are arrested between formation of haustorial mother cell (HMC) and first haustoria often accompanied with limited cell collapse. In nonhost resistance analysis of *Arabidopsis* to *Phytophthora infestans* infection, penetrated epidermal cells with rapid hypersensitive response was observed, although no symptoms could be detected (Huitema et al.,

Table 5. Correlation coefficients (*r*) among infection parameters measured from four rust fungi.

Parameter	RLP *Ph*	RIF*Pt*	EA*Pt*	RIF*Phs*	EA*Phs*	RIF*Phm*	EA*Phm*
RLP *P. hordei* isolate 1.2.1	1.00						
RIF *P. triticina*'Flamingo'	-0.81	1.00					
EA *P. triticina*'Flamingo'	0.85	-0.84	1.00				
RIF *P. hordei-secalini*	-0.87	0.93	-0.86	1.00			
EA *P. hordei-secalini*	0.94	-0.91	0.90	-0.93	1.00		
RIF *P. hordei-murini*	-0.92	0.94	-0.86	0.98	-0.92	1.00	
EA *P. hordei-murini*	0.81	-0.79	0.87	-0.80	0.91	-0.76	1.00

RLP = relative latency period; RIF = relative infection frequency; EA = percentage of early abortion.

2003). Therefore, HR that cannot be detected on visual symptoms may be observed at the single cell level in Type I NHR, which is probably related to low infection probability and an extremely rapid HR on non-host plants.

The established colonies were classified according to their phase of development into two categories, namely, those with sporogenic tissues (WST) and without sporogenic tissues (WOST). There is a significant variation between QTL-NILs and reference line, in proportion of established infection units with and without sporogenic tissues at seven days after inoculation (Data not shown).

Significantly larger proportions of established colonies with sporogenic tissues were observed in SusPtrit as compared to SusPtrit NILs with PR and non-host QTLs. Microscopical observations made in this study on the mechanism of non-host resistance confirm that for a large part of the resistance is pre-haustorial. Large proportions of colonies were arrested before HMC formation (Table 4). From all tested NILs, lower percentages of established infection units (*P. triticina* 49.0%, *Phm* 29.5% and *Phs* 23.6%) were observed in NIL with *Rphq2*.

In NILs with *Rnhq* (Su-*Rnhq-V* and Su-*Rnhq-L*), the proportions of established colonies with sporogenic tissues were lower than in SusPtrit infected with all three inappropriate rust species, while the percentage is higher than that of SusPtrit for established colonies without sporogenic tissues (Data not shown).

Correlations between measured components of resistances for tested rusts

The association in prehaustorial resistance was quantified by calculating correlation coefficients (*r*) among the infection parameters measured for partial resistance and nonhost resistance. Higher negative correlation was observed between RLP of *P. hordei* isolate 1.2.1 and RIF of *P. triticina, Phm* and *Phs*, indicating that some of the genes for resistance to these rusts are either linked or have pleiotropic effects. The higher negative correlation was also observed between parameters measured from those tested inappropriate rust fungi (Table 5).

Furthermore, the higher positive correlation (*r* = 0.81 to 0.94) was also observed between RLP of *P. hordei* isolate 1.2.1 and EA of *P. triticina* isolate 'Flamingo', *Phm* and *Phs* (Table 5). Correlation between RIF of *P. triticina* isolate "Flamingo" and RIF of *Phm* and *Phs* was also higher. Higher positive association was observed between different parameters measured (RLP, RIF, and EA), indicating that there is a possible association between partial resistance quantitative trait loci and nonhost resistance quantitative trait loci. As stated in Qi et al. (1998, 1999), Niks et al. (2000) and Jafary et al. (2006), this significant association between parameters for PR to *P. hordei* and the loci for resistance to heterologous rusts revealed that these two traits are associated with each other.

Conclusion

The result of current study illustrated that PR QTLs, *Rphq2, Rphq3, Rphq11 and Rphq16* and the non-host resistances QTL, Rnhq, in barley, have effects on both partial resistance towards homologous leaf rust and non-host resistance towards heterologous leaf rusts. Furthermore, higher positive correlation was observed between parameter of relative latent period in seedling stage and proportion of early abortion at infection sites, which indicated that there is a possible association between partial resistance QTLs and non-host resistance QTLs.

Conflict of Interests

The authors have not declared any conflict of interests.

ACKNOWLEDGMENTS

This work is part of M.Sc. thesis of the senior author. The study was financially supported by Netherlands Fellowship Program (NFP-AP).

REFERENCES

Atienza SG, Jafary H, Niks RE (2004). Accumulation of genes for

susceptibility to rust fungi for which barley is nearly a nonhost results in two barley lines with extreme multiple susceptibility. Planta 220:71-79

Fan J, Doerner P (2012). Genetic and molecular basis of nonhost disease resistance: complex, yes; silver bullet, no. Curr. Opin. Plant Biol. 15:400-406.

Huitema E, Vleeshouwers V, Francis DM, Kamoun S (2003). Active defence responses associated with non-host resistance of Arabidopsis thaliana to the oomycete pathogen *Phytophthora infestans*. Mol. Plant Pathol. 4:487-500.

Jafary, H, Szabo LJ, Niks RE (2006). Innate nonhost immunity in barley to different heterologous rust fungi is controlled by sets of resistance genes with different and overlapping specificities. Mol. Plant Microbe Interact. 19(11):270-1279.

Kikuchi S, Taketa S, Ichii M, Kawasaki S (2004). Efficient fine mapping of the naked caryopsis gene (nud) by HEGS (High Efficiency Genome Scanning)/AFLP in barley. Theor. Appl. Genet. 108(1):73-78.

Lindhout P (2002). The perspectives of polygenic resistance in breeding for durable disease resistance. Euphytica 124:217-226.

Lipka U, Fuchs R, Kuhns C, Petutschnig E, Lipka V (2010). Live and let die-*Arabidopsis* nonhost resistance to powdery mildew. Eur. J. Cell Biol. 89:194-199.

Marcel TC, Varshney RK, Barbieri M, Jafary H, de Kock MJD, Graner A, Niks RE (2007). A high-density consensus map of barley to compare the distribution of QTLs for partial resistance to *Puccinia hordei* and of defence gene homologues. Theor. Appl. Genet 114:487-500.

Marcel TC, Gorguet B, Ta MT, Vels A, Niks RE (2008). The verification of QTLs for partial resistance to *Puccinia hordei* in NILs of barley confirms an isolate-specific effect. New Phytol. 177:743-755.

Niks RE, Marcel TC (2009). Nonhost and basal resistance: how to explain specificity? New Phytol. 182:817-828.

Niks RE, Rubiales D (2002). Potentially durable resistance mechanisms in plants to specialized fungal pathogens. Euphytica 124:201-216.

Niks RE, Fernández E, Van Haperen B, Bekele AB, Martínez F (2000). Specificity of QTLs for partial and non-host resistance of barley to leaf rust fungi. Acta Phytopathol. Entomol. Hung. 35(1/4):13-21.

Qi, X, Jiang, G, Chen, W, Niks, RE, Stam, P, Lindhout, P (1999). Isolate-specific QTLs for partial resistance to *Puccinia hordei* in barley. Theor. Appl. Genet. 99:877-884

Qi, X, Niks, RE, Stam, P, and Lindhout P (1998). Identification of QTLs for partial resistance to leaf rust (*Puccinia hordei*) in barley. Theor. Appl Genet 96:1205-1215.

Uma B, Swaroopa RT, Podile AR (2011). Warriors at the gate that never sleep: non-host resistance in plants. J. Plant Physiol. 168:2141-2152.

van Berloo R, Aalbers H, Werkman A, Niks RE (2001). Resistance QTL confirmed through development of QTL-NILs for barley leaf rust resistance. Mol. Breed. 8:187-195.

Wulff BBH, Horvath DM, Ward ER (2011). Improving immunity in crops: new tactics in an old game. Curr. Opin. Plant Biol. 14:468-476.

academicJournals

Vol. 15(40), pp. 2209-2214, 5 October, 2016
DOI: 10.5897/AJB2016.15623
Article Number: 3001A7F60834
ISSN 1684-5315

http://www.academicjournals.org/AJB

African Journal of Biotechnology

Full Length Research Paper

Screening of spontaneous castor bean accesses for genetic improvement programs

Rener Luciano de Souza Ferraz[1], Jane Lima Batista[2], Marcelo de Andrade Barbosa[3]*, Ivomberg Dourado Magalhães[4], Alberto Soares de Melo[5] and Antonio Sergio Ferraudo[6]

[1]Department of Agricultural Engineering, Federal University of Campina Grande Avenue Aprígio Veloso, CEP: 58429-140 - Campina Grande, PB, Brazil.
[2]Department of Biofuels, Technology Faculty of Jaboticabal, Eduardo Zambianchi Ave., 31, CEP: 14883-130 - Jaboticabal, SP, Brazil.
[3]Department of Soils and Fertilizers, Paulista State University, Access Road Prof. Paulo Donato Castellane, CEP: 14884-900 - Jaboticabal, SP, Brazil.
[4]Department of Plant Production, Federal University of Alagoas, Access road Lourival Melo Mota, s/n, CEP: 57072-900 - Alagoas, AL, Brazil.
[5]Department of Agricultural Sciences, Paraíba State University/Embrapa Cotton Baraúna Integration Center - Room 310, 3° floor, CEP: 58429-500 - Campina Grande, PB, Brazil.
[6]Department of Exact Sciences, Paulista State University, Access road Prof. Paulo Donato Castellane, CEP: 14884-900 - Jaboticabal, SP, Brazil.

Received 23 August, 2016; Accepted 21 September, 2016

The objective of this work was to identify, through the use of multivariate analysis, the spontaneous accesses of castor bean that show promising characteristics for inclusion in genetic improvement programs of this culture in Brazil. The study was conducted at the Paulista State University, Jaboticabal Campus. The accesses of castor bean seeds obtained were identified as ACS-001-CRSP, ACS-001-JASP, ACS-001-MASP, ACS-001-SESP, ACS-002-JASP, ACS-002-SESP and ACS-003-JASP, from the municipalities of Jaboticabal, Monte Alto, Santa Ernestina and from the District of Córrego Rico. The seeds' biometric variables and germination potential were measured, in addition to the biomass accumulation of the seedling's vegetative parts. The experimental design was completely randomized, with seven treatments and four replications. The original data was standardized and submitted to multivariate analysis of principal components and grouping. Through the results obtained, it is possible to reduce the number of original variables into two latent variables with discriminant power between the castor bean accesses, being the multivariate analysis efficient in this process. The castor bean accesses ACS-001-CRSP and ACS-001-MASP are promising for introduction in genetic improvement programs of this culture.

Key words: *Ricinus communis* L., genotype, multivariate statistics, bioenergy.

INTRODUCTION

Climate change has often been featured in numerous discussions around the world, especially when emphasizing the consequences of human actions in the environmental context (Cera and Ferraz, 2015; Klein et al., 2016.). In fact, some activities developed by man are potentially harmful to the environment, for example,

processes that result in greenhouse gases emission, such as oil and gas, which are non-renewable energy sources and major precursors of CO_2 emissions into the atmosphere (Anifowose and Odubela, 2015). In this context, Shahraeeni et al. (2015) reported that the mitigation of global warming is possible through reducing atmospheric concentrations of pollutant gases.

The choice of biofuels consists of a promising strategy for environmental improvement, being from renewable sources (Lima et al., 2015; Lu et al., 2015). In this scenario, the cultivation of castor bean (*Ricinus communis* L.) can be highlighted as an alternative source of vegetable oil for biodiesel generation, and several other industrial applications with the possibility of viable fuel supply to the Brazilian energy matrix (Dutra et al., 2015; Kallamadi et al., 2015; Lara-Fioreze et al., 2015).

Brazil is characterized by its edaphoclimatic diversity, featuring varied ecosystems throughout the country, with large potential agricultural areas for the production of oilseeds. Castor bean has a high productivity capacity, high adaptability to different climate and soil, and the oil produced by the plant does not compete with edible ones, making it a promising bioenergy alternative (Paes et al., 2015). There are several varieties of castor oil plants with significant genetic diversity, making them suitable for genetic improvement (Kallamadi et al., 2015).

Therefore, research should be intensified aiming the generation of academic and scientific information, besides the possibility of introducing technologies from screening of castor-oil-plant accesses that have potential for use in genetic improvement programs in Brazil and in the world (Singh et al., 2015).

In recent studies, the use of data analysis by univariate methods is efficient, particularly when the objective is to differentiate genotypes of the same species, for example *R. communis* L. (Moraes et al., 2015). However, there is significant increase in the literature of the use of multivariate data analysis for discrimination of genotypes or accesses with desirable agronomic characteristics or for genetic improvement (Rodrigues et al., 2014).

The germplasm's genetic variability is vital for the success of a genetic improvement program, and furthermore, the diversity analysis allows the identification of divergent genitors suited to obtain hybrids of greater heterotic effect. To this end, the application of multivariate statistical techniques such as the principal component analysis (PCA) and grouping enables the differentiation between accesses and optimization of germplasm collection, in order to promote a more efficient use of available genetic resources (Reis et al., 2015).

The objective of this study was to identify, through the use of multivariate analyses, accesses of spontaneous castor bean with promising characteristics for inclusion in genetic improvement programs of this culture in Brazil, increasing the availability of raw material for biofuel production.

MATERIALS AND METHODS

The experiment was conducted between the months of July and August 2014 in a greenhouse, followed by laboratory, both belonging to the Department of Agriculture Applied Biology (DAAB) located at the Faculty of Agricultural and Veterinary Sciences (FCAV) of the Paulista State University (UNESP).

Initially, accesses castor bean seeds were obtained from the micro-region of Jaboticabal, SP. To this end, areas were identified as infested by the species (*R. communis* L.) in reproductive phase, and the racemes with 70% of fruits maturing or dry were collected and arranged inside the greenhouse for sun drying. Then, the berries were opened for removal of the seeds, which were placed in polyethylene trays staying in the greenhouse for drying and subsequent selection according to color pattern, weight, health, physical damage and pathogen attacks. The selected seeds were identified as ACS-001-CRSP, ACS-001-JASP, ACS-001-MASP, ACS-001-SESP, ACS-002-JASP, ACS-002-SESP and ACS-003-JASP, from the municipalities of Jaboticabal, Monte Alto, Santa Ernestina and District of Córrego Rico.

Evaluations were performed for longitudinal diameter (SLD, mm), transverse diameter (STD, mm) and thickness (ST, mm) using a digital caliper, and fresh mass of a hundred seeds (HSM, g) in analytical scale, according to the criteria of Embrapa (2006). The germination potential of the seeds was carried out according to the rules established in Brasil (2009). The evaluation of germination percentage (GP, %), emergency speed index (ESI), mean germination time (MGT, days), and germination rate (GR, days), were performed as described in Carvalho and Carvalho (2009). For this purpose, the seeds were sown in August 3, 2015, and 14 days after sowing, five uniform seedlings were collected per share, which was separated into root, stem and leaves. In order to obtain the dry mass of the roots (RDM, g), stems (SDM, g) and leaves (LDM, g), these vegetative parts were placed in paper bags and dried in a forced air oven at 60°C until a constant weight.

The experimental design was completely randomized, with treatments consisting of seven castor bean accesses with four replications of 25 seeds. The data were subjected to standardization in such a way to make the mean zero and the variance unitary. The multivariate structure of the results was evaluated by means of PCA in order to condense the amount of relevant information in the original set of data into a smaller number of dimensions (principal components, PC), resulting from linear combinations of the original variables generated from the higher eigenvalues in the covariance matrix. For each PC, we proceeded to cluster analysis by hierarchical method, Ward's minimum variance, considering the variables relevant in the composition of each principal component (Hair et al., 2009).

RESULTS AND DISCUSSION

Through the use of PCA, it was possible to condense the number of original variables into two main components (PC1 and PC2), which together hold 79% of the total accumulated variance. The choice of these PCs was

*Corresponding author. E-mail: barbosamarcelo.unesp@hotmail.com.

Table 1. Loads of variables, eigenvalues and cumulative variance associated with the two principal components formed from 11 variables measured in seven castor bean accesses.

PCs	SLD	STD	ST	HSM	GP	ESI	MGT	GR	RDM	SDM	LDM	λ	σ²
PC1	0.58	0.52	0.79	0.55	-0.60	-0.52	0.68	-0.75	-0.91	-0.85	-0.83	5.42	49.26
PC2	0.78	0.82	0.57	0.78	0.04	0.62	-0.50	0.40	0.28	0.27	0.35	3.29	29.95

PC, Principal component; SLD, seed longitudinal diameter; STD, seed transverse diameter; ST, seed thickness; HSM, a hundred seed mass; GP, germination percentage; ESI, emergency speed index; MGT mean germination time; GR, germination rate; RDM, root dry mass; SDM, stem dry mass; LDM, leaf dry mass; λ, eigenvalue; σ², variance.

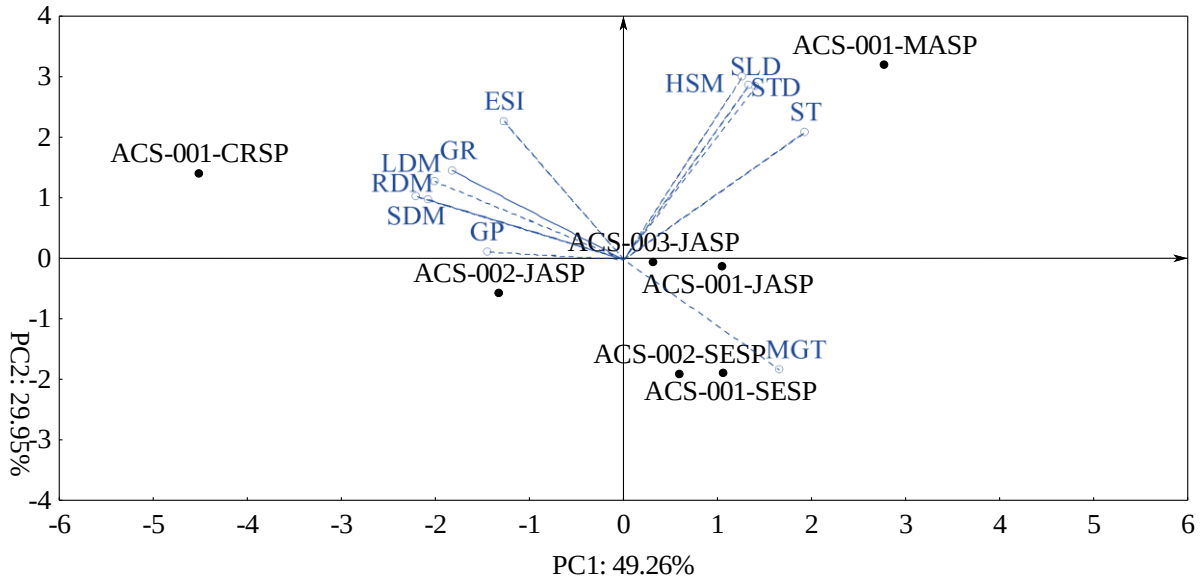

Figure 1. Two-dimensional projection (biplot) of castor bean accesses and the variables in the two principal components (PC1 and PC2).

based on the eigenvalues ≥ 1.00. For the selection of the variables, values ≥ 0.60 were adopted (absolute values) according to the Kaiser criteria (Table 1).

The first principal component (PC1) explained 49.26% of the total variance. In this component, the accesses ACS-001-CRSP and ACS-001-MASP were discriminated, in which the biometric variables (ST), seed vigor (GP, MGT and GR) and dry mass of seedlings (RDM, SDM and LDM) contributed to the cumulative variance for presenting factor loads above 0.60 (absolute value) (Figure 1). The second Principal Component (PC2) holds 29.95% of the remaining variance. In this component, the access ACS-001-MASP was separated from the accesses ACS-001-SESP and ACS-002-SESP, and it should be highlighted that the biometric variables (SLD, STD and HSM) and emergency speed index (ESI) of the seeds contribute with significant actor loadings in screening of these castor bean accesses (Figure 1).

The knowledge of differences in genetic constitutions within groups or between genotype groups is important to any genetic improvement program (Rodrigues et al., 2014). Therefore, the results of this study contribute to the state of the art and scientific development, by increasing the genetic amplitude with new materials, according to the statement Cruz and Regazzi (1997), which emphasize the importance of identification of genitors with genetic differences that produce progeny of higher heterosis, thereby increasing the probability for obtaining superior individuals.

The search for genetic variability and the introduction of new genetic material into existing germplasm banks are important strategies to guarantee the goals of improvement programs (Reis et al., 2015). Most species exploited agriculturally had their genetic amplitude drastically reduced as a result of domestication, selection processes and plant improvement (Gonçalves et al., 2008).

The lower growth of plants can be considered an indicator of adaptive defense strategies, especially in situations of abiotic stresses (Freitas-Silva et al., 2016; Li et al., 2016). The variation in seedling growth, aerial part and root system denotes more or less adaptation to the

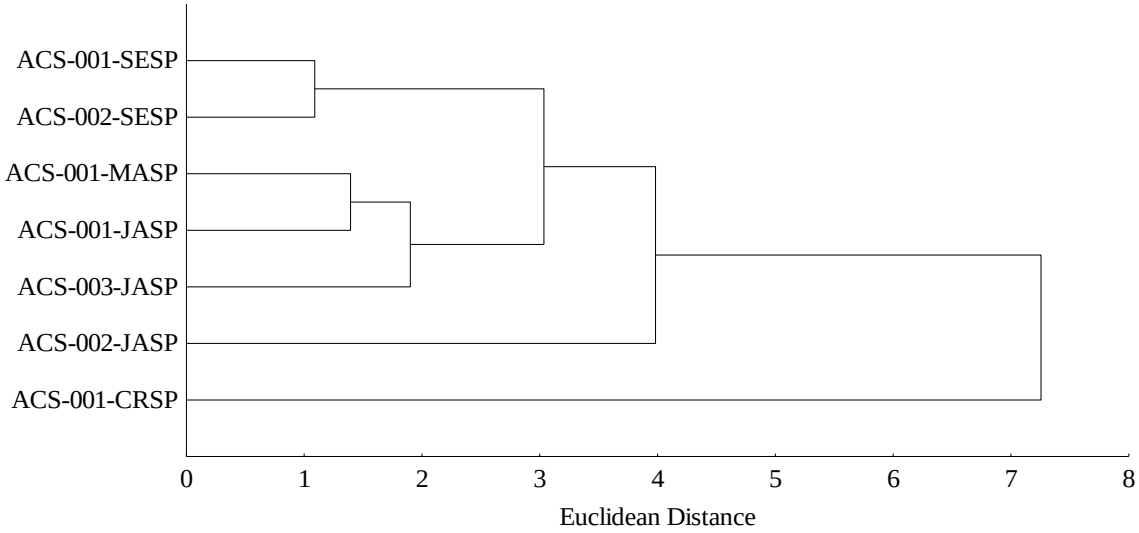

Figure 2. Dendrogram showing the structure of groups contained in the seven castor bean accesses, built with the expressive variables PC1.

environment (Mesquita et al., 2015). Based on this information, there is further need to study the ACS-001-CRSP for its capacity of adjustment in the growth of root system and aerial part, as a defense strategy to abiotic stresses such as water deficit and salt stress, which should lead to greater stability in the field.

Variations in the biometric characteristics of the seeds can be attributed to various factors, from physiological maturity to differences in genetic make-up, so that such situations act directly on the proliferation and development of cells that constitute the embryo axis and reserve tissues (Severino et al., 2015). According to Paes et al. (2015), due to the large number of varieties, the oil content may vary from 44-55% of the seeds' dry mass. Still, these authors emphasize the relationship between biometrics and oil content in castor beans. Thus, considering the results obtained in this study, the access CCS-001-MASP can be explored for oil production purposes, mainly for standing out for the peculiar characteristics of its seeds, which gives it potential in oil accumulation.

In order to express structure groups contained in the accesses, cluster analysis was performed based on PC1 variables. Through this technique, it was verified that the ACS-001-CRSP access has high dissimilarity compared with others, followed by ACS-002-JASP, while the accesses ACS-003-JASP, ACS-001-JASP and ACS-001-MASP form an intermediate group, with significant dissimilarity regarding the accesses ACS-001-SESP and ACS-002-SESP (Figure 2).

The grouping of accesses based on the variables with high factor loadings in PC2, shows that the ACS-001-MASP access has great dissimilarity when compared with others (Figure 3). The ACS-003-JASP and ACS-001-SESP accesses form an intermediate group, while the rest are grouped into two subdivisions consisting of ACS-001-JASP and ACS-001-CRSP; and ACS-002-JASP and ACS-002-SESP (Figure 3).

The data clustering process consists in the vectorization of similar multidimensional data in a number of clusters, and currently this type of analysis is widely used in exploratory analyses (Wang et al., 2016). The use of this technique is justified by the practicality in the visualization of the results by interest group, even when the number of genotypes involved in the research is high (Laurindo et al., 2015). Vargas et al. (2015) add that the increased use of multivariate techniques to quantify the genetic divergence is relevant, because these analyses allow considering simultaneously a large number of features, which facilitate the decision-making process based on a joint response, unlike studies that assess the variables in an isolated manner.

Rodrigues et al. (2014), studying castor bean accesses from the state of Minas Gerais, found the formation of groups and dissimilarity among the accesses with peculiar characteristics promising for improvement, and concluded that the employment of the multivariate technique (cluster analysis) proved efficient for the investigation of genetic variability among the studied materials.

Conclusions

1) The original set of variables may be reduced in two latent variables with discriminating power among the castor bean plant accesses.
2) The accesses of castor bean ACS-001-CRSP and ACS-001-MASP have high potential for introduction in genetic improvement programs of the culture.

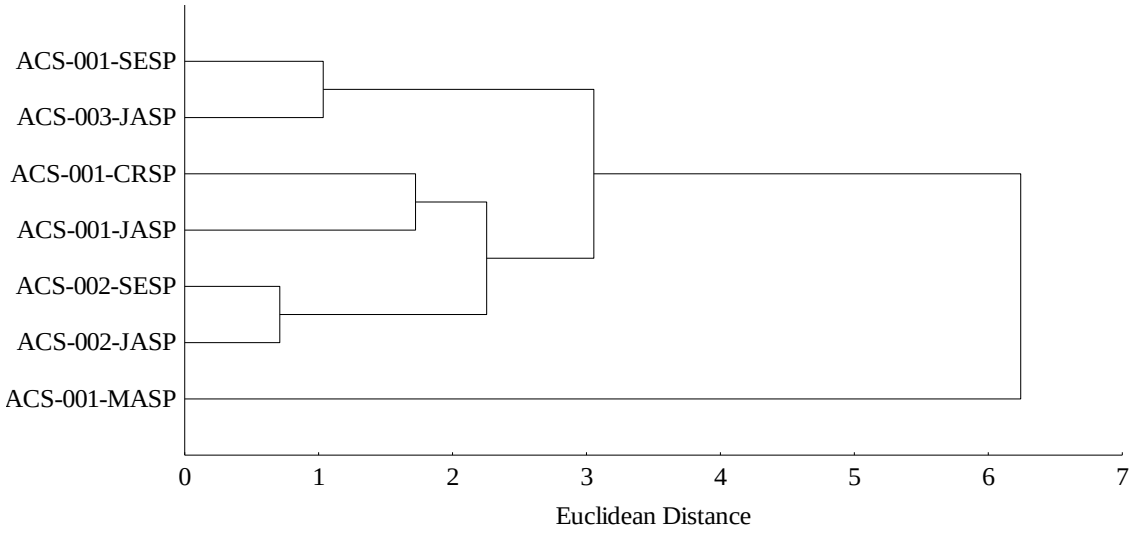

Figure 3. Dendrogram showing the structure of groups contained in the seven castor bean accesses, built with significant variables in PC2.

3) The use of multivariate data analysis shows efficiency in screening studies of castor bean accesses.

Conflict of Interests

The authors have not declared any conflict of interest.

REFERENCES

Anifowose B, Odubela M (2015). Methane emissions from oil and gas transport facilities-exploring innovative ways to mitigate environmental consequences. J. Clean. Prod. 92(4):121-133.

Brasil (2009). Ministério da Agricultura, Pecuária e Abastecimento. Regras para análise de sementes. Ministério da Agricultura, Pecuária e Abastecimento. Secretaria de Defesa Agropecuária. Brasília, DF: MAPA/ACS, 2009. 395 p. Available in: <http://www.agricultura.gov.br/arq_editor/file/2946_regras_analise__sementes.pdf>. Access at 7 March 2015.

Carvalho DB, Carvalho RIN (2009). Qualidade fisiológica de sementes de guanxuma em influência do envelhecimento acelerado e da luz. Acta Sci. Agron. 31(3):489-494.

Cera JC, Ferraz SET (2015). Variações climáticas na precipitação no sul do brasil no clima presente e futuro. Rev. Bras. Met. 30(1):81-88.

Cruz CD, Regazzi AJ (1997). Divergência genética. In. Cruz D, Regazzi, A.J. Métodos Biométricos Aplicados ao Melhoramento Genético. Viçosa: UFV, cap. 6: 287-324.

Dutra AF, Melo AS, Dutra WF, Silva FG, Oliveira IM, Suassuna JF, Véras Neto JG (2015). Agronomic performance and profitability of castor bean (*Ricinus communis* L.) and peanut (*Arachis hypogaea* L.) intercropping in the Brazilian semiarid region. Aust. J. Crop Sci. 9(2):120-126.

Embrapa (2006). Caracterização Taxonômica de Acessos de Mamona (*Ricinus communis* L.) do Banco Ativo de Germoplasma da Embrapa Algodão. Campina Grande: Embrapa Algodão. 17 p. (Embrapa Algodão. Boletim de Pesquisa e Desenvolvimento, 67).

Freitas-Silva L, Araújo TO, Silva LC, Oliveira JÁ, Araújo JM (2016). Arsenic accumulation in Brassicaceae seedlings and its effects on growth and plant anatomy. Ecotoxicol. Environ. Saf. 124:1-9.

Gonçalves LSA, Rodrigues R, Sudré CP, Bento CS, Moulin MM, Araújo ML, Daher RF, Pereira TNS, Pereira MG (2008).Divergência genética em tomate estimada por marcadores RAPD em comparação com descritores multicategóricos. Hortic. Bras. 26(3):364-370.

Hair JF, Black WC, Babin BJ, Anderson RE, Tatham RL (2009). Análise Multivariada de Dados. Porto Alegre: Bookman, 6.ed. P 688.

Kallamadi PR, Nadigatlab VPRR, Mulpurib S (2015). Molecular diversity in castor (*Ricinus communis* L.). Ind. Crops Prod. 66(4):271-281.

Klein D, Wolf C, Schulz C, Weber-Blaschke G (2016). Environmental impacts of various biomass supply chains for the provision of raw wood in Bavaria, Germany, with focus on climate change. Sci. Total Environ. 539(1):45-60.

Lara-Fioreze ACC, Fioreze SL, Pivetta LG, Zanotto MD (2015). Nitrato de prata como indutor de flores masculinas em linhagem pistilada de mamona. Glob. Sci. Technol. 8(1):61-69.

Laurindo LS, Laurindo RDF, Azevedo AM, Nick C, Silva DJH, Mizubuti ESG (2015). Seleção de acessos de tomateiro resistentes à pinta-preta pela análise de agrupamento das curvas de progresso da doença. Pesq. Agropec. Bras. 50(2):106-114.

Li X, Wan S, Kang Y, Chen X, Chu L (2016). Chinese rose (*Rosa chinensis*) growth and ion accumulation under irrigation with waters of different salt contents. Agric. Water Manage. 163:180-189.

Lima GS, Nobre RG, Ghey HR, Soares LAA, Pinheiro FWA, Dias AS (2015). Crescimento, teor de sódio, cloro e relação iônica na mamoneira sob estresse salino e adubação nitrogenada. Comun. Sci. 6(2):212-223.

Lu X, Withers MR, Seifkar N, Field RP, Barrett SRH, Herzog HJ (2015). Biomass logistics analysis for large scale biofuel production: Case study of loblolly pine and switch grass. Bioresour. Technol. 183(5):1-9.

Mesquita FO, Nunes JC, Lima Neto, AJ, Souto AGL, Batista RO, Cavalcante LF (2015). Formação de mudas de nim sob salinidade da água, biofertilizante e drenagem do solo. Irriga 20(2):193-203.

Moraes PF, Laat DMD, Santos MEAHP, Colombo CA, Kiihl T (2015). Expressão gênica diferencial em genótipos de mamona (*Ricinus communis* L.) submetidos a déficit hídrico induzido por PEG. Bragantia 74(1):25-32.

Paes JB, Souza AD, Lima CR, Santana GM (2015). Rendimento e características físicas dos óleos de nim (*Azadirachta indica*) e mamona (*Ricinus communis*). Floresta Ambient. 22(1):134-139.

Reis MVM, Damasceno Junior PC, Campos TO, Diegues IP, Freitas SC (2015). Variabilidade genética e associação entre caracteres em germoplasma de pinhão-manso (*Jatropha curcas* L.). Rev. Ciênc. Agron. 46(2):412-420.

Rodrigues HCA, Carvalho SP, Carvalho AA (2014). Determinação da divergência genética entre acessos de mamoneira por meio de

caracteres binários e multicategóricos. Rev. Ciênc. Agron. 13(3): 247-254.
Severino LS, Mendes BSS, Lima GS (2015). Seed coat specific weight and endosperm composition define the oil content of castor seed. Ind. Crops Prod. 75:14-19.
Shahraeeni M, Ahmed S, Malek K, Drimmelen BV, Kjeang E (2015). Life cycle emissions and cost of transportation systems: Case study on diesel and natural gas for light duty trucks in municipal fleet operations. J. Nat. Gas Sci. Eng. 24(3):26-34.
Singh AS, Kumari S, Modi AR, Gajera BB, Narayanan S, Kumar N (2015). Role of conventional and biotechnological approaches in genetic improvement of castor (*Ricinus communis* L.). Ind. Crops Prod. 74(1):55-62.
Vargas TO, Alves EP, Abboud ACS, Leal MAA, Carmo MGF (2015). Diversidade genética em acessos de tomateiro *heirloom*. Hortic. Bras. 33(2):174-180.
Wang R, Zhou Y, Qiao S, Huang K (2016). Flower pollination algorithm with bee pollinator for cluster analysis. Inf. Proc. Lett. 116(1):1-14.

academicJournals

Vol. 15(40), pp. 2215-2223, 5 October, 2016
DOI: 10.5897/AJB2016.15563
Article Number: 1346E3D60837
ISSN 1684-5315

http://www.academicjournals.org/AJB

African Journal of Biotechnology

Full Length Research Paper

Assessment of the genetic diversity of Kenyan coconut germplasm using simple sequence repeat (SSR) markers

Maurice E. Oyoo[1]*, Najya Muhammed[2], Kimani N. Cyrus[3] and Simon M. Githiri[3]

[1]Department of Crops, Horticulture and Soil Sciences, Egerton University, P. O. Box 536-20115, Egerton, Kenya.
[2]Department of Chemistry and Biochemistry, Pwani University, P. O. Box 195-80108, Kilifi, Kenya.
[3]Jomo Kenyatta University of Agriculture and Technology, P. O. Box 62000-00100, Nairobi, Kenya.

Received 13 July 2016, Accepted 7 September, 2016.

Genetic diversity and relationship among 48 coconut individuals (*Cocos nucifera* L.) collections from the Coastal lowland of Kenya were analyzed using 15 simple sequence repeat (SSR) primer pairs. Diversity parameters were calculated using Popgene Software version 1.31. The gene diversity values ranged from 0.0408 (CAC68) to 0.4861 (CAC23) with a mean value of 0.2839. The polymorphic information content (PIC) values ranged from 0.0400 to 0.3680 with a mean value of 0.2348. Marker CAC23 had the highest PIC and revealed highest gene diversity values in this study. Analysis of the molecular variation indicated that within individual variation was 98% while among materials, variation was low at 2% suggesting that molecular variation was not defined by region of production. Cluster analysis was constructed using DARwin program version 6.0. Forty eight (48) coconut individuals were clustered into three groups.

Key words: Coconut palm (*Cocos nucifera* L., Arecaceae), germplasm, simple sequence repeat (SSR) markers, cluster analysis, diversity.

INTRODUCTION

The coconut palm (*Cocos nucifera* L., Arecaceae) is a crop mostly cultivated in the coastal lowlands of Kenya and plays an important role in the economy. However, Kenya has been lagging behind in technology development for product diversification and by product utilization. Beside this, the coconut grows well in agro-ecological coastal lowlands (CL), where frequent droughts in these zones have been affecting the coconut yields with most trees drying up or tipping off. The unavailability of drought resistant varieties and poor access to quality planting materials are another major hindrance to growth and productivity in the coconut industry in Kenya (Muhammed et al., 2013). Furthermore, the slow growth and long pre-breeding period of palm does not promote the genetic enhancement of coconut palm for productivity and tolerance to biotic and abiotic

*Corresponding author. Email: mauriceoyoo464@gmail.com.

Table 1. Coastal AEZ characteristics.

AEZ	Temperature (°C)	Altitude (m)	Rainfall (mm)	Natural vegetation	Number of individuals sampled
CL1	24-30	0-900	1100-2700	Moist and forest	12
CL2	24-30	0-900	1000-1600	Moist and dry forest	26
CL3	24-30	0-900	800-1400	Dry forest, moist woodland	06
CL4	24-30	0-900	600-1100	Dry woodland and highland	04

stresses (Rajesh et al., 2008). Current estimate put total number of plants in Kenyan coastal lowlands at about 4.4 million with an average nut yield of 1.5 t ha^{-1}, while that of copra is as low as 0.45 t ha^{-1}. Germplasm collections, containing significant amount of genetic diversity within and among coconut populations, are essential for an effective crop improvement programme. Therefore, the assessment of genetic diversity within coconut populations becomes increasingly significant in germplasm conservation and utilization. Since morphological characterization in the coast of Kenya has shown diversity (Oyoo et al., 2015), the coconut genetic diversity in Kenya shall provide sufficient scientific data for germplasm management and utilization. Diversity analysis in coconut palm has been done by morphological traits, biochemical and molecular markers (Rajesh et al., 2005). Morphological and biochemical markers are not desirable due to the long juvenile phase of palms, high cost of conducting investigations, long-term of field evaluation, influence of environment factors on the phenotype and limited number of available phenotypic markers (Manimekalai et al., 2006). Molecular markers, detect variation at the DNA level and are detectable at all stages of development. Since they can also cover the entire genome, DNA markers overcome most limitations of morphological and biochemical markers (Ashburner et al., 1997; Teulat et al., 2000; Upadhyay et al., 2004; Manimekalai et al., 2006). Among available molecular marker techniques, simple sequence repeat (SSR) markers provide good signal in evaluating genetic diversity and genetic relationships in plants. The increased number of coconut SSR markers greatly improves the previously established genetic relationships among coconut populations.

Three types of coconut palms have been described in Kenya, the East African tall (EAT) Dwarf types and the hybrids. The EAT yield good quality copra and toddy but with inferior coconut water as compared to the Dwarf coconut (Gethi and Malinga, 1997). Just as in Asia, the Talls are naturally cross-pollinating types, vigorous growing, comparatively late to flowering and the fruits are with intermediate colors of brown, green, yellow, orange among individual palms. Dwarfs, in contrast, are naturally self-pollinating types with reduced growth habitat, early flowering and produce large number of medium to small, distinctly colored (green or yellow or orange or brown) fruits (Dasanayaka et al., 2009). To date, little information is available on the genetic diversity among Kenyan coconut palms. For sustainable breeding, adoption and conservation *in situ*, it is important to develop a strategy to use coconut diversity for socio-economic benefits (Batugal and Oliver, 2003). In the current study, 48 coconut individuals from four administrative units of Kenyan coast were assessed using 15 SSR markers.

In Kenya, coconut is cultivated in six counties; Kwale, Kilifi, Mombasa, Tana River, Lamu and Taita Taveta. With the exception of Taita Taveta, the other five counties have a high concentration of coconut tree population and a total coastline of 640 km of the Indian Ocean. Coastal Kenya covers areas from the sea with ample amount of rainfall to the far west with 600 mm of rainfall per year, usually with poor distribution. Rainfall is bimodal with major rainy season beginning in April and lasts till July. Short rainy season is seen in October to November (Jaetzold and Schmidt, 1983). The coastal lowlands zone is divided into five sub zones called coastal lowlands (CL): Cl2-CL6. These zones are sub-divided based majorly on topography, soil and water which influence agricultural development (Jaetzold and Schmidt, 1983).

The assessment of genetic diversity and structure of germplasm is essential for the efficient organization of breeding material. The objective of this research was to estimate genetic variation of coconut germplasm in Kenyan coast and suggest how that knowledge might lay the groundwork for the genetic improvement and breeding of coconut in Kenya.

MATERIALS AND METHODS

Germplasm sampling

Coconut leaf samples were collected *in situ* and coded as previously described by Oyoo et al. (2015). Coding the palms sampled was done to reflect the county, district, division, sub division, village and the collection number. If collection was from Kilifi county, Magarini district, Magarini division, Gogoni location, Ngarite village and it was the first palm sampled, the code name given was: KLF/MAG/MAG/GOG/NGA/01. Sampling was done at different agro ecological zones (Table 1) and the GPS data was recorded. The focus was in areas where palms grown were morphologically different with a marked change in altitude or cropping systems, a formidable barrier such as a mountain or a river exists, or local people ethnically different (in terms of dialect) from previous collection site. The priority of taking sample was farmers' field while avoiding collecting duplicates. A major challenge was that farmers had no clear distinct local names for coconut at the coast and insisted '*nazi ni nazi tu*' (coconuts are just

Table 2. List of coconut-specific microsatellite primer pairs with their forward and reverse sequences.

Primer	Repeat type	F	R	Size range	Tm
CAC02	$(CA)_{15}(AG)_7$	AGCTTTTTCATTGCTGGAAT	CCCCTCCAATACATTTTTCC	225~240	49
CAC04	$(CA)_{19}(AG)_{17}$	CCCCTATGCATCAAAACAAG	CTCAGTGTCCGTCTTTGTCC	185~207	53
CAC06	$(AG)_{14}(CA)_9$	TGTACATGTTTTTTGCCCAA	CGATGTAGCTACCTTCCCC	146~164	49
CAC10	$(AG)_{13}(CA)_9$	GATGGAAGGTGGTAATGCTG	GGAACCTCTTTTGGGTCATT	156~163	53
CAC21	$(CA)_{11}$	AATTGTGTGACACGTAGCC	GCATAACTCTTTCATAAGGGA	149~151	53.7
CAC23	$(CA)_8$	TGAAAACAAAAGATAGATGTCAG	GAAGATGCTTTGATATGGAAC	170~179	53.9
CAC56	$(CA)_{14}$	ATTCTTTTGGCTTAAAACATG	TGATTTTACAGTTACAAGTTTGG	138~162	53.9
CAC68	$(CA)_{13}$	AATTATTTTCTTGTTACATGCATC	AACAGCCTCTAGCAATCATAG3	130~146	54
CAC71	$(CA)_{17}$	ATAGCTCAAGTTGTTGCTAGG3	ATATTGTCATGATTGAGCCTC3	172~283	54
CAC72	$(CA)_{18}$	TCACATTATCAAATAAGTCTCACA	GCTCTCTTTCTCATGCACA	124~132	54
CAC84	$(CA)_{13}$	TTGGTTTTTGTATGGAACTCT	AAATGCTAACATCTCAACAGC	150~163	54
CN11E6	$(CT)_{21}$	TACTTAGGCAACGTTCCATTC	TAACCAGAAAGCAAAAAGATT	85~128	50
CN1C6	$(CT)_1$`TT$(GT)_5$	AGTATGTGAGTAGGATTATGG	TTCCTTGGACCCTTATCTCTT	175~184	52
CN1H2	$(GA)_{18}$	TTGATAGGAGAGCTTCATAAC	ATCTTCTTTAATGCTCGGAGT	230~321	52
CNZ01	$(CT)_{15}(CA)_9$	ATGATGATCTCTGGTTAGGCT	AAATGAGGGTTTGGAAGGATT	109~131	52

The SSR primers were developed by Perera et al. (1999, 2000) and Teulat et al. (2000)

coconuts). In addition, the general structure of parents and progeny was a mixture in a population. Estimating the age of the population was not easy. The fields were uncultivated with low input or none at all. The collected leaf samples were labeled and stored in silicon gels.

DNA extraction

DNA was extracted from dry leaf samples using a CTAB protocol modified from the Doyle and Doyle (1990) method. The modification involved omission of the ammonium acetate step and a longer DNA precipitation time of 12 h. The quality and quantity of the extracted DNA samples were ascertained by running them on a 1% agarose gel and by using a nanodrop spectrophotometer. The DNA samples were then diluted to a working concentration of 30 ng/µl. The primer sequences and associated information are given in Table 2.

SSR markers amplification and electrophoresis

The PCR amplification was performed in a 10 µl volume mix consisting of 5 U Dreamtaq polymerase enzyme (Thermo scientific corp, Lithuania), x 6 Dreamtaq buffer (Thermo scientific corp, Lithuania), 2.5 mM of each dNTPS (Bioneer corp, Republic of Korea), $MgCl_2$, 5 µM of each primer (Inqaba biotec, S.A) and 30 ng DNA template in an Applied Biosystems 2720 thermocycler (Life Technologies Holdings Pte Ltd,Singapore). The PCR cycles consisted of initial denaturation at 94°C for 5 min followed by 35 cycles of denaturation at 94°C for 30 s, annealing at 54-59.7°C (depending on the primer), extension at 72°C for 1 min followed by one cycle of final extension at 72°C for 10 min. The amplicons were mixed with 6x Orange DNA loading dye (Thermo scientific corp, Lithuania) and separated on a 2% agarose gels (Duchefa, Netherlands) stained with Invitrogen life technologies ethidium bromide (Invitrogen corp, U.S.A) in a 0.5x TBE buffer. The separated amplicons were visualized on an Ebox-VX5 gel visualization system (Vilber Lourmat inc, France). The alleles were scored as absent or present based on the size of the amplified product using a 100 bp O'geneRuler ready to use DNA Ladder (Thermo Scientific Corp, Lithuania).

Data analysis

Cluster and principal component analyses

Genetic dissimilarities between all the germplasm was calculated using DARwin version 6.0 (Perrier et al., 2003; Perrier and Jacquemoud-Collet, 2006) using simple matching coefficient. The dissimilarity coefficients were then used to generate an unweighted neighbour-joining tree (Saitou and Nei, 1987) with Jaccard's similarity coefficient. Bootstrapping value of 1,000 was used. Principal component analyses were also estimated by using Darwin version 6.0.

Analysis of diversity parameters

The amplified SSR markers were scored as present (1) or absent (0), and then recorded into a binary matrix as discrete variables. Markers which could be amplified and interpreted consistently were omitted from the analysis. The diversity studies of the 48 coconut ecotypes (from different AEZ) were conducted using Popgene version 1.31. The following parameters were estimated: number of alleles per locus (*N*), polymorphic information content (*pic*), m* = major allele frequency, ne = effective number of alleles (Kimura and Crow, 1964), * h = Nei's (1973) gene diversity, I = Shannon's information index (Lewontin, 1972) and the percentage of polymorphic loci. Other diversity parameters measured were Ht = gene diversity in the total population, Hs = gene diversity within and between sub populations Gst = gene differentiation relative to the total population, Nm = estimate of gene flow from Gst, which in this case is equivalent to Wright F statistics (*Fst*) (Nei, 1978). Analysis of molecular variance (AMOVA) was computed using Powermarker software version 3 (Liu and Muse, 2005).

Table 3. Diversity parameters for 15 SSR loci used to analyze genetic diversity of coconut germplasm in Kenya.

Locus	Sample size	Allele no.	m*	ne*	h*	i*	PIC	Amplified bands (no.)
CAC02	48	2.0	0.8333	1.3846	0.2778	0.4506	0.2392	40
CAC04	48	2.0	0.6667	1.8000	0.4444	0.6365	0.3457	32
CAC06	48	2.0	0.8958	1.2295	0.1866	0.3341	0.1692	43
CAC10	48	2.0	0.6875	1.7534	0.4297	0.6211	0.3374	43
CAC21	48	2.0	0.9583	1.0868	0.0799	0.1732	0.0767	46
CAC23	48	2.0	0.5833	1.9459	0.4861	0.6792	0.368	28
CAC56	48	2.0	0.8125	1.4382	0.3047	0.4826	0.2583	39
CAC68	48	2.0	0.9792	1.0425	0.0408	0.1013	0.04	47
CAC71	48	2.0	0.875	1.2800	0.2188	0.3768	0.1948	42
CAC72	48	2.0	0.9167	1.1803	0.1528	0.2868	0.1411	44
CAC84	48	2.0	0.8542	1.3318	0.2491	0.4154	0.2181	41
CNZ01	48	2.0	0.6042	1.3846	0.2778	0.4506	0.3639	40
CN1C6	48	2.0	0.7708	1.5463	0.3533	0.5383	0.2909	37
CN11E6	48	2.0	0.8333	1.3846	0.2778	0.4506	0.2392	40
CN1H2	48	2.0	0.8333	1.9168	0.4783	0.6713	0.2392	29
Mean		2.0	0.8069	1.4470	0.2839	0.4445	0.2348	39.4
SD				0.288	0.137	0.173		

m* = Major allele frequency; *ne = Effective number of alleles [Kimura and Crow (1964)]. *h = Nei's (1973) gene diversity; *I = Shannon's Information index [Lewontin (1972)]; Smith et al., (1997) polymorphic information content (PIC). The number of polymorphic loci is: 15. The percentage of polymorphic loci is 100.00%.

RESULTS AND DISCUSSION

Diversity parameters

The major allele frequency value ranged from 0.5833 for CAC23 to 0.9792 for CAC68 with a mean of 0.8069 (Table 3). The number of effective alleles values ranged from 1.0425 to 1.9459 with a mean value of 1.4470. It was observed that marker CAC68 had the lowest values while marker CAC23 had the highest value. The gene diversity values ranged from 0.0408 to 0.4861 with a mean value of 0.2839. Marker CAC68 had the lowest value while marker CAC23 had the highest value, suggesting that CAC23 loci could be useful in revealing genetic diversity of coconut accessions in Kenya. This observation was also confirmed by Shannon's information index at locus CAC23 (p = 0.6792), which had the highest value as compared to the lowest value of p = 0.1013 at locus CAC68. Marker CAC23 also showed greatest PIC (0.3680%) as opposed to marker CAC68 which revealed the lowest PIC values (0.0400%). An average of 34.9 bands were amplified with the highest number of bands amplified being observed for marker CAC68. Least number of bands (29) was amplified by marker CN1H2.

The weighted average of estimated haplotype diversities in the total population (*Ht* = 0.4884) and weighted average of estimated haplotype diversities in the subpopulation (*Hs* = 0.4686) were best revealed at the CAC23 locus. The lowest (*Ht* = 0.408 and Hs=0.0382) were recorded at the CAC68 locus (Table 4). The highest gene differentiation relative to the total population studied, *Gst* = 0.2016 recorded for marker CAC04, and the lowest *Gst* = 0.0378 was recorded at CN11E6 locus. The highest estimate of gene flow from Gst, Nm = 28.0937, was recorded for marker CAC56, while the least *Nm* = 1.9801 was recorded at the CAC04 locus

Results presented in Table 5 also reveal that genetic similarity were very high in the subpopulations. It ranged from 0.9502 (genetic identity between Kilifi and Lamu counties) to 0.9891 (between Lamu and Kilifi counties). Genetic distances were very low among the subpopulations and they ranged from 0.011 (Kwale and Lamu) to 0.511 (Lamu and Kilifi).

Further, when the genetic variation of the coconut germplasm was partitioned by analysis of molecular variance (AMOVA), 2% of the variation was revealed among the germplasm that were produced within the counties (Table 6), while the within population variation was 98%, further suggesting genetic redundancy of coconut at the coastal Kenya on the basis of where grown.

Cluster analysis

The dendrogram was constructed from the genetic dissimilarities among all the individuals using DARwin 6. The 48 germplasm were clustered into three distinct groups (Figure 1). Groups II and III were further

Table 4. Nei's (1978) analysis of gene diversity in subdivided and total populations.

Locus	Sample size	Ht	Hs	Gst	Nm*
CAC02	48	0.2477	0.2208	0.1083	4.1153
CAC04	48	0.394	0.3146	0.2016	1.9801
CAC06	48	0.1665	0.1494	0.1026	4.374
CAC10	48	0.4217	0.3807	0.0972	4.6424
CAC21	48	0.0703	0.0675	0.0394	12.1961
CAC23	48	0.4884	0.4689	0.0399	12.0332
CAC56	48	0.3073	0.3019	0.0175	28.0937
CAC68	48	0.0408	0.0382	0.0638	7.3333
CAC71	48	0.2491	0.2315	0.0707	6.5759
CAC72	48	0.1298	0.1253	0.0352	13.6981
CAC84	48	0.2156	0.2041	0.0533	8.8874
CNZ01	48	0.4639	0.4334	0.0657	7.1065
CN1C6	48	0.3567	0.3315	0.0705	6.592
CN11E6	48	0.2874	0.2765	0.0378	12.714
CN1H2	48	0.2491	0.2049	0.1777	2.3137
Mean	48	0.2726	0.25	0.0829	5.5296
St. Dev		0.0186	0.0159		

Ht = Gene diversity in the total population; Hs = gene diversity within and between sub populations; Gst=gene differentiation relative to the total population; Nm = estimate of gene flow from Gst.

Table 5. Genetic identity (above diagonal) and genetic distance (below diagonal).

Population ID	Kilifi	Kwale	Lamu	Tana River
Kilifi	****	0.9563	0.9502	0.9638
Kwale	0.0447	****	0.9891	0.9697
Lamu	0.0511	0.011	****	0.9565
Tana River	0.0369	0.0308	0.0445	****

Table 6. Analysis of molecular variance (AMOVA) for 48 coconut individuals sampled from four counties of the coastal lowlands of Kenya.

Source	df	SS	MS	Est. Var.	%
Among populations	3	7.871	2.624	0.042	2
Within populations	44	94.317	2.144	2.144	98
Total	47	102.188		2.185	100

subdivided into two groups with one sub group in group III consisting of solely collections from Kilifi County. The dendrogram revealed that materials sampled from same counties were not assigned to the same group. Group I consisted of only two germplasm lines from Kilifi; KLF/MAG/MAG/NGA/02 and KLF/MAL/MAL/GED/CHA/03. Group II was composed of germplasm sampled from Lamu county and a few materials from Kwale and three from Kilifi. Only one material, TR/TD/KIP/KIP/WAK/34 from Tana River clustered in this group, while the rest of materials from this county were clustered in group III. Group III consisted of germplasm from all the four counties; however samples from Kilifi formed the majority with up to six samples all clustering from node 76 to 80. Clustering failed to group the germplasm solely on the basis of the origin.

Principal coordinate analysis (PCoA) (Figure 2) was carried out to determine genetic relationship among the coconut germplasm studied. The first three axes accounted for the majority of total cumulative variation (61.64%) (Table 7) with the three axes accounting for

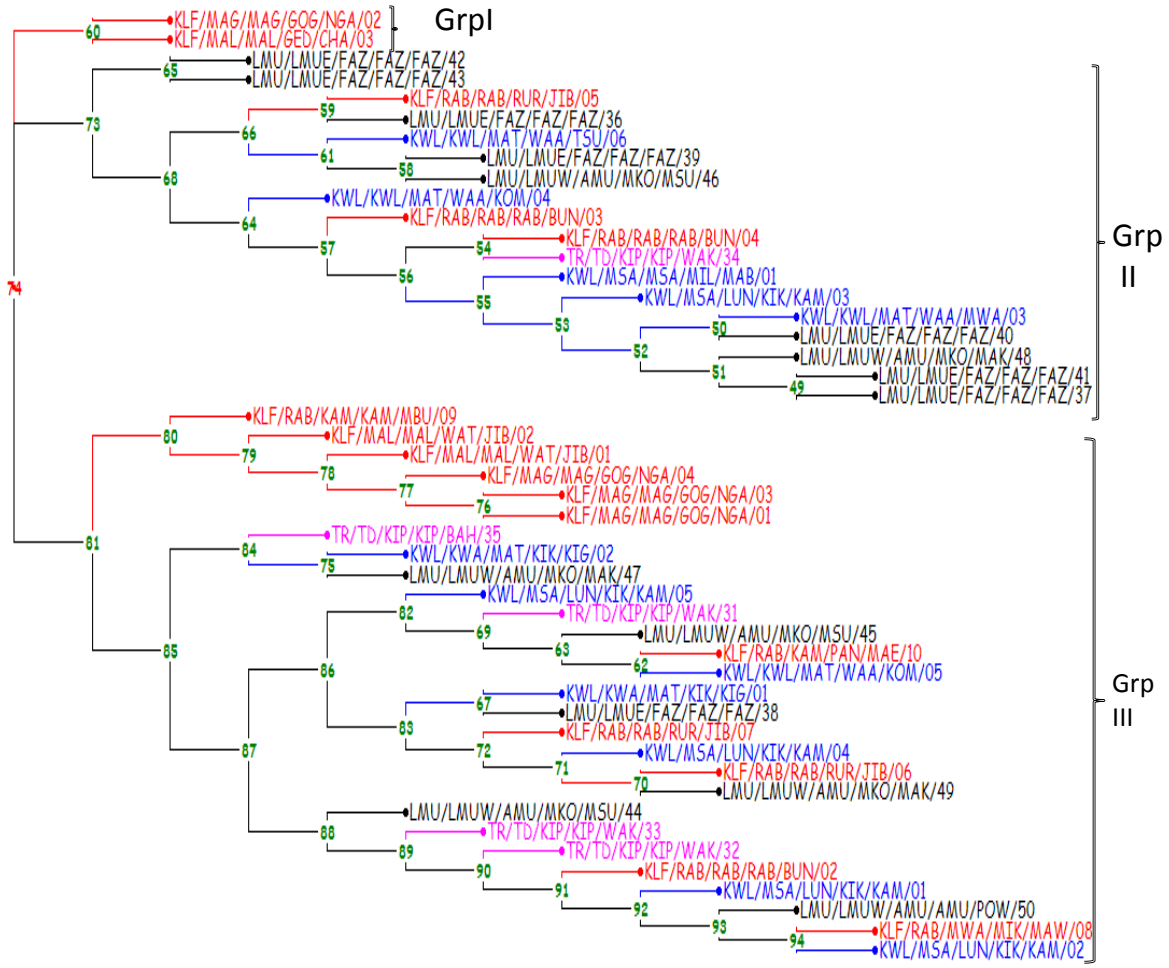

Figure 1. Dendrogram based on genetic dissimilarities between 48 individuals sampled at the Kenyan coast. Numbers represent bootstrap confidence limits for 1000 replicates.

37.61, 14.02 and 10.02%, respectively. Individual counties total cumulative percent variations were higher than the overall trial percent cumulative variation. Total cumulative variation was highest in Tana River (97.88%); and it was explained by only two axes. The county was followed by Lamu (91.15%), Kwale (90.51%) and Kilifi (90.19%) in that order. These results could be corroborated by results (Figure 2) that shows that germplasm did not cluster around each other in Tana River. Coconut is an important tropical economic crop, but not many studies have been conducted in relation to diversity based on molecular markers. Due to a lack of available molecular markers, Akpan (1994) and Sugimura et al. (1997) indicated that previous assessment and characterization of coconut germplasms relied mostly on morphological and agronomic traits. However, these traits do not generally provide an accurate measure of genetic diversity, because many show complex inheritance and are easily influenced by the external environment. To mitigate, this problem (Rivera et al., 1999) described the development and characterization of microsatellite markers for *Cocos nucifera* using genomic-SSR hybrid screening. Recently, Xiao et al. (2013) used computational methods to utilize sequence information from next-generation sequencing as described by Fan et al. (2013) to develop SSR markers.

UPGMA dendrogram was drawn to visualize relationships among 48 coconut studied. The dendrogram of cluster analysis of individuals clearly illustrated population structure of the tested varieties. It showed the presence of subpopulations in all the cluster and different levels of similarity between the localities. It however failed to cluster germplasm per counties grown as expected. This could be as a result of farmers exchanging planting materials within the coastal Kenya. As described by Aremu et al. (2007), principal component analysis (PCA) reveals the pattern of character variation among genotypes. In this study, PCA failed to cluster coconut materials based on their counties where they are grown. This could be explained by the low coefficient of

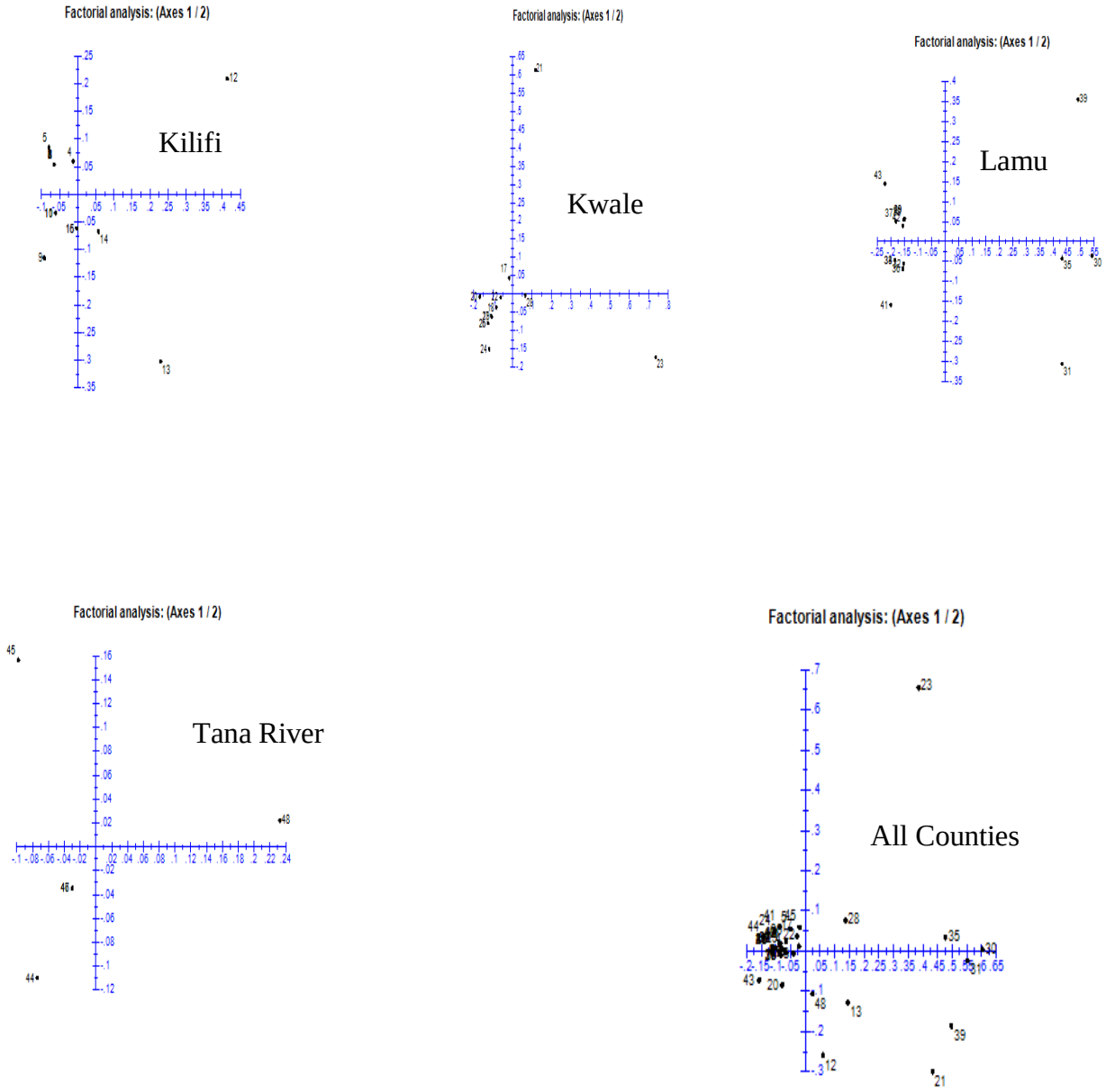

Figure 2. PCoA of axes 1 and 2 based on dissimilarity of 15 loci across 48 coconut individuals from different counties.

variation realized in coconut at the Coastal Kenya, probably suggesting high level of genetic similarity and very low genetic distances as shown in Table 6. This conclusion could also be deduced from the analysis of molecular variance (Table 7), which suggested that more variation existed within individual coconut as opposed to among groups based on the areas where they are produced.

PIC provides an estimate of discriminatory power of a marker by taking into account not only the number of alleles at a locus, but also their relative frequencies. Table 4 shows that loci CAC23 (0.368), CAC10 (0.3374), CCZ01 (0.3639) and CAC04 (0.3457) revealed a higher PIC levels than other loci, indicating that these primers are suitable for detecting the genetic diversity of coconut accessions in Kenyan Coast These markers also revealed a higher weighted average of estimated haplotype diversities in the total population (*Ht*). The *Ht* values for these markers as compared to others are relevant in view of the fact that there are only two alleles per locus. Furthermore, SSR analysis also showed that the mean gene flow, *Gst* of coconut in Kenya was 0.0829, suggesting that the gene exchange between individuals was minimal. Based on the fact there are

Table 7. Eigen value and percentage of total variation accounted for by the first three principal component axes.

Axis	Eigen value	Proportion (%)	Cumulative (%)
Kilifi County			
1	0.01721	48.65	48.65
2	0.01191	33.68	82.33
3	0.00278	7.86	90.19
Kwale County			
1	0.05584	46.56	46.56
2	0.03757	31.33	77.89
3	0.01513	12.62	90.51
Lamu County			
1	0.08289	68.27	62.27
2	0.1956	16.11	84.38
3	0.0822	6.77	91.15
Tana River County			
1	0.1422	62.93	62.93
2	0.0079	34.95	97.88
All Counties			
1	0.03838	37.61	37.61
2	0.01429	14.01	51.62
3	0.01023	10.02	61.64

only two alleles per locus in this study, *Gst* is identical to *Fst*, Wright F statistics. *Gst* is indepen-dent of gene diversity within subpopulation and can be used to compare differentiation in different organisms. For this reason, *Hs* could be very small but the absolute *Gst* is small. Genetic analysis (Table 6) also revealed that these genetic similarities were very high while genetic distances were very low. This is an indication that coconuts within a region were not genetically diverse from those of the other regions. Coconut germplasm were sampled from random mating groups or individuals, thus gene diversity may be replaced with heterozygosity while gene identity may be referred to as homozygosity.

Conclusion

Coconut sampled from different ecological zones failed to cluster per county or AEZ from where they were sampled. Molecular variability within the individuals was high while within individuals was low. This is an indication of the narrow genetic diversity in Kenya. Coconut breeding scheme should therefore be initiated to enhance variability. Such a scheme should include introductions from other areas while conserving the Kenyan coconut germplam for future crop improvement.

Conflict of interests

The authors have not declared any conflict of interest.

ACKNOWLEDGEMENT

The authors are greatly indebted to the National Council for Science, Technology and Innovation (NACOSTI) Kenya for the financial support AND Kenya coconut Development Authority (KCDA) for the collection of the coconut samples.

REFERENCES

Akpan EEJ (1994). Evaluation of tall coconut (*Cocos nucifera* L.) genotypes within the Nigerian coconut germplasmbank. Oleagineux. 49:13-20.

Aremu CO, Adebayo MA, Ariyo OJ, Adewale BB (2007). Classification of genetic diversity and choice of parents for hybridization in cowpea *Vigna unguiculata* (L.) Walp for humid savanna ecology. Afr. J. Biotechnol. 6(20):2333-2339.

Ashburner GR, Thompson WK, Halloran GM (1997). RAPD analysis of South Pacific coconut palm populations. Crop Sci. 37(3):992-997.

Batugal P, Oliver JT (2003). Poverty reduction in coconut growing communities, vol.I: The Framework and Project Plan, International Plant Genetic Resources Institute Regional Office for Asia, the Pacific and Oceania (IPGRI-APO), Serdang, Selangor, Malaysia. pp. 1-350.

Dasanayaka PN, Everard JMDT, Karunanayaka EH, Nandadasa HG (2009). Analysis of coconut (*Cocos nucifera* L.) diversity using microsatellite markers with emphasis on management and utilization of genetic resources. J. Natl. Sci. Found. 37:99-109.

Doyle JJ, Doyle JL (1990**)**. Isolation of plant DNA from fresh tissue. Focus. 12:13-15.

Fan H, Xiao Y, Yang Y, Xia W, Mason AS, Xia Z, Qiao F, Zhao S, Tang H (2013). RNA-Seq Analysis of *Cocos nucifera*: Transcriptome sequencing and *De Novo*assembly for Subsequent Functional Genomics Approaches. PLOS ONE 8:e59997.

Gethi JG, Malinga WK (1997). Kenya Coconuts: Present Past and Future: Pp155-158. In: CP Topper. PDS Caligari, AK Kallaya, SH Shomari, PAL Masawe and A. Mpunani (Eds). Proceedings of the International Cashew and Coconut Conference: 'Trees for Life-Key to development'. Bio-Hybrids International, Reading, UK.

IPGRI (1995**)**. Descriptors for Coconut (*Cocos nucifera* L.). International Plant Genetic Resource Institute, Rome, Italy.

Jaetzold R, Helmut S (1983). Farm Management Handbook of Kenya*.* 4 vols. Nairobi: Kenya Ministry of Agriculture.

Kimura M, Crow JF (1964). The number of alleles that can be maintained in a finite population. Genetics 49:725-38.

Lewontin RC (1972). Testing the theory of natural selection. Nature 236:181-182.

Lewontin RC (1972**)**. The apportionment of human diversity. Evol. Biol. 6:381-398.

Liu K, Muse SV (2005). Power Marker: an integrated analysis environment for genetic marker analysis. Bioinform. 21:2128-2129.

Manimekalai R. Nagarajan P (2006). Assessing genetic relationships among coconut (*Cocos nucifera* L.) accessions using inter simple sequence repeat markers. Sci. Hort. 108:49-54.

Manimekalai R, Nagarajan P (2007). Use of Simple Sequence Repeat markers for estimation of genetic diversity in coconut (*Cocos nucifera* L.) germplasm accessions, J. Plant Biochem. Biotechnol. 16(1):29-33.

Muhammed N, Nyamota R, Hashim S, Malinga JN (2013). Zygotic embryo *in vitro* culture of *Cocos nucifera* L. (sv. East African Tall variety) in the coastal lowlands of Kenya. Afr. J. Biotechnol. 12(22):3435-3440.

Nei M (1973). Analysis of gene diversity in subdivided populations. Proc. Natl. Acad. Sci. USA 70:3321-3323.

Nei M (1978). Estimation of average heterozygosity and genetic distance from a small number of individuals. Genetics. 89(3):583-90.

Oyoo ME, Muhammed N, Githiri SM, Ojwang PO, Muniu FK, Masha E, Owuoche J (2015). *In-situ* morphological characterization of coconut in the coastal lowlands of Kenya. Afr. J. Crop Sci. 9(2):65-74.

Perera L, Russell JR, Provan J, Powell W (2000). Use of microsatellite DNA markers to investigate the level of genetic diversity and population genetic structure of coconut (*Cocos nucifera* L.). Genome 43(1):15-21.

Perera L, Russell JR, Provan J, Powell W (1999). Identification and characterization of microsatellites in coconut (*Cocos nucifera* L.) and the analysis of coconut population in Sri Lanka, Molecular. Ecology 8(2):344-346.

Perrier X, Jacquemoud-Collet JP (2006). DARwin software.

Rajesh MK, Arunachalam V, Nagarajan P, Lebrun P, Samsudeen K, Thamban C (2008). Genetic survey of 10 Indian coconut landraces by simple sequence repeats (SSRs). Scientia Horticulturae 118(4):282-287.

Rajesh MK, Sabana AA, Rachana KE, Shafeeq Rahman, Jerard BA, Anitha K (2005). Genetic relationship and diversity among coconut (*Cocos nucifera* L.) accessions revealed through SCoT analysis. 3 Biotech. 5(6):999-1006.

Rivera R, Edwards KJ, Barker JHA, Arnold GM, Ayad G, Hodgkin T Karp A (1999). Isolation and characterization of polymorphic microsatellites in *Cocos nucifera* L. Genome.42:668-675.

Smith J, Chin E, Shu H, Smith O, Wall S, Senior M, Mitchell S, Kresovich S and Ziegle J (1997). An evaluation of the utility of SSR loci as molecular markers in maize (*Zea mays* L.): Comparisons with data from RFLPs and pedigree. Theor. Appl. Genet. 95:163-173.

Sugimura Y, Itano M, Salud CD, Otsuji K, Yamaguchi H (1997). Biometric analysis on diversity of coconut palm: cultivar classification by botanical and agronomical traits. Euphytica 98:29-35.

Teulat B, Aldam C, Trehin R, Lebrun P, Barker JHA, Arnold GM, Karp A, Baudouin L, Rognon F (2000). An analysis of genetic diversity in coconut (*Cocos nucifera* L.) populations from across the geographic range using sequence-tagged microsatellites (SSRs) and AFLPs, Theor. Appl. Genet. 100(5):764-771.

Upadhyay A, Jayadev K, Manimekalai R, Parthasarathy VA (2004). Genetic relationship and diversity in Indian coconut accessions based on RAPD markers. Sci. Hortic. 99(3-4):353-362.

Xiao Yong, YiLuo, YaodongYang, HaikuoFan,Wei Xia, Annaliese S. Mason, SonglinZhao, Ross Sager FeiQiao (2013**)**. Development of microsatellite markers in *Cocos nucifera* and their application in evaluating the level of genetic diversity of *Cocosnucifera.* Plants Omics J. 6(3):193-200.

academicJournals

Vol. 15(40), pp. 2224-2233, 5 October, 2016
DOI: 10.5897/AJB2016.15418
Article Number: A542F8260840
ISSN 1684-5315

http://www.academicjournals.org/AJB

African Journal of Biotechnology

Full Length Research Paper

Evaluation of various pesticides-degrading pure bacterial cultures isolated from pesticide-contaminated soils in Ecuador

Pérez Mónica[1]*, Rueda O. Darwin[2], Bangeppagari Manjunatha[2], Johana J. Zúñiga[2], Ríos Diego[2], Rueda B. Bryan[3], Sikandar I. Mulla[4] and Naga R. Maddela[5]

[1]Faculty of Environmental Engineering in Prevention and Remediation, Ministry of Environment, Universidad de las Américas-UDLA, Quito, South America, Ecuador.
[2]Department of Life Sciences, Universidad de las Fuerzas Armadas-ESPE, Sangolquí- P. O. Box: 171-5-231B, South America, Ecuador.
[3]Faculty of Biotecnology, Universidad de las Américas -UDLA, Quito, South America, Ecuador.
[4]Department of Biochemistry, Karnatak University, Dharwad, Karnataka, India.
[5]Department of Environmental Engineering, Universidad Estatal Amazonica, Puyo, South America, Ecuador.

Received 18 April, 2016; Accepted 19 September, 2016

Due to the intensive use of pesticides within the greenhouse-rose production, remediation of polluted soils has become a hot topic for researchers in recent decades. Several bacterial strains having the ability to utilize various pesticides as a sole source of carbon and energy were isolated from pesticide-contaminated soils of Urcuquí, Ecuador. According to phenotypical, physiological, and biochemical characterizations, and 16S rRNA gene sequence analysis, the isolated pure bacterial cultures were identified as *Pseudomonas putida* sp. strain B1, *Acinetobacter* sp. strain B2 and *Arthrobacter* sp. strain B3. The bacterial isolates were used individually and mixed cultures were used in the laboratory and field experimentations for the degradation of various pesticides like Ridomil MZ 68 MG, Fitoraz WP 76, Cleaner, Decis 2.5 CE, Score 250 EC, Zero 5 EC, Bravo 720 SC, Meltatox, Mirage 45 CE and Teldor Combi at 50 mgL^{-1}. The bacterial growth was monitored on both liquid culture medium (in laboratory) and field experiments by spectrophotometer method, *Neubauer camera* and colony-forming units. In addition, the degradation of individual pesticides (50 mgL^{-1}) was determined by ultra-high performance liquid chromatography-tandem mass-spectrometry and UV-VIS spectrophotometer. The results showed that the highest growth rate of microbial consortium was observed during degradation of various pesticides than individual pure bacteria for both experiments. In addition, most pesticides were completely degraded by microbial consortium after 60 days.

Key words: Bioremediation, spectrophotometer, bioreactors, pesticides, consortium.

INTRODUCTION

In Ecuador, flower farming was started with a non-surpassing area of 30 hectares in 1970. This is how Ecuadorian valleys were devoted to the diversification of flowers which intern changing the old existing landscape for greenhouse production systems, focused on enhancing the production of flowers (Lopez, 2011). This enhancement turned out to be such a profitable business that led to the beginning of Ecuadorian flower exportation

in 1985. However, like any high-production crop, floriculture requires intensive farming which along with monocultural systems, may lead to pests and diseases outbreaks. This is why pesticides are required in flower cultivation to counter any diseases or pests (Seoanez et al., 2004). These pests can potentially cause damage during storage, transportation or commercialization of roses. Furthermore, pesticides are used during most phases of rose-cultivation to minimize any pest infestation, and there by protect crops from any potential yield losses or reduction of product quality (Hernandez and Hansen, 2010).

Despite the beneficial impacts that pesticides have, such as subduing pest infestation to stabilize and improve agricultural productivity, overusing them may lead to the contamination of agricultural land, water, crops, and adversely end up affecting non-target organisms (Gooty et al., 2015; Xiao et al., 2013). Toxic chemical use in soils represents a serious threat to the health of human beings, animals and aquatic systems around the globe. Subsequently, it makes both publicly and scientifically concerns become noticeable all over the world (Aparicio, 2015).

Bioremediation is an eco-friendly and cost-effective method, that involves use of microorganisms, such as bacteria and fungi, to degrade or mineralize the hazardous/toxic chemicals which might be harmful to the environment (Mulla et al., 2012). Hence, in this technique, the organisms break down the toxic substances in the presence of enzymes, turning them into absorbable energy and nutrients for their growth, nowadays, this biological remediating method has become widely used.

The isolation of microorganisms involved in pesticide/ fungicide degradation has been broadly described in the literature (Megadi et al., 2010a, b; Yu et al., 2013; Tallur et al., 2015). In several cases, a prevailing microorganism is likely to have a key role in the degradation process (Wang et al., 2010). In other instances though, such as the well-known case of the Carbendazim fungicide, a variety of microorganisms has been known to be isolated as degraders (Zuniga, 2015). These microorganisms show high efficiency as pesticide-degraders. Keeping in view of this, the present study was focused on the isolation and characterization of bacterial cultures having the ability to degrade the most commonly-used pesticides in flower farming.

MATERIALS AND METHODS

Chemicals

Several pesticides, such as Ridomil MZ 68 MG (64% Mancozeb + 4% Metalaxil) by Sygenta, Fitoraz WP 76 (6% Cymoxanil + 70% Propineb) by Bayer Crop Science, Cleaner (180 g/L Cyhalofop Butyl) by Consul LMZ, Decis 2.5 EC (2.8% Deltamethrin) by Bayer Crop Science, Score 250 EC (23.5% Difenoconazole) by Sygenta, Zero 5 EC (50 g/L Lambda cyhalothrin) by Ecuaquimica, Bravo 720 SC (72% clorotanonil) by Sygenta, Meltatox (425 g/L Acetato de Dodemorph) by Basf, Mirage 45 CE (45% Prochloraz) by Proficol Andina, Teldor Combi (350 g/L Fenhexamid + 66.7 g/L Tebuconazole) by Bayer Crop Science were used in this study.

Table 1. Physicochemical properties of the soils.

Properties	Sample soil
Texture	Sandy-clay
pH (in H_2O)	7.2
Organic matter (%)	6.8
Ion exchange capacity (meq/100 g)	19.2
Electrical conductivity (mS/cm)	0.31
Nitrates (NH_3)	37.1
Phosphates (PO_4)	19.1
Chlorides (Cl^-)	8.7

Agroprojekt, consultancy and Laboratory services, 2012.

Soils

The pesticide-contaminated soil samples were collected from pencaflor floricultural farm, located in Urcuquí, province of Imbabura, Ecuador. Latitude: 0° 22' 31.0906 "; Length: - 78° 13' 54.4923 "; altitude: 2149.00 m; area: 17UTM to a depth of 20 cm, air dried at room temperature before use. Physico-chemical characteristics of the soil samples were analyzed by standard methods (Agroprojekt, 2012) and are shown in Table 1.

Observation of microorganisms in soil samples under the microscope

In order to observe the microorganisms present in the soil samples, microscopic observation was performed. Four small parts of the soil samples were taken and placed in test tubes containing 1 ml of sterilized distilled water and tightly covered by aluminum foil. The sample was homogenized by vortex at a rate of 600-revolution-per-minute for 60 s. An aliquot was further observed by microscope.

Experimental design and soil incubation studies

Isolation of microorganisms

In order to isolate the microorganisms capable of degrading various pesticides by enrichment technique, the following protocol was adopted, 20 mg of soil samples were placed into 10 Petri plates, one for each pesticide (50 mg L^{-1}). The soils were supplemented with the pesticides dilution. The Petri plates were incubated at 50°C for 24 h under sterilized condition. 2 mg soil sample were taken from Petri plates and placed in a clean and sterilized test tube with

*Corresponding author. E-mail: monygp_804@hotmail.com.

appropriate distilled water (sterilized), mixed and filtered. The few micro liters of filtrate was cultivated onto pesticide (50 mg L^{-1})-mineral-salts agar plates and incubated at 30°C for 3 days. The well grown different colored colonies were picked and transferred for further purification on pesticide-mineral salts agar plates. The bacterial strains (B1, B2 and B3), which are capable of utilizing pesticides as a sole carbon and energy source, were isolated from soils samples taken for the production of roses.

Microorganisms identification

The purified organisms were determined by their physiological as well as morphological characterizations and then biochemical tests. The morphology of the isolated colony was monitored for 3 days at 25°C after incubation, by using light microscopy on mineral salt medium plates with pesticides. Cells were stained according to the classical Gram-stain procedure. Oxidase activity was determined according to Garcia et al. (2010). Catalase activity was determined as described by Rodriguez and Gamboa (2009). Fermentation of glucose, King B and Indol tests were performed according to methods described by Faddin (2007).

Growth of microorganisms

Microbial counts in liquid culture

The experimental study of Mendoza et al. (2011) was adapted with little modification in the present study. In order to examine the bacterial growth, 150 ml of sterilized minimal salts medium (K_2HPO_4, 3 g; KH_2PO_4, 0.5 g; $(NH_4)_2SO_4$, 1.25 g; NaCl, 0.01 g; $MgSO_4$, 0.1 g; $FeSO_4.7H_2O$, 0.001 g for each liter) (pH 7.0) containing 79 µl of pesticides (50 mg L^{-1}) was transferred into sterilized flasks. Further, each flask were inoculated separately with approximately 27 µl of *Pseudomonas*, 2.7 µl of *Acinetobacter*, 28 µl of *Arthrobacter* and 2.8 µl of bacterial consortium (*Pseudomonas* + *Acinetobacter* + *Arthrobacter*, 1:1:1 ratio), in order to reach biomass level of CFU = 100000. All the flasks were incubated in a rotary shaker at 90 rpm and 25°C under dark condition and the samples were withdrawn at different intervals like 15, 30, 45 and 60 days, respectively, to measure growth rate of the organisms. The calculation of the pesticide was taken into account in the dosage of the pencaflor for the treatment of disinfection of roses.

Microbial counts in solid cultures

150 g of soil samples were weighed and autoclaved so that examination of material growth found in soils is achieved. The sample then was dried at 450°C for 24 h. The soil subsequently, was placed in a polypropylene flask. 10 ml of sterilized mineral-salts-medium (pH 7.0) was supplemented with 50 mg L^{-1} of pesticides as the sole source, according to the humidity loss. Each flask was inoculated with a suspension of 27 µl of *Pseudomonas putida* sp. strain B1, 2.7 µl of *Acinetobacter* sp., 28 µl of *Arthrobacter* sp. and 2.8 µl of bacterial consortium (*P. putida* + *Acinetobacter* sp. + *Arthrobacter* sp.), in order to reach biomass level of CFU= 100000. All the flasks were incubated into an automated greenhouse at 21.1°C having 54.4% of humidity. By utilizing the spectrophotometry method, the bacterial quantification process was performed. Three repetitions per treatment were employed.

Chromatography for determination of pesticides in cultures

The residual analysis of pesticides degradation were performed for both liquid and soils samples. All the treatments were replicated three times, samples were collected on 0 day and subsequently at 1, 15, 30, 45, 60 days after inoculation. For Score, Teldor, Mirage, Cleaner, Bravo and Ridomil, the measurement was performed following an ultra-high performance liquid chromatography-tandem mass-spectrometry (LC–MS/MS). Chromatographic separation was achieved by Agilent C_{18} column. The mobile phase contained the solvent A: H_2O/0.1% formic acid and solvent B acetonitrile/0.1% formic acid in a composition of 95% solvent A in 5% Solvent B at a flow rate of 0.20 mL/min. For Decis and Zero pesticides, the mobile phase was: water/methanol 90:10 with 5 mM ammonium formate at a flow rate of 400 µl/min. The retention time were: Score (8.35 min), Teldor (Fenhexamid 7.04 min + Tebuconazole 7.8 min), Mirage (8.29 min) and Ridomil (6.13 min), Cleaner (8.2 min), Bravo(2.3 min), decis (15 min), Zero (15 min). On the other hand, for the pesticides Fitoraz and Metatox, UV-VIS spectrophotometer was used, the wave length of maximum absorption used was 284-293 nm according to the pesticide.

RESULTS AND DISCUSSION

Identification of microorganisms

The bacterial cultures were isolated from soil samples by enrichment with pesticides (Ridomil, Cleaner, Decis, Meltatox, Mirage, Bravo, Zero, Fitoraz, Score and Teldor) as a sole source of carbon and energy. The three strains were characterized by their cultural, morphological and biochemical properties. The B1 strain is Gram negative, aerobic, shows catalase, oxidase and King B test positive, while glucose and Indol production turned out negative. The B2 strain is Gram negative, aerobic, catalase and King B test was positive, while the oxidase, glucose fermentation, Indol was negative. The B3 strain is Gram positive, aerobic, catalase, oxidase and King B test were positives, while glucose fermentation and Indol were found to be negatives. The isolates were further identified by phylogenetic analysis based on 16S rRNA gene sequences (Figure 1). The complete sequence of 16S rRNA gene of the isolated organisms (B1, B2 and B3) was determined. Analysis of sequences was done at NCBI, where relevant sequences were downloaded for further analysis in order to identify the isolates (Mulla et al., 2011). The isolate strain B1 was identified as *P. putida*, strain B2 as *Acinetobacter* sp. and strain B3 as *Arthrobacter* sp.

Growth of microorganisms

Microbial measurement in liquid culture

The growth of *Acinetobacter*, *Arthrobacter*, *Pseudomonas* and bacterial consortium showed similar growth rate in the presence of 10 different pesticides in the liquid culture media. By utilizing the SPSS Statistics software package, the data was evaluated with a 95% confidence interval using a marginal means analysis. The analysis showed that microbial consortium had reached the highest cell proliferation rate on the liquid media containing various

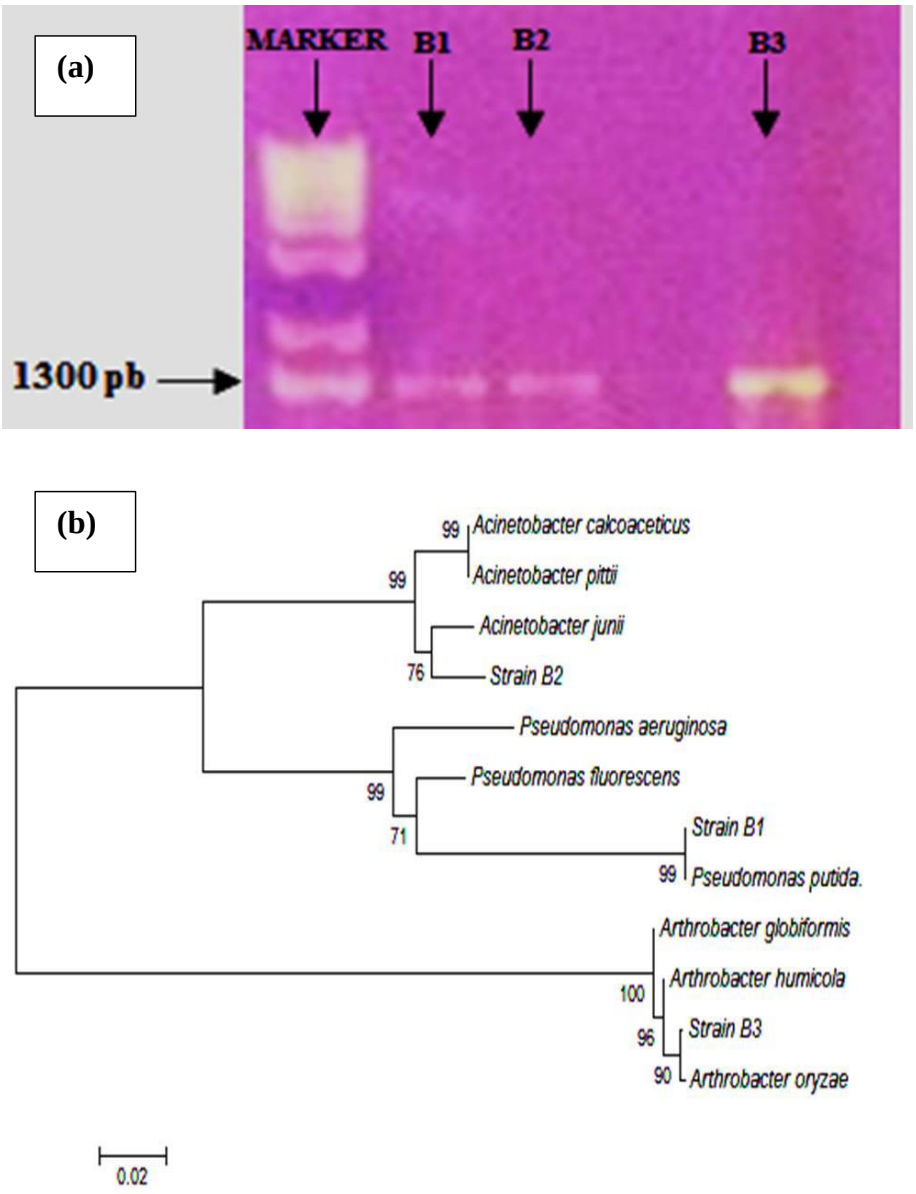

Figure 1. Agarose gel electrophoresis of 16S rDNA gene amplified from the isolate B1, B2 and B3 (a). Neighbour joining tree, based on 16S rRNA gene sequences, showing the phylogenetic relationships among the B1, B2 and B3 strains, along with their closest relatives (b). The Bootstrap values (expressed as percentages of 1000 replications), which surpassed the 50%-range, are shown at branch point. The bar indicates a 2%-sequence divergence (b).

pesticides like Ridomil, Bravo, Cleaner, Mirage, Score and Teldorat (50 mg L^{-1}). Following *P. putida* strain B1, this showed the highest microbial growth on Decis and Zero pesticides (50 mg L^{-1}). *Acinetobacter* sp. strain B2 showed high growth rate on Mitaraz and Meltatox (50 mg L^{-1}), whereas *Artrobacter* sp. strain B3 showed the lowest bacterial growth on the studied pesticides. Number of colonies of consortium reached a maximum of 8.40 $\log_{10}$ CFU mL^{-1} on 30th day. After 30th day, all three strains and consortium decreased in growth rate (Figure 2).

Microbial measurement in solid culture

The solid phase showed a higher bacterial growth rate than the liquid phase. At day 15, strains B1, B2, B3 and consortium were inoculated in the autoclaved soils, the bacterial consortium of colonies reached highest rate of 9 $\log_{10}$ CFU g^{-1}. Further, all three strains and consortium decreased in growth rate. Results indicated that *P. putida* strain B1, *Acinetobacter* sp. strain B2, *Arthrobacter* sp. strain B3 and consortium exhibited similar population

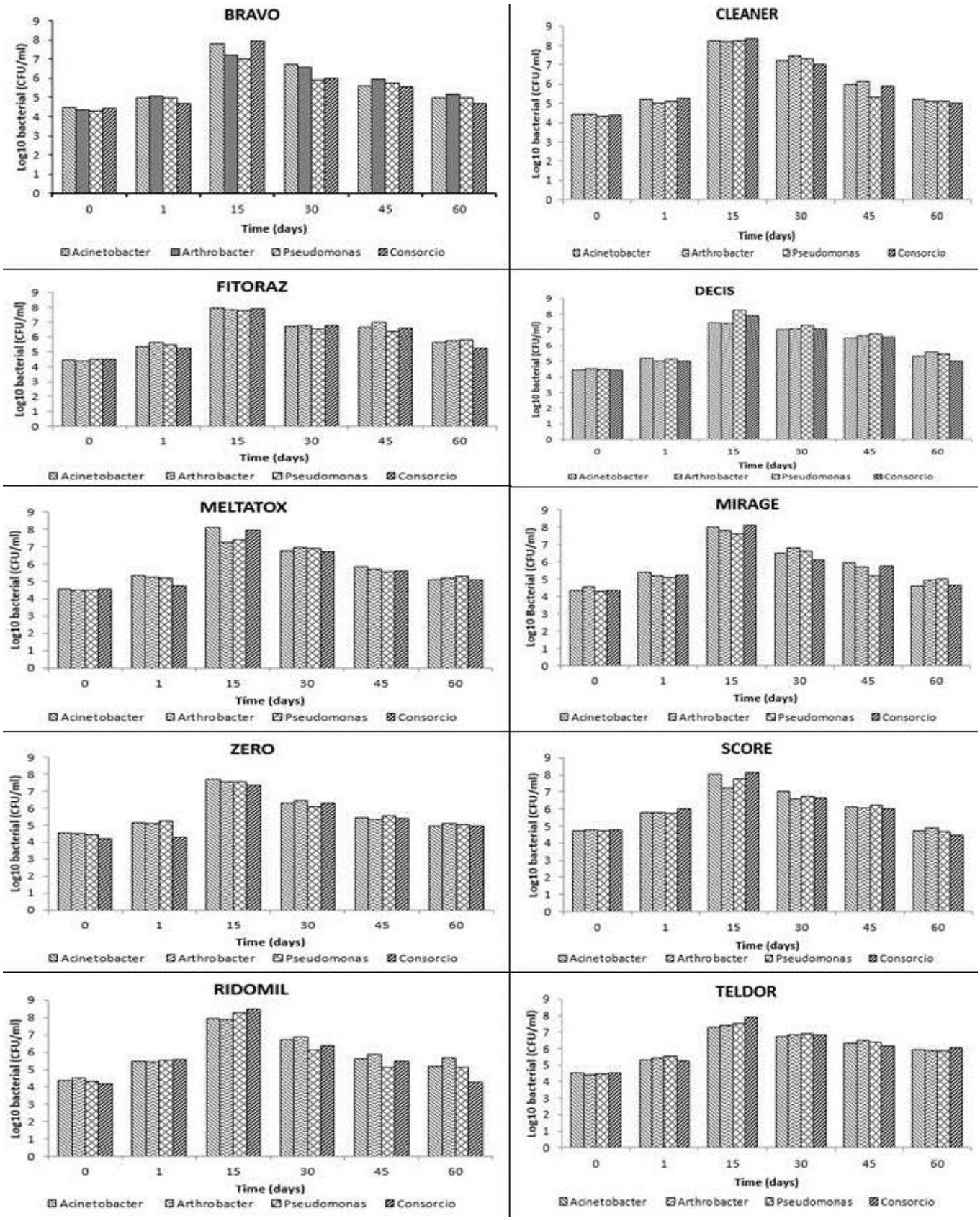

Figure 2. *Acinetobacter*, *Arthrobacter*, *Pseudomonas* and bacterial consortium growth of in liquid culture incubated at 25°C at 90 rpm in the presence of 10 different pesticides.

dynamics throughout the time of study (Figure 3). In solid culture, the bacterial consortium showed the highest growth rate on Ridomil, Bravo, Mirage, Cleaner, Score, Teldor, Fitoraz pesticides than individual pure cultures. The controls did not show a significant growth.

Degradation of pesticides

The growth of the bacterial cultures such as strains B1, B2, B3 and consortium on various pesticide-solid phase, confirmed a pesticide concentration reduction. The solid media showed higher cell proliferation rate in contrast to the liquid media.

The ability of *P. putida* sp. strain B1, *Acinetobacter* sp. strain B2, *Arthrobacter* sp. strain B3 and consortium to degrade different pesticides in solid media is shown in Figure 4. The organisms were able to use the 10 different pesticides as a sole carbon source. Additionally, the consortium managed to grow and had better degrading-pesticide ability than pure bacterial strains.

LC-MS/MS and spectrometer analysis indicated pesticides, such as Ridomil, Bravo, Mirage, Cleaner, Score and Fitoraz could no longer be detected after 30 days of incubation in the consortium culture filtrates. Teldor was degraded up to 93% by the bacterial consortium. Meltatox and Zero were degraded upto 98% rate by *Acinetobacter* sp., Decis was degraded up to 98% by *P. putida* sp, while the *Artrobacter* sp. isolate only degraded at 94% after a 30-day incubation period in all the treatments. In all the controls without the isolates, the hydrolysis percentages of pesticides were less than 15%. As compared to the controls without inoculation, degradation of all pesticides was enhanced obviously by the addition of isolates.

The *Pseudomonas* species has shown high metabolic adaptability to several toxic pollutants such as mancozeb (Pirahuata et al., 2006), metalaxyl (Massoud et al., 2008), methyl parathion, endosulfan, dimetoato, malation (Hussaini et al., 2013); parathion (Rosenberg and Alexander, 1979), monocrotophos (Bhadbhade et al., 2002a), lambda cyhalothrin (Manigandan et al., 2013), cymoxanil (Derbalah and Belal, 2008), cyhalop of butyl (Nie et al., 2011), chlorothalonil (Wang et al., 2011), and also consortium of *Pseudomonas* reduced Chlorothalonil (Rios and Penuela, 2015). However, there is no report on degradation of propineb, deltamethrin, dodemorph acetate, prochloraz, fenhexamid or tebuconazole by *Pseudomonas* sp. The present study indicates that *P. putida* strain B1 was able to show a higher degradation ratio in pesticides such as Meltatox, Fitoraz, Decis, Mirage and Teldor.

There are studies on the use of *Acinetobacter* to degrade pesticides such as atrazine (Pooja et al., 2004), methilparation (Liu et al., 2007), chloroanilines (Hongsawat and Vangnai, 2011), malation (Ahmed et al., 2015) and metalaxil (Zuno-Floriano et al., 2012). However, no studies mention the use of *Acinetobacter* to degrade pesticides such as mancozeb, cyhalopof butyl, deltamethrin, difenoconazole, lambda cyhalothrin, clorotanolil, dodemorph acetate, prochloraz or mixed-up pesticides (Fitoraz, Teldor). In strain B2, the rate degradation of various pesticides reached between 90 and 98% (Figure 4). *Acinetobacter* degrade 98% of dodemorph acetate and lambda cyhalothrin than strain B1, strain B3 and consortium. However, *Acinetobacter* sp. strain B2 showed the lowest degrading rate only up to 90% of Teldor.

There are reports on the degradation of various chemicals like diazinon (Barik et al., 1979), fenitrothion (Ohshiro et al., 1996), parathion (Nelson et al., 1982), and monocrotophos (Bhadbhade et al., 2002b) by *Arthrobacter*. However, *Arthrobacter* has not been tested before on any of the currently studied pesticides. Despite showing low bacterial growth unlike other strains, *Arthrobacter* sp. strain B3 has been able to degrade up to 94% of all 10 pesticides.

The bacterial consortiums are able to complement each other's metabolic functions by recycling the whole pesticide. A microbial consortium contains degraders of target compound and can utilize the metabolic intermediates of the parent compound (Pattanasupong et al., 2003). Toxic intermediates may sometime continue to persist when using a pure bacterium. In this study, the microbial consortium was able to quickly adapt to the stress caused by the xenobiotic on solid media, showing a 100% degradation of ridomil, bravo, mirage, cleaner, score and fitoraz within 60 days of investigation. These results imply that the microbial consortium will therefore significantly enhance the soil conditions by reducing the pesticide concentration.

As shown in Figures 2 and 3, a higher bacterial growth was achieved by the cells in solid phase within 30 days, than free cells suspended on liquid media (both in pre-cultivated conditions). The exponential phase takes place during day 15 on liquid media, while on solid media, it can be perceived on day 13. This result matches what Salunkhe et al. (2014) mentioned: the *B. subtilis* strains experience an exponential phase 3 days after inoculation on liquid media. Nevertheless, this phase takes place on the sixth day in soil. This may be caused by masses-transference intensification and a high microorganism-pollutant interaction. The toxic-metabolites transference, which precedes degradation, is faster on liquid media. This ends up affecting bacterial growth by reducing the population. On liquid media though, the thicker contact surface leads to bacteria growth in a shorter period of time using the pesticide as a carbon source.

Conclusions

Microbial degradation is one of the most important techniques to dissipate pesticides found in soils. The present study concluded that *P. putida* sp. strain B1, *Acinetobacter* sp. strain B2*, Artrobacter* sp. stain B3 and

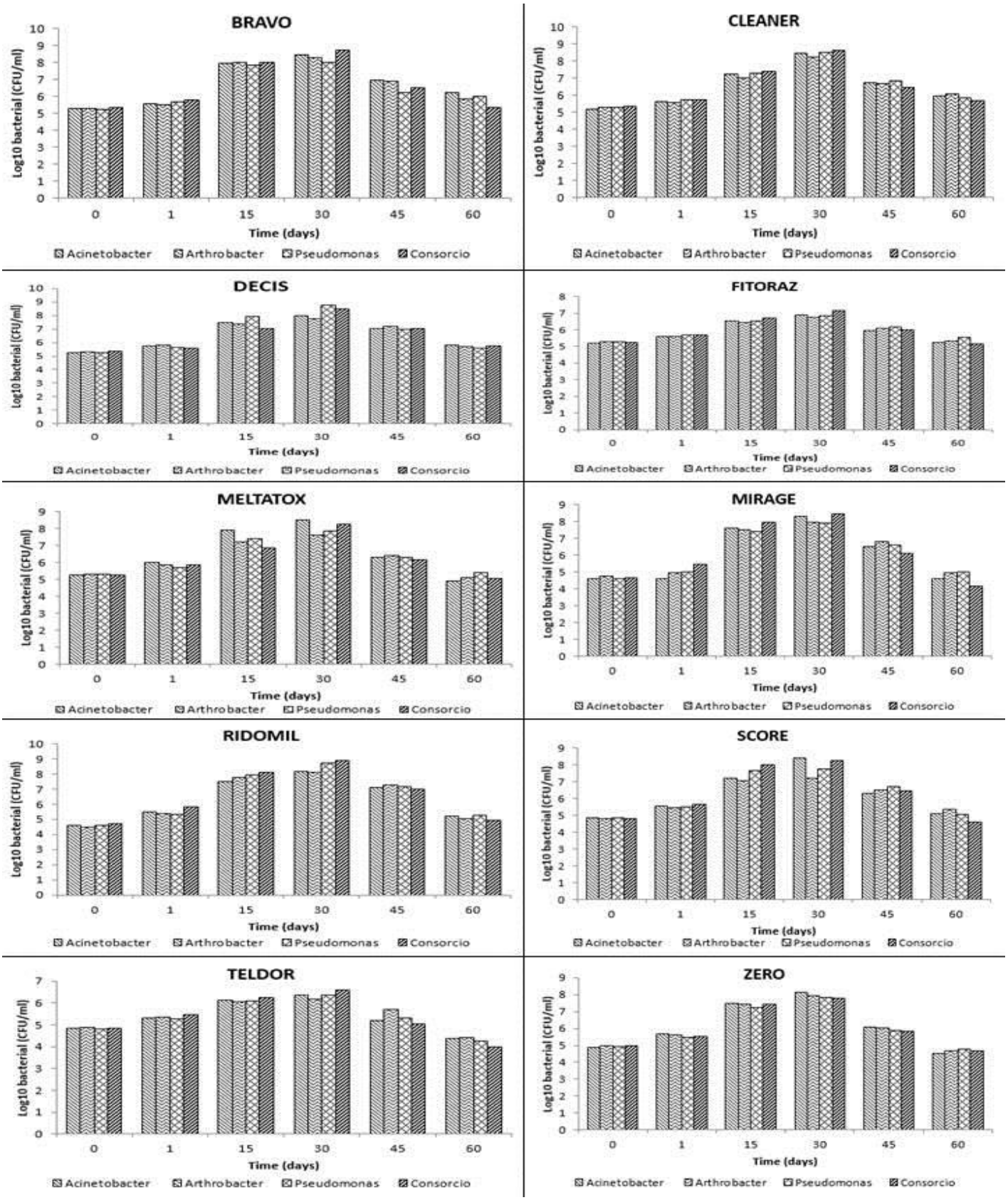

Figure 3. *Acinetobacter*, *Arthrobacter*, *Pseudomonas* and consortium growth in solid culture (soils) incubated at 21.1°C and 54.4% humidity in the presence of 10 different pesticides.

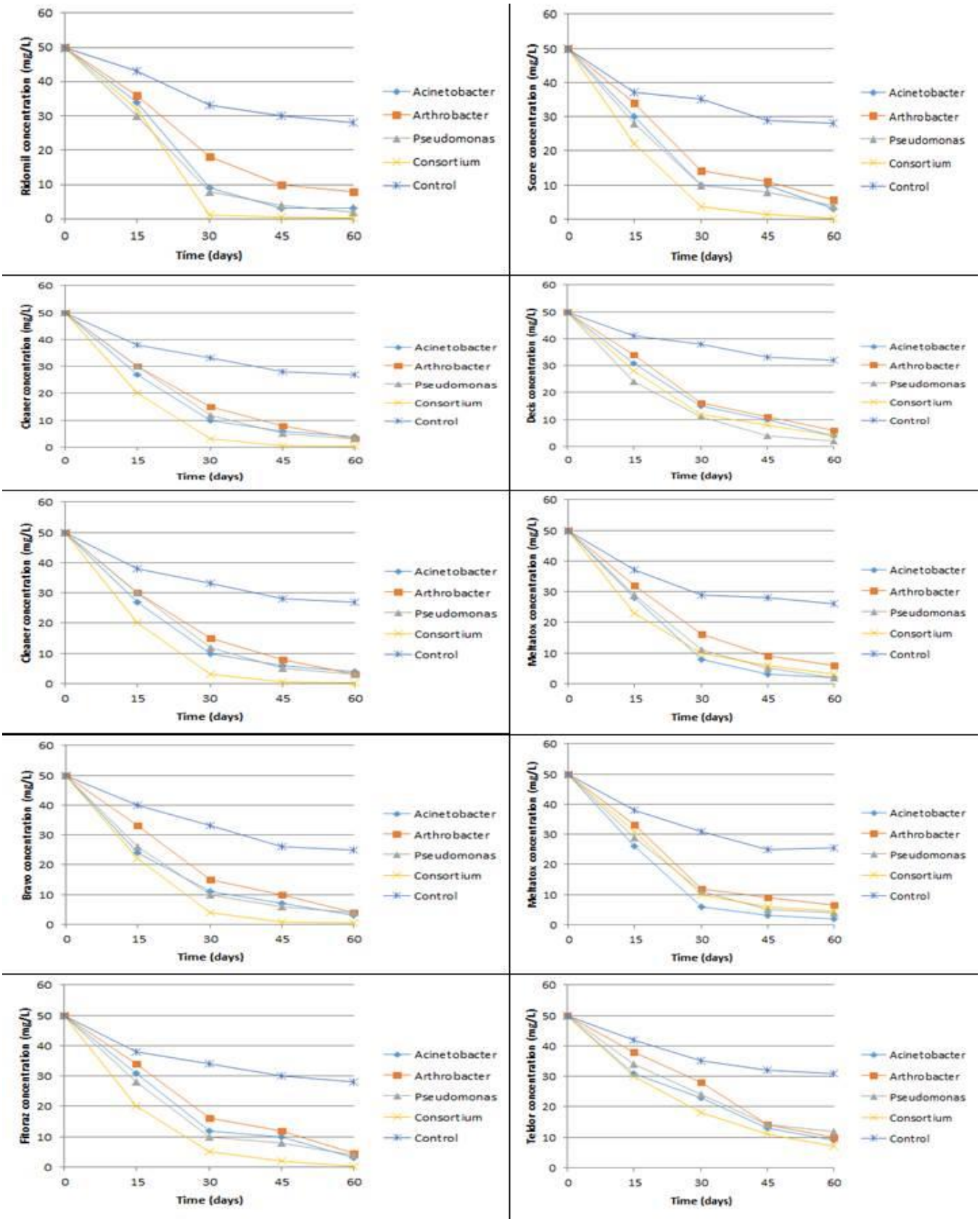

Figure 4. Various pesticides residual concentration observed in *Acinetobacter*, *Arthrobacter* and bacterial consortium in autoclavated soils (solid media). Each value is mean of three replicates.

the bacterial consortium have proven to have the capacity to utilize different pesticides as a carbon source and enhance the dissipation in soils and liquid medium. The bacterial consortium was more effective. All the strains can be applied in flower farming as a bioaugmentation process in order to reduce the pesticide residues in soils.

Conflict of Interests

The authors have not declared any conflict of interests.

ACKNOWLEDGEMENTS

The authors are thankful to Agrobiotecnología Laboratory, Universidad de las Fuerzas Armadas-ESPE and Ciencias Agropecuarias Department - Universidad de las Americas for providing all necessary facilities for this study.

REFERENCES

Agroprojekt SA (2012). Consultancy and Laboratory Services, Quito – Ecuador.

Ahmed I, Azmy A, Tamer M, Essan A, Shaban H (2015). Biodegradation of Malathion by *Acinetobacter baumannii* strain ADA isolated from domestic sewage in Egypt. Int. J. Biotecnol. Eng. 9:11.

Aparicio V (2015). Los plaguicidas agregados al suelo y su destino en el ambiente, INTA Ediciones, Argentina. pp. 1-74.

Barik S, Wahid P, Ramakrishnan C (1979). A change in degradation pathway of parathion in natural ecosystem. J. Environ. Qual. 7:346-357.

Bhadbhade B, Dhakephalkar P, Sarir S (2002a). Plasmid associated biodegradation of an organophosphorus pesticides, monocrotophos by *Pseudomona mensocina*. Biotechol. Lett. 2:647-650.

Bhadbhade B, Sarnik S, Kanekar P (2002B). Biomineralization of an organophosphorus pesticide, monocrotophos by soil bacterial. J. Appl. Microbiol. 93:224-234.

Derbalah A, Belal E (2008). Biodegradation kinetics of cymoxanil in aquatic system. Chem. Ecol. 24(3):169-180.

Faddin M, (2007). Pruebas bioquímicas para la identificación de bacterias. 4ta edición. Buenos Aires, Argentina, Editorial Médica Panamericana. Pp. 1-250.

Garcia LC, Martínez-Molina E, Trujillo ME (2010). *Micromonosporapisi* sp. nov., isolated from root nodules of *Pisumsativum*. Int. J. Syst. Evol. Microbiol. 60:331-337.

Gooty J, Shrinivasulu M, Maddela N, Manjunatha B, Rangaswamy V, Koch A, Rueda D (2015). Influence of the insecticides acetamiprid and carbofuran on arylamilase and myrosinase activities in the tropical black and red clays soils. Environ. Monit. Asses. 187(6):1-9.

Hernandez A, Hansen A (2010). Uso de plaguicidas en dos zonas agrícolas de México and evaluación de la Contaminación de agua and sedimentos. Rev. Int. Contam. Ambient. 27(2):115-127.

Hongsawat P, Vangnai A (2011). Biodegradation pathways of chloroanilines by *Acinetobacter baylyo* stain SF02. J. Hazard. Mater. 186(2):1300-1307.

Hussaini S, Shaker M, Asef M (2013). Isolation of Bacterial for Degradation of selected pesticides. Bull. Environ. Pharmacol. Life Sci. 2(4):50-53.

Liu F, Hong M, Liu D, Li X, Show P (2007). Biodegradation of methyl parathion by *Acinetobacter radioresistens* UBTB-04. J. Environ. Sci. 19(10):1257-1260.

Lopez CEM (2011). Producción, comercialización, exportaciones de flores en el Ecuador and su rol en las exportaciones no tradicionales, Facultad de Ciencias Económicas, Universidad de Guayaquil. pp. 1-76.

Manigandan G, Nelson R, Jeevan P (2013). Biodegradation of Lambda cyhalothrin by *Pseudomonas fluorescend* and *Trchoderma viridae*. J. Microbiol. Biotechnol. Res. 3(5):42-45.

Massoud A, Derbalah A, Belal S (2008). Microbial detoxification of metalaxl in aquatic system. J. Environ. Sci. 20(3):262-267.

Megadi VB, Tallur PN, Hoskeri RS, Mulla SI, Ninnekar HZ (2010a). Biodegradation of Pendimethalin by *Bacillus circulans*. I. J. Biotechnol. 9(2):173-177.

Megadi VB, Tallur PN, Mulla SI, Ninnekar HZ (2010b). Bacterial Degradation of Fungicide Captan. J. Agric. Food. Chem. 58:12863-12868.

Mendoza JC, Perea YS, Salvador JA, Pérez JAMG (2011). Biodegradación bacteriana de plaguicidas Permetrina y Cipermetrina en cultivo de lote. Avances En Ciencias E Ingeniería 2(3):45-55.

Mulla SI, Hoskeri RS, Shouche YS, Ninnekar HZ (2011). Biodegradation of 2-nitrotoluene by *Micrococcus* sp. strain SMN-1. Biodegradation 22(1):95-102.

Mulla SI, Talwar MP, Hoskeri RS, Ninnekar HZ (2012). Enhanced degradation of 3-nitrobenzoate by immobilized cells of *Bacillus flexus* strain XJU-4. Biotechnol. Bioproc. Eng. 17:1294-1299.

Nelson M, Yaron B, Nye P (1982). Biologically induced hydrolysis of parathion in soil: kinetics and modelling. Soil. Biol. Biochem. 14:223-228.

Nie Z, Hang B, Cai S, Xie X, He J, Li S (2011). Degradation of cyhalofop butyl (CYB) by *Pseudomona azotoformans* strain QDZ and cloning of a novel gene encoding CYB hydrolyzing esterease. J. Agric. Food. Chem. 11:6040-6046.

Ohshiro K, Kakuta T, Sakai T (1996). Biodegradation of organophosphorus insecticide by bacterial isolated from turf soil. J. Fermen. Bioeng. 82:299-305.

Pattanasupong A, Nagase H, Inoue M (2003). Ability of a microbial consortium to remove pesticide, carbendaim and 2,4-dichlorophenoxyacetic acid. World. J. Microniol. Biotechnol. 20(5):517-522.

Pirahuata M, Mojica M, Baquero E (2006). Aislamiento, purificacion and seleccion de bacterias como candidatos para ser utilizados en prcesos de biorremediacion de manczebutilizado en cultivo de papa. Universidad Distrital Francisco Jose de Caldas. 8:157-171.

Pooja S, Suri C, Cameotra S (2004). Isolation for a member of *Acinetobacter* species involved in atrazine degradation. Biochem. Biophys. Res. Common. 317(3):697-702.

Rios K, Penuela G (2015). Degradacion del clorotalonilo por un consorcio microbiano aislado de humedales constantes en laboratorio. Actual. Biol. 37(102):255-265.

Rodriguez E, Gamboa M (2009). Bacteriología General. 2da edición. Barcelona, España. Editorial García. Pp. 1-170.

Rosenberg A, Alexander M (1979). Microbial cleavege of various organophosphorus insecticide. Appl. Environ. Microbiol. 37:886-891.

Salunkhe V, Sawat I, Banerjee K, Wadkar P, Sawat S, Hingmire S (2014). Kinetics of degradation of carbendazim by *Bacillus subtilis* strains: possiility of in situ detoxification. Environ. Monit. Asses. 186(12):8599-8610.

Seoanez M, Chacón A, Gutiérrez A, Angulo L (2004). Contaminación del Suelo. Madrid, España: Ediciones Mundi-Prensa. Pp.1-17.

Tallur PN, Mulla SI, Megadi VB, Talwar MP, Ninnekar HZ (2015). Biodegradation of cypermethrin by immobilized cells of *Micrococcus* sp. strain CPN 1. Braz. J. Microbiol. 46:667-672.

Wang G, Chen M, Bi M, Li S (2011). Bioremediation of chlotothalonil contaminated soil by utilizing *Pseudomonas* sp. strain CTN-3. Ying Yong Sheng Tai Xue Bao 23(3):807-811.

Wang Z, Xu J, Li Y, Wang K (2010). *Rhodococcus jialingiae* sp. nov., an actinobacterium isolated from sludge of a carbendazim wastewater treatment facility. Int. J. Sist. Evol. Microbiol. 60(2):378-381.

Xiao W, Wang H, Li T, Zhu Z, Zhang J, He Z, Yang X (2013). Biorremediationof Cd and carbendazim co-contaminated soil by Cd-hyperaccumulator Sedum alfredii associated with carbendazim-degradating bacterial strain. Environ. Sci. Pollut. Res. 20(1):380-389.

Yu FB, Shan SD, Luo LP, Guan LB, Qin H (2013). Isolation and characterization of a *Sphingomonas* sp. strain F-7 degrading fenvalerate and its use in bioremediation of contaminated soil. J. Environ. Sci. Health B 48(3):198-207.

Zuniga J (2015). Evaluación *in vitro* de la degradación del pesticida

carbendazim mediante bacterias aisladas e identificadas, a partir de suelos cultivados con papa (*Solanum tuberosum*). en la parroquia.

Zuno-Floriano FG, Miller MG, Aldana-Madrid ML, Hengel MJ, Gaikwad NW, Tolstikov V, Contreras-Cortés AG (2012). Effect of *Acineto bacter* sp. on metalaxyl degradation and metabolite profile of potato seedling (*Solanum tuberosum*) alpha variety. Plos One 7(2):e31221.

academicJournals

Vol. 15(40), pp. 2234-2242, 5 October, 2016
DOI: 10.5897/AJB2016.15484
Article Number: 7EDFC2760844
ISSN 1684-5315

http://www.academicjournals.org/AJB

African Journal of Biotechnology

Full Length Research Paper

Use of response surface methodology to optimize the drying conditions of a bioactive ingredient derived from the African opaque sorghum beer

I. B. Chabi[1], A. P. P. Kayodé[1]*, B. P. Agbobatinkpo[1], A. Adénilé[2], O. A. Mamadou[1], G. Vieira-Dalodé[1], L. Baba-Moussa[3] and J. T. C. Codjia[4]

[1]Laboratoire de Valorisation et de Gestion de la Qualité de Bioingrédients Alimentaires, Faculté des Sciences Agronomiques, Université d'Abomey-Calavi, 01 BP 526 Cotonou, Bénin Republic.
[2]Laboratoire d'Ethnopharmacologie et de santé animale Faculté des Sciences Agronomiques, Université d'Abomey-Calavi, 01 BP 526 Cotonou, Bénin Republic.
[3]Laboratoire de Biologie et de Typage Moléculaire en Microbiologie, Faculté des Sciences et Techniques, Université d'Abomey-Calavi, 05 BP 1604 Cotonou, Bénin Republic.
[4]Laboratoire de recherche en Ecologie Animale et Zoogéographie, Faculté des Sciences Agronomiques, Université d'Abomey-Calavi, 01 BP 526 Cotonou, Bénin Republic.

Received 22 May, 2016; Accepted 15 September, 2016

The present work aims to optimize the heat drying conditions of a bioactive feed ingredient derived from the African opaque sorghum beer. The bioactive ingredient was dried at various temperatures 35 to 50°C and times 5 to 24 h. The effects of the drying conditions on the dry matter, water activity, pH, titratable acidity, bacteriocin, ethanol, lactic acid, yeasts, lactic acid bacteria contents and antimicrobial activity against indicator pathogens (*Staphylococcus aureus* ATCC 27844, methicillin resistant *S. aureus* (MRSA), *Salmonella typhi* R 30951401, *Klebsiella pneumoniae* ATCC 35657, *Escherichia coli* ATCC 25922, *E. coli* O157:H7 ATCC 700728 and *Candida albicans* MHMR) were studied. Results showed that the temperature was the main factor that affects the bioactivity indicators of the ingredient. The optimal conditions ensuring the best functionality of the ingredient were as follows: Temperature 42°C and drying duration, 24 h. At this optimum condition, water activity (0.49) was low enough to warrant adequate shelf life to the ingredient.

Key words: Bioactive ingredient, drying, optimization, response surface methodology.

INTRODUCTION

Thermal drying is a process of removing moisture from wet materials and is an important technique for the processing and preservation of some foodstuffs (Chen et al., 2013). It has a decisive effect on the quality of most

*Corresponding author. E-mail: polykap@yahoo.fr. Tel: (+229) 97870734.

Table 1. The central composite experimental design matrix (coded and real values for independent variable levels) for drying of antimicrobial ingredient.

Run	Levels of temperature		Levels of time	
	Coded value (X_1)	Real value (°C)	Coded value(X_2)	Real time (h)
1	0	42.5	0	14.5
2	0	42.5	0	14.5
3	0	42.5	0	14.5
4	0	42.5	0	14.5
5	0	42.5	0	14.5
6	0	42.5	0	14.5
7	+1	47	+1	20.2
8	-1	38	+1	20.2
9	-1	38	-1	8.79
10	+1	47	-1	8.79
11	+α	50	0	14.5
12	0	42.5	+α	24
13	-α	35	0	14.5
14	0	42.5	-α	5

commercial food products (Mujumdar, 2007). Sun drying has some significant disadvantages. It is time-consuming and labor-intensive, weather-dependent and may result in nutrients loss. Moreover, environmental contamination may occur during the sun drying (Maskan, 2001). Drying of biological materials such as bioactive ingredients containing living organisms is a complex process due to the simultaneous phenomenon of heat and mass transfer which occurs inside each particle (Torrez Irigoyen et al., 2014). In such conditions, the goal of drying is to preserve all functional properties of the ingredients after drying. To preserve the quality characteristics of such biological materials, a number of drying parameters could be optimized. These include drying temperature, flow-rate of drying air, pressure, power intensity, thickness of slices and drying time, which are dependent on the drying method (Singh et al., 2008; Sobukola et al., 2010; Manivannan and Rajasimman, 2011).

Response surface methodology (RSM) is a useful optimization tool, which has been applied in research to study the effect of individual variables and their interactions on response variables (Ahmed et al., 2014). It uses quantitative data from an appropriate experimental design to determine and simultaneously solve multivariate problems. Equations describe the effect of test variables on responses, determine interrelationships among test variables and represent the combined effect of all test variables in any response. This approach enables an experimenter to make efficient exploration of a process or system (Madamba, 2002). In the present study, we used the Response Surface Methodology to evaluate the simultaneous effects of the drying temperature and duration of a bioactive feed ingredient on its dry matter, water activity, pH, titratable acidity, bacteriocin, ethanol, lactic acid, yeasts, and lactic acid bacteria contents. Its antimicrobial activities against indicator pathogens such as *Staphylococcus aureus* ATCC 27844, methicillin resistant *S. aureus* (MRSA), *Salmonella typhi* R 30951401, *Klebsiella pneumoniae* ATCC 35657, *Escherichia coli* ATCC 25922*, E. coli* O157:H7 ATCC 700728 and *Candida albicans* MHMR were investigated and optimized.

MATERIALS AND METHODS

Inoculums and origin

The inoculum used is *kpete-kpete* which is the sediment of the Benin opaque sorghum beers known as tchoukoutou. *Kpete-kpete* consists of a mixture of lactic acid bacteria and yeasts (Kayodé et al., 2007) and is usually used as starter by women beer producers for a new beer production. The inoculum was supply by a woman producer of tchoukoutou in Abomey-Calavi.

Preparation of antimicrobial ingredient

Sorghum flour (75% of dehulled sorghum grains and 25% of sorghum malt) is mixed with distilled water to obtain a dough with a water content of 45% The dough is inoculated with 10% (w/w) of *kpete-kpete*, kneaded into dough and allowed to ferment in a plastic bucket with lid for 36 h to allow optimum microorganisms propagation. The fermented dough samples were dried in a ventilated oven drier (Venticell, Fisher, Bioblock Scientific, MMM, Medcenter) for an indicated time and temperature as specified in the experimental design (Table 1). At each time and temperature point, samples were aseptically taken and put in the flask for microbiological analysis and antimicrobial tests.

Experimental design

An orthogonal rotatable Central Composite Design (CCD) for k = 2 factors was used to investigate the simultaneous effects of two

process variables on the dry matter (DM), water activity (a_w), pH, lactic acid (LA), lactic acid bacteria count (LAB), yeasts and moulds count (YM), bacteriocin production (BE) and the antimicrobial activity against indicator pathogens (*S. aureus* ATCC 27844, methicillin resistant *S. aureus* (MRSA), *S. typhi* R 30951401, *K. pneumoniae* ATCC 35657, *E. coli* ATCC 25922*, E. coli* O157:H7 ATCC 700728 and *C. albicans* MHMR) in a quadratic function. The design generated fourteen observations including six central points, four kernel points and four axial points. The design matrix and variable combinations are shown in Table 1.

Microbiological analysis

Total counts of LAB, yeasts and moulds were performed according to the method described by Nout et al. (1987). At each sampling time, duplicate samples (10 g) were diluted in 90 ml sterile peptone physiological saline solution (5 g peptone, 8.5 g NaCl, and 1000 ml distilled water, pH = 7.0) and homogenized with a Stomacher lab-blender (type 400, London, UK). Decimal dilutions were plated. Viable counts of lactic acid bacteria were determined on de Man, Rogosa and Sharpe Agar (MRSA, CM 361, Oxoid, Hampshire, England) containing 0.1% (w/v) natamycin (Delvocid, DSM, The Netherlands) with incubation in anaerobic jar (Anaerocult A, Merck KGaA, Germany) for 72 h. Yeasts and moulds were enumerated using Malt Extract Agar (MEA, CM 59 Oxoid, Basingstoke, Hampshire, England). MEA plates were incubated at 25°C for 72 to 120 h. The colonies were then counted and expressed as logarithmic colony forming units per gram (log_{10} cfu/g) of sample.

Antimicrobial activity

The capacity of bioactive ingredient to inhibit the indicator pathogens was determined by modifying the disc diffusion method of NCCLS (2003). Twenty milliliters (20 mL) of molten Mueller-Hinton Agar (MHA, CM 337, Oxoid, Hampshire, UK) were poured into sterile Petri dishes and allow to solidify. Hundred microliters (100 µL) of the overnight Mueller-Hinton broth (Oxoid, CM 405, Hampshire, UK) culture of each pathogen strain, which have been adjusted to 0.5 McFarland-turbidity, was spread on the plates. Once the plates were dried aseptically, five blank discs papers (6 mm in diameter) were placed onto the surface of the agar. The moist or dried sample of bioactive ingredient was reconstituted with sterile distilled water to obtain a solution of 500 mg mL^{-1}. This solution was stirred vigorously using a magnetic stirrer for 30 min and then centrifuged at 3 500 g for 30 min. Forty microliters (40 µL) of each supernatant were delicately placed into the discs. The plates were left at room temperature for 1 h so that the absorbed supernatant become diffused into the agar, and then incubated at 37°C for 24 h.

Physicochemical analysis

Determination of dry matter, pH, titratable acidity and a_w

The dry matter content was determined by oven drying of 5 g of grinded at 105°C until a constant weight was reached (AACC, 44-15 A, 1984). Titratable acidity and pH were determined as described by Hounhouigan et al. (1993). The pH was measured using a digital pH-meter (JENWAY, Model 3505, UK) calibrated with buffers at pH 4.0 and 7.0 (WTW, Weilheim, Germany). The water activity (a_w) of the dried samples was measured using a water activity meter (Rotronic HygroLab 2, 8303 Bassersdorf).

HPLC determination of lactic acids and ethanol

Lactic acids and ethanol were extracted in 1.5 ml centrifuge tubes from 50 mg samples with 1 ml of sulphuric acid (H_2SO_4, 5 mM) under mild agitation for 30 min. After extraction, samples were centrifuged at 3500 x g for 30 min then filtered through a 0.45 µm sieve before separation by HPLC using an Aminex HPX-87H^+cation-exchange column (BioRad Hercules, USA) at a column temperature of 37°C with UV-(210 nm) and IR-detectors (Mestres and Rouau, 1997). The eluent was 5 mM sulphuric acid at a flow rate of 0.6 ml min^{-1}. The injection volume of the sample was 20 µl. Lactic acids and ethanol was expressed as mg/g dry matter.

Bacteriocin extraction

Bacteriocin was measured by the method of Burianek and Yousef (2000) modified as follows: 10 g of the tested ingredient were withdrawn in a Falcon tube to which one added 30 ml of distillated water stirred vigorously using a magnetic stirrer for 60 min. Blend was centrifuged at 3 500 g for 30 min. The supernatant fluid was harvested and chloroform was added (1:2, v/v) then stirred vigorously using a magnetic stirrer for 30 min. The blend was allowed to settle for 30 min and the aqueous layer was removed delicately, using a micropipette. Afterward, the precipitated phase (interface between aqueous layer and solvent) and solvent (chloroform) were removed and dried. The residual aqueous layer remaining in the flask was cooled and weighed. The solvent (chloroform) is evaporated using a rotary evaporator. After one hour of drying in the oven (130°C) the flask is cooled with the desiccators then weighed again. The weight (m) of bacteriocin expressed in mg/g is calculated as follows:

$$m = \frac{[(m_f - m_i) - m_0]}{m_e}$$

Where m_i is an initial mass of flask, m_f is final mass of flask; m_o is mass of peptide initially contained in sorghum flour used.

Statistical analysis

All statistical analyses were carried out by employing the statistical package Minitab 14 (Minitab Inc., USA). A second order polynomial model was fitted to the mean data values to obtain regression equations. The independent variables were the temperature (X_1) of drying (35 to 50°C) and the duration (X_2) of drying (5 to 24 h). The chosen model was a second degree polynomial regression with interaction for Y variables.

$$Y = b_0 + b_1X_1 + b_2X_2 + b_3X_1^2 + b_4X_2^2 + b_5X_1X_2.$$

Where Y is the response, b_0, b_1, b_2, b_3, b_4 and b_5 are model coefficients for intercept, linear, quadratic and interaction terms, respectively, and x_i are coded independent variables.

The fitted polynomial equations were expressed in 3D response surface graphs, in which the response is presented on the vertical axis and two factors at the two horizontal perpendicular axes. The analysis of variance (ANOVA) was used to determine significant differences between independent variables ($p < 0.05$).

Verification of the model

The criteria for evaluating the reliability of the simulations were the percentage error observed between experimental and predicted values. Thus, the experimental value was compared with the predicted one from the optimized model by calculating the percentage error to determine the adequacy of the drying process and response surface models. The percentage error, PE which is lower than 10 % indicates a good fit (McLaughlin and Magee, 1998; Kek et al., 2014).

Table 2. The measured data for response surface analysis of the effect of drying conditions on the quality of antimicrobial ingredient.

Code	D.M	a_w	pH	TA	Alcool	LA	BE	O157 :H7	E. coli	S. aureus	MRSA	C. albicans	S. typhi	K. pn	LAB	YM
1	67.64	0.86	4.15	1.95	0.85	10.15	19.55	13.12	12.75	12.25	12.50	14.62	13.25	12.12	7.93	7.71
2	66.58	0.88	3.86	3.64	0.34	12.28	12.81	12.62	13.25	13.00	12.00	13.12	12.00	12.00	7.83	7.17
3	69.84	0.85	3.92	3.33	0.11	17.23	11.92	14.12	13.62	12.00	13.50	13.00	16.00	12.12	7.92	7.09
4	68.25	0.86	3.88	3.45	0.89	12.46	13.09	12.00	12.00	13.75	13.00	15.12	14.12	11,75	7.93	7.14
5	69.87	0.85	3.91	3.43	0.60	21.11	12.11	12.12	11.75	12.25	12.87	12.75	13.50	10.75	7.44	7.08
6	69.61	0.85	3.93	3.35	0.67	20.54	15.95	11.25	13.12	14.00	11.12	13.25	14.00	13.25	8.10	7.25
7	92.59	0.26	4.61	2.07	0.08	15.19	13.82	13.00	12.62	12.50	12.12	13.00	12.12	10.25	5.16	0.00
8	74.80	0.84	3.95	3.16	0.57	19.83	16.36	12.62	13.50	12.25	13.00	14.87	13.25	11.00	8.06	7.10
9	62.62	0.90	3.94	3.56	1.19	13.12	15.97	12.00	12.75	13.00	13.50	15.00	14.50	12.12	8.12	7.22
10	77.76	0.84	4.15	3.4	0.20	14.95	12.47	12.87	12.50	13.62	11.00	14.12	15.00	13.00	7.14	6.24
11	90.72	0.31	4.43	2.15	0.01	13.44	13.23	12.25	12.12	12.00	11.87	12.00	13.12	10.00	5.03	0.00
12	90.74	0.40	4.27	2.47	0.02	10.18	13.67	11.87	12.00	11.87	13.00	13.62	12.00	10.87	7.35	6.19
13	65.02	0.89	3.91	3.34	0.99	17.34	13.58	13.12	12.25	13.00	12.25	14.87	15.00	12.12	8.22	7.13
14	59.78	0.88	3.89	3.81	1.54	17.99	16.73	14.00	13.62	12.00	12.62	14.25	15.50	14.12	8.43	7.95

O157,H7, E. coli O157,H7 ATCC 700728; E. coli*, E. coli* ATCC 25922; S. aureus*, Staphylococcus aureus* ATCC 27844; MRSA, methicillin resistant *Staphylococcus aureus; C. albicans, Candida albicans* MHMR*; S. typhi, Salmonella typhi* R 30951401 and *K. pn, Klebsiella pneumoniae* ATCC 35657.

$$PE(\%) = \left(\left| \frac{m_{exp} - m_{pre}}{m_{exp}} \right| \right) * 100$$

Where m_{exp} is experimental value and m_{pre} is predicted value.

RESULTS AND DISCUSSION

Effects on physic-chemical properties

Long shelf life of dried product is closely related to their low moisture content (Atalar and Dervisoglu, 2015). For all treatments (Table 2) the dry matter varied from 59.78 to 92.59%. The highest dry matter was obtained for the treatment 7 and the lowest for the treatment 14. The linear and quadratic regression model for dry matter was given in Table 3. As could be expected, it clearly appears that the drying temperature as well as the drying duration significantly influenced the dry matter of the bioactive ingredient. Only 3% of the total variations are not explained by the model. Additionally, the significant p-value of F, particularly for linear and quadratic regression model indicates that dry matter from bioactive ingredient had a good model fit due to the high value of R^2 and F. Figure 1a shows the surface plots for the effect of the independent variables on the moisture content. From this figure., it was observed that water content decreases continuously with drying time and increasing drying temperature. Such increase in the product dry matter content, due to water loss, is desirable since it could improve shelf life of the product (Kayodé et al., 2012).

Besides, the main objective of drying is to decrease the a_w of various perishable materials to values <0.5, in order to enable their storage at ambient temperature (Bonazzi and Dumoulin, 2011). Water activity of wet bioactive ingredient was 0.93. During the drying process, it decreased significantly to reach the value of 0.26 for treatment 7 (Table 2). Table 3 shows that the linear, quadratic and interaction terms of all independent variables (drying time and drying temperature) was highly significant and negatively affected the water activity of the bioactive ingredient. This is confirmed by its surface plot (Figure 1b). The same trend was reported by Kek et al. (2014) for drying of guava.

For all the treatments applied, the pH values of dried bioactive ingredient range from 3.86 to 4.61. Figure 1d shows the trend in the pH as function of the two independent variables. As shown in Table 3, pH was found to be a function of the linear and quadratic effects of drying temperature and drying

Table 3. Regression coefficients, coefficient of determination (R^2), and p-values for the second order polynomial equations.

Coef.	D.M	a_w	pH	TA	Alcool	L.A	Bac.	*E. coli* O157:H7	*E. coli*	*S. aureus*	MRSA	*C. albicans*	*S. typhi*	*K. pn*	LAB	YM
Constant																
b_0	68.936	0.861	3.952	3.195[a]	0.5634	15.7211	14.282	12.5251	12.7808	12.5251	12.4927	13.711	13.7926	11.9693	7.796	7.1558
Linear																
b_1	7.935[a]	-0.168[a]	0.1819[a]	-0.3386	-0.3261[b]	-0.9749	-0.6942	-0.0208	-0.1411	-0.0833	-0.4206	-0.7889[b]	-0.3940	-0.3562	-1.0585[a]	-2.0918[a]
b_2	8.232[a]	-0.151[a]	0.1155[b]	-0.4151[b]	-0.3427[b]	-0.6340	-0.3515	-0.2930	-0.1914	-0.2187	-0.1313	-0.2409	-1.0435[b]	-0.9726[a]	-0.3068[c]	-0.9726[b]
Quadratic																
b_3	3.653[a]	-0.090[a]	0.0933[c]	-0.1568	-0.0415	-0.0109	-0.2552	-0.0392	-0.1695	-0.0809	-0.1641	-0.0045	0.0697	-0.3691	-0.5107[a]	-1.4146[a]
b_4	2.710[b]	-0.076[a]	0.0608	-0.0142	0.0595	-0.4601	0.3928	-0.1294	-0.0562	-0.2849	0.1066	-0.176	-0.0422	0.1489	-0.0541	-0.1494
Interaction																
b_5	0.662	-0.130[a]	0.038	-0.2325	0.1250	-1.6175	0.24	-0.1225	-0.1575	-0.0925	0.4050	-0.2475	-0.4075	-0.4075	-0.2525	-1.5275[b]
R^2	**0.972**	**0.995**	**0.881**	**0.629**	**0.772**	**0.149**	**0.148**	**0.129**	**0.207**	**0.234**	**0.392**	**0.555**	**0.582**	**0.750**	**0.932**	**0.953**

b_1 and b_3, Coefficients for temperature; b_2 and b_4, coefficients for time; b_5, coefficient for interaction (temperature × time). [a] Significant at $p<0.001$, [b] significant at $p<0.01$, [c] significant at $p<0.05$; R^2 coefficient of determination.

time. The linear and quadratic effects ($p<0.01$) were positive. The interaction effect between time and temperature was found to be not significant (Table 3). Titratable acidity (Figure 1g) was mainly a function of the drying time with a negative linear effect ($p<0.05$) and insignificant linear effect of the drying temperature. Besides, the quadratic and interaction effects with temperature and time were found to be not significant (Table 3).

Effects on bacteriocin production, organic acid and ethanol contents

Bacteriocin, organic acids (such as lactic acid, acetic acid), ethanol, hydrogen peroxide are part of components capable of inhibiting pathogenic microorganisms. Statistical analysis showed no significant effect of the drying parameters on bacteriocin and lactic acid as reflected by the low values of the respective coefficients of determination (Table 3). Ahmad et al. (2014) reported that activity of bacteriocin is heat stable at temperature up to 80°C. The drying duration and temperature had not significant effect on bacteriocin activity of bioactive ingredient.

Yeasts are mainly responsible for ethanol production. The yeasts involved in the bioactive ingredient under study were previously reported to belong essentially to *Saccharomyces cerevisiae* (Kayodé et al., 2007). The ethanol content of the product decreases significantly with increasing temperatures. This could be expected since ethanol is highly volatile even at ambient temperature. Among the different treatments applied, the highest ethanol rate (1.54 mg/g) of bioactive ingredient was obtained with the treatment 14 and the lowest (0.01 mg/g) with the treatment 11 (Table 2). As shown in Table 3 and Figure 1c, only the linear effect of the drying parameters was significant on the ethanol content of the ingredient. The quadratic and interaction effects were not significant.

Effects on functional microorganisms

Surface plots and the model coefficients for viable microorganisms are presented in Figure 1e and f and Table 3, respectively. The total count of viable microorganisms is relatively constant at drying temperature between 35 and 43°C. Beyond this temperature, the viable microorganisms decreased sharply to reach a minimum level at 50°C. Thus, viable yeasts decreased from 6.24 to 0.0 log cfu/g whereas LAB decreased from 7.14 to 5.03 log cfu/g. In similar study, Kayodé et al. (2012) reported that the yeasts were much more sensitive to temperature compared to LAB which are able to survive at temperatures as high as 45°C. Higher temperatures and longer drying durations affect negatively the total count of viable microorganisms in the bioactive ingredient. Specifically, the linear and quadratic effects of the parameters are significant. It is well established that the loss of probiotics viability during convective thermal processing is related to cell injuries resulting from the combined effects of heat and mechanical stress (Behboudi-Jobbehdar et al., 2013). The interactive effects of the duration and temperature were not significant for LAB,

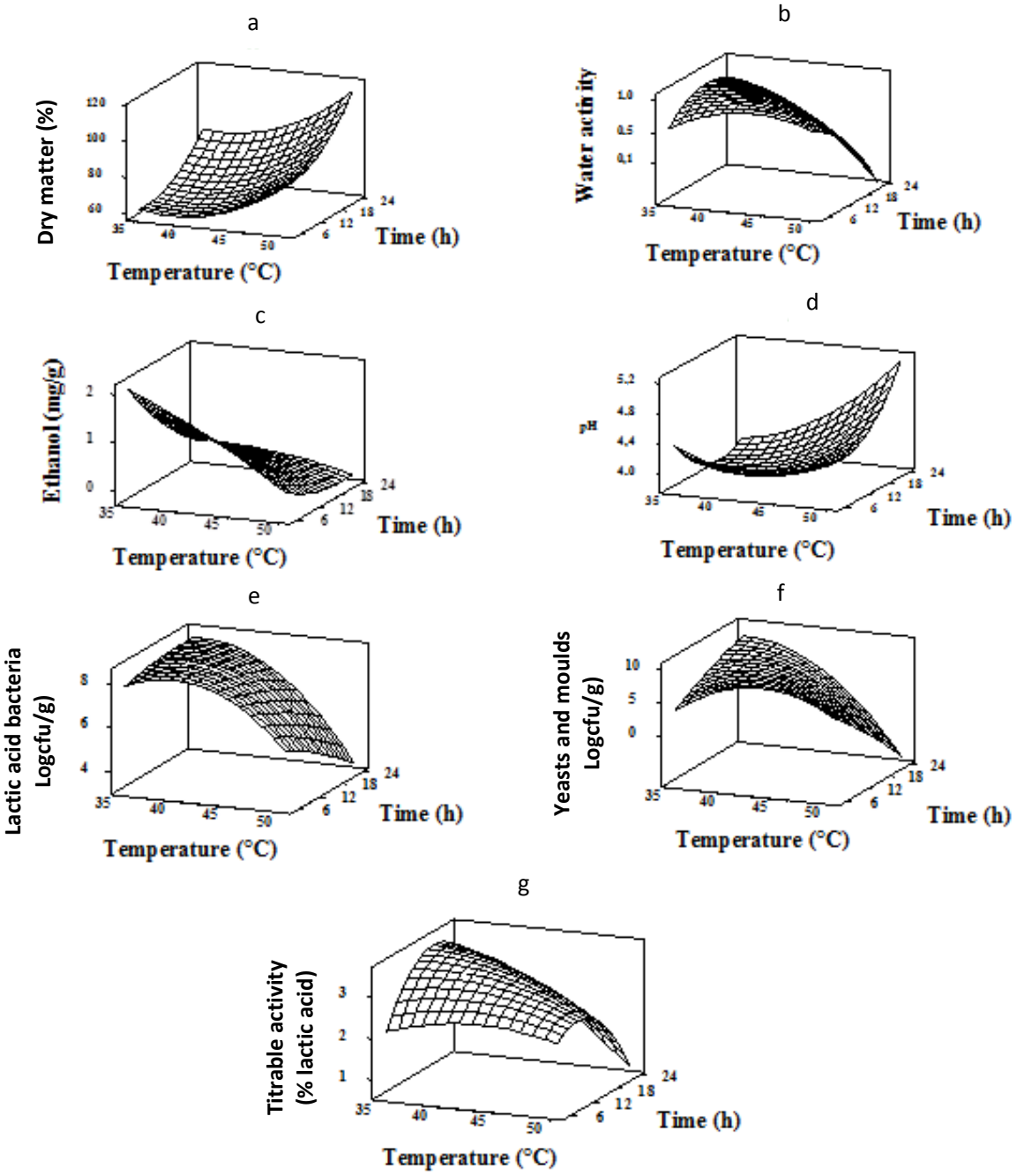

Figure 1. Response surface curves (3D) depicting the effects of drying temperature and time on (a) dry matter, (b) water activity, (c) ethanol, (d) pH, (e) lactic acid bacteria, (f) Yeasts and moulds and (g) titratable acidity with respect to significant process parameters.

whereas it significantly affect the yeasts and moulds contents of the product (Table 3).

Effects on antimicrobial properties

The inhibition diameter was used as an index for the antimicrobial activity of the bioactive ingredient investigated. The inhibition diameter of all indicator pathogens tested ranged from 10 mm (on *K. pneumoniae*) to 15.50 mm (on *S. typhi*). Clearly, the bioactive ingredient dried at different temperatures (35-50°C), preserved its antimicrobial properties. However, the analysis of variance (Table 3) indicated that the

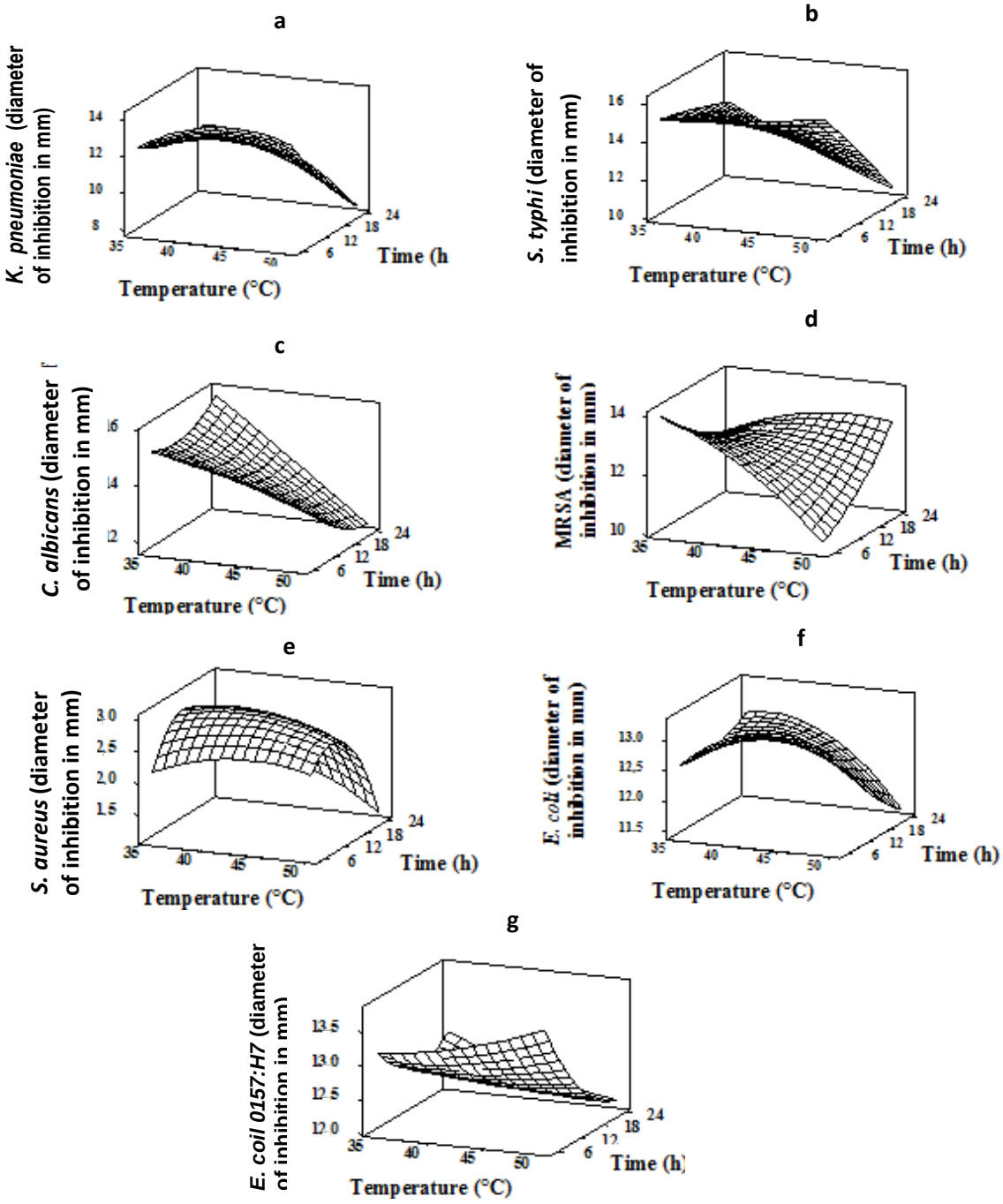

Figure 2. Response surface curves (3D) showing the effects of dried antimicrobial ingredient on (a) *K. pneumoniae*, (b) *S. typhi*, (c) *C. albicans*, (d) MRSA, (e) *S. aureus*, (f) *E. coli*, (g) and *E. coli* .O157:H7.

antimicrobial activity on three indicator pathogens (*K. pneumoniae* ATCC 35657, *S. typhi* R 30951401 and *C. albicans* MHMR) was closely related to the linear effects of temperature and time with significant values of the relative coefficients of determination values (R^2) which ranged from 0.56 to 0.75. As shown in Table 3 and Figure 2a, b and c, inhibitions of *C. albicans* MHMR, *S. typhi* R 30951401 and *K. pneumoniae* ATCC 35657 mainly depend on drying temperature. The quadratic and interactive effects of time and temperature were not significant. The coefficient of determination (R^2) obtained for the four (Table 3 and Figure 2d, e, f and g) remaining pathogens (methicillin resistant *S. aureus* (MRSA), *S. aureus* ATCC 27844, *E. coli* ATCC 25922 and *E. coli*

Table 4. Pearson's correlation coefficients between microbial inhibitions and some physicochemical and microbiological parameters.

	a_w	pH	*S. typhi* ATCC	*K. pneumoniae*	*E. coli O157 :H7*	*E. coli* ATCC	*S. aureus*	*MRSA*	*C. albicans*	LAB
a_w										
pH	-0.916**									
S. typhi	0.077	0.099								
K. pneumoniae	0.306	-0.268	0.649*							
E. coli O157 :H7	0.205	-0.053	0.478	0.282						
E. coli ATCC	0.170	-0.021	0.310	0.519	0.510					
S. aureus ATCC	-0.047	0.041	0.161	0.403	-0.457	-0.095				
MRSA	-0.338	0.424	0.121	-0.221	0.204	0.060	-0.504			
C. albicans	-0.248	0.327	0.312	0.402	0.062	0.096	0.311	0.296		
LAB	0.820**	-0.881**	-0.248	0.103	-0.112	-0.133	-0.085	-0.393	-0.352	
YM	0.889**	-0.878**	-0.018	0.160	0.129	-0.065	-0.168	-0.325	-0.423	0.931**

*Significant at 0.05; **Significant at 0.01.

Table 5. Predicted and experimental values of the response variables at optimum processing parameters by desirability function of RSM.

Variable	Optimum product				
	Limit	Desirability	Predicted values	Experimental values	PE(%)
pH	3.90-4.50	0.587	4.26	4.11±0.21	3.65
Water activity	0.4-0.5	0.999	0.45	0.49±0.01	8.16
Titratable acidity (%)	2.0-3.50	0.747	2.56	2.63±0.08	2.66
LAB (Log cfu/g)	7.0-8.0	0.649	7.33	7.63±0.27	3.93
Antimicrobial activity **					
K. pneumoniae	11.95-13.73	0.827	12.41	12.67±0.63	2.05
S. typhi	11.95-13.73	0.827	12.41	12.63±0.53	1.74
C. albicans	11.95-13.73	0.827	12.41	13.81±0.44	10.13

**Inhibition diameter (mm) of antimicrobial ingredient against some indicator pathogens.

O157:H7 ATCC 700728) were rather weak. There were no significant effects of the drying time and temperature on the antimicrobial activities of the ingredient vis-à-vis of these pathogens.

Relationship between some measured parameters

The Pearson's correlation coefficients between some measured parameters are presented in Table 4. High negative correlation exists between the a_w and the pH ($r = -0.916$; $p<0.01$). Except the correlation between microbial inhibition on *K. pneumoniae* and *S. typhi* ($r = 0.649$; $p<0.05$), no other significant correlation could be observed between microbial inhibition on indicator pathogens. Lactic acid bacteria, yeasts and moulds were positively correlated with a_w ($r = 0.820$; $r = 0.889$; $p<0.01$ respectively) and negatively with pH ($r = -0.881$; $r = -0.878$; $p<0.01$ respectively). It was clear that the lower the a_w the lower the viable cells count during the drying process. Interestingly, a low a_w is an indicator of a good viability of such microorganisms during storage (Vesterlund et al., 2012).

Optimization of process parameters and verification of models

To achieve optimum drying conditions for the bioactive ingredient in terms of optimal functionality, the desirability function was used to optimize the drying time and temperature. The desired goals for each response are summarized in Table 5. The limits of all responses at operating conditions were converted to a desirability function. The optimal conditions were found to be: temperature = 41.893°C and drying duration = 24.0 h. The composite desirability value of the optimum solution was 0.749 for the optimized temperature and time. Once the optimum conditions have been determined, we conducted additional independent experiments at these values. The experimental values were compared with the predicted from the optimized model and the PE was

calculated to determine the adequacy of the drying and response surface models. After verification, the experimental values were very close to the predicted responses (Table 5) and the percentage error indicated that the observed values were the same as the predicted values. Thus, all optimized models gave good fits to experimental data over the range of limit employed (PE<10%).

Conclusion

In the present research, we successfully used response surface methodology with CCD to optimize the drying process of bioactive ingredient containing viable thermo sensitive microorganisms. Statistical models show that the independent variables mostly marked the responses. Dry matter, water activity and viable microorganisms showed pronounced dependence on drying durations and temperatures. The optimal conditions for drying ensuring the best functionality of bioactive ingredient were found to be 42°C and 24 h. Under these conditions, experimental and predicted responses were not significantly different. At these water activity and water content values, the bioactive ingredient can be preserved and stored at ambient temperature with good shelf life.

Conflict of Interests

The authors have not declared any conflict of interests.

ACKNOWLEDGEMENT

This research was sponsored by the "Conseil Scientifique de l'Université d'Abomey-Calavi (Benin)" through the BioZoo project. The authors are thankful to the university's officials.

REFERENCES

AACC (1984). Approved methods of the American Association of cereal chemists, 8th Edition, St. Paul, MN, USA.

Ahmad V, Iqbal ANMZ, Haseeb M, Khan MS (2014). Antimicrobial potential of bacteriocin producing *Lysinibacillus* jx416856 against foodborne bacterial and fungal pathogens, isolated from fruits and vegetable waste. Anaerobe 27:87-95.

Ahmed ZS, Abozed SS, Abd El-Kader AE (2014). Extraction Optimization and Quality Characterization of Traditionally Prepared *Hibiscus sabdariffa* Beverage Using Response Surface Methodology. World J. Dairy Food Sci. 9:154-165.

Atalar I, Dervisoglu M (2015). Optimization of spray drying process parameters for kefir powder using response surface methodology. LWT Food Sci. Technol. 60:751-757.

Behboudi-Jobbehdar S, Soukoulis C, Yonekura L, Fisk I (2013). Optimization of Spray-Drying Process Conditions for the Production of Maximally Viable Microencapsulated *L. acidophilus* NCIMB 701748. Drying Technol. 31:1274-1283.

Bonazzi C, Dumoulin E (2011). Quality changes in food materials as influenced by drying processes. In. Modern Drying Technology Volume 3: Product Quality and Formulation, First Edition.

Burianek LL, Yousef AE (2000). Solvent extraction of bacteriocins from liquid cultures. Lett. Appl. Microbiol. 31:193-197.

Chen H, Zhang M, Fang Z, Wang Y (2013). Effects of different drying methods on the quality of squid cubes. Drying Technol.16:1911-1918.

Hounhouigan DJ, Nout MJR, Nago CM, Houben JH, Rombouts FM (1993). Changes in the physicochemical properties of maize during natural fermentation of *mawè*. J. Cereal Sci. 17:291-300.

Kayodé APP, Deh DC, Baba-Moussa L., Kotchoni SO, Hounhouigan JD (2012). Stabilization and preservation of probiotic properties of the traditional starter of African opaque sorghum beers. Afr. J. Biotechnol. 30:7725-7730.

Kayodé APP, Hounhouigan JD, Nout MJR (2007). Impact of brewing process operations on phytate, phenolic compounds and in vitro solubility of iron and zinc in opaque sorghum beer. LWT Food Sci. Technol. 40:834-841.

Kek SP, Chin NL, Yusof YA (2014). Simultaneous time-temperature-thickness superposition theoretical and statistical modelling of convective drying of guava. J. Food Technol. 51:3609-3622.

Madamba PS (2002). The Response Surface Methodology: an application to optimize dehydration operations of selected agricultural crops. LWT Food Sci. Technol. 35:584-592.

Manivannan P, Rajasimman M (2011). Optimization of process parameters for the osmotic dehydration of beetroot in sugar solution. J. Food Process. Eng. 34:804-825.

Maskan M (2001). Kinetics of color change of kiwifruits during hot air and microwave drying. J. Food Eng. 48:169-175.

McLaughlin CP, Magee TRA (1998). The determination of sorption isotherm and the isosteric heats of sorption for potatoes. J. Food Eng. 35:267-280.

Mestres C, Rouau X (1997). Influence of natural fermentation and drying conditions on the physicochemical characteristics of cassava starch. J. Sci. Food Agric. 74:147-155.

Mujumdar AS (2007). An overview of innovation in industrial drying: current status and R&D needs. Transp. Porous Med. 66:3-18.

NCCLS-National Committee for Clinical Laboratory Standards (2003). Method for antifungal disk diffusion susceptibility testing of yeast: Proposed Guideline M44-P. NCCLS, Wayne, PA, USA.

Nout MJR, Beernink G, Bonants-Van Laarhoven TMG (1987). Growth of *Bacillus cereus* in soyabean tempeh. Int. J. Food Microbiol. 4:293-

Singh B, Panesar PS, Nanda V, (2008). Optimization of osmotic dehydration process of carrot cubes in sucrose solution. J. Food Process Eng. 31:1-20.

Sobukola OP, Awonorin SO, Oladimeji SL, Olukayode BF (2010). Optimization of pre-fry drying of yam slices using response surface methodology. J. Food Process Eng. 33:626-648.

Torrez Irigoyen RM, Goñi SM, Giner SA (2014). Drying–toasting kinetics of presoaked soybean. A mathematical model considering variable diffusivity, shrinkage and coupled heat transfer. J. Food Eng. 142:70-79.

Vesterlund S, Salminen K, Salminen S (2012). Water activity in dry foods containing live probiotic bacteria should be carefully considered: A case study with *Lactobacillus rhamnosus* GG in flaxseed. Int. J. Food Microbiol. 157:319-321.

academicJournals

Vol. 15(40), pp. 2243-2250, 5 October, 2016
DOI: 10.5897/AJB2016.15580
Article Number: 9A26B8160847
ISSN 1684-5315

http://www.academicjournals.org/AJB

African Journal of Biotechnology

Full Length Research Paper

Enzymatic regulation of organic acid metabolism in an alkali-tolerant halophyte *Chloris virgata* during response to salt and alkali stresses

Huan Wang[1], Bing Bai[1], Ziyu Bai[1], Lijun Shi[1], Jinlin Ye[1], Siwen Fan[1], Huahua Xu[2] and Decheng Shi[1]*

[1]Department of Agronomy, Jilin Agricultural University, Changchun 130118, Jilin Province, China.
[2]Dongfeng High School, Daqing 163311, Heilongjiang Province, China.

Received 22 July, 2016; Accepted 15 September, 2016

***Chloris virgata*, an alkali-tolerant halophyte, was chosen as the test material for our research. The seedlings of *C. virgata* were treated with varying salt and alkali stress. First, the composition and content of organic acids in shoots were analyzed and the results indicated that there was not only a significant increase in total organic acids, but there were also obvious changes in different components of organic acids under alkali stress. The increments in citrate were the largest, followed by malate. However, none of the organic acids showed significant alterations in the content and components under salt stress. Also, activity of some enzymes (citrate synthase, malate synthase, NADP-isocitrate dehydrogenase, and isocitrate lyase) associated with such organic acids did not change significantly under alkali stress, but malate dehydrogenase activity markedly decreased under a stronger alkali stress (80 mM). Under salt stress as well as increased malate synthase (MS) activity, however, there was no significant change for other enzymes. These results strongly demonstrated that the enzymatic regulation of organic acid metabolism may be the biochemical basis of alkali tolerance for *C. virgata*. Citrate synthase (CS), MS and isocitrate lyase (ICL) might be the key enzymes that determine the alkali tolerance of *C. virgata*.**

Key words: Salinity, ion balance, enzyme activity, *Chloris virgata*.

INTRODUCTION

More than 800 million hectares of land throughout the world are affected by salt level. This amount accounts for more than 6% of the world's total land area. The salinization of soil is a widespread environmental problem and an important factor in limiting plant growth and productivity (Allakhverdiev et al., 2000). The detrimental effects of high salinity on plants can be observed at the whole-plant level as the death of plants and/or decreases in productivity. Some reports have clearly classified natural salt stress, in terms of salt characteristics, into neutral, alkaline and mixed salt-stress. It has also been shown that alkaline and neutral salt-stress are two

*Corresponding author. E-mail: 45447087@qq.com. Tel: +86 431 5269590. Fax: +86 431 5684009.

distinct kinds of stress for plants and should be called alkali and salt stress, respectively (Shi and Yin, 1993; Yang et al., 2008a, b, c; Wang et al., 2015b). Although some researches had focused on alkali tolerance of plants (Wang et al., 2012, 2015a, b; Gong et al., 2014; Sun et al., 2014), little is known about physiological mechanisms of plant alkali tolerance.

The presence of different concentrations of organic acids among various plants in their natural habitat is evident (Miyasaka et al., 1991); these organic acids play essential roles in interactions between the soil and various microorganisms (Yang and Crowley, 2000), making sparingly soluble soil Fe, P and other metals available to growing plants (Johnson et al., 1994). Many studies have demonstrated that plants secrete considerable amounts of citrate, malate and oxalate from roots in response to some abiotic stresses (Delhaize et al., 1993; Yang et al., 2007). The low-molecular weight organic acids may play important roles in protecting plants against abiotic stresses around the rhizosphere. Although some studies have shown that the total organic acids accumulated in shoots of *Kochia sieversiana* and other plants under alkali stress (Yang et al., 2007), only a few reports have demonstrated the organic acids metabolism under alkali stress. The total organic acids and oxalate content of shoots increased in *K. sieversiana* and *Suaeda glauca* under alkali stress (Yang et al., 2007) and the increase in the content of citrate was also detected in *Puccinellia tenuiflora* and sunflower (Shi et al., 2002; Shi and Sheng, 2005). The accumulation of organic acids might be responsible for coping with the imbalance of charges and high pH stress, but the biochemical basis and metabolic control mechanisms of accumulated organic acids is still unclear.

Some researchers have shown that the accumulation and exudation of citrate in root tips with aluminium (Al) treatments is associated with increased citrate synthase (CS) activity and decreased aconitase activity (Yang et al., 2004). There are also a few reports showing the influence of salt stress on organic acid metabolism. It had been indicated that NaCl salinity *in situ* causes an increase in all three MDH activities (total NAD-MDH, mitochondrial NAD-MDH, and chloroplastic NADP-MDH) in salt-tolerant cultivars CSR-1 and CSR-3, whereas 16 to 100% inhibition in activities was noted in salt-sensitive cultivars Ratna and Jaya (Kumar et al., 2000). In *Mesembryanthemum crystallinum* Linn, steady-state transcript levels for chloroplast NADP-MDH decreased transiently in the leaves after salt stress and then increased to levels greater than two-fold higher than levels in unstressed plants, whereas transcript levels in roots were extremely low and were unaffected by salt stress treatment (Cushman, 1993). Popova et al. (2002) reported that the activity of NADP-ICDH in plants adapted to high salinity increased in leaves and decreased in roots, and expression of Mc-ICDH1 was found to be stimulated in leaves in salt-adapted *M. crystallinum* by transcript analyses and western blot hybridizations. These results indicated that organic acid metabolism is influenced by salt stress due to the alteration of some enzyme activities under salt stress, and this kind of change might play a key role in enhancing salt resistance. However, the content of accumulated organic acids under alkali stress was greater than that under salt stress based on a few comparative tests of the two kinds of stress (Yang et al., 2007, 2008c). Therefore, studying organic acid metabolism in plants under alkali stress is becoming more important.

In this study, an alkali-resistant halophyte, *C. virgate*, a grass with high protein content, which makes it a high-quality forage plant (Zheng and Li, 1999) was used as material. The seedlings were treated with varying salt stress and alkali stress to explore the metabolic control mechanisms of organic acid accumulation in *C. virgata* during responses to alkali stress.

MATERIALS AND METHODS

Plant

In this study, an alkali-resistant halophyte, *C. virgata,* a grass with high protein content, which makes it a high-quality forage plant (Zheng and Li, 1999) was used as material. Seeds of *C. virgata* were collected from native grassland in Changling County, Jilin Province, Northeast China, and sown in 17-cm diameter plastic pots containing washed sand. Each pot contained 13 seedlings and seedlings were sufficiently watered with Hoagland nutrient solution every 2 days. Quantity of evaporation was evaluated with weight method (weight of each pot was recorded two times at 8:00 and 16:00). Evaporation was compensated for with distilled water at other times. The research was carried out at Northeast Normal University, Changchun, China during April to July. All pots were placed outdoors and protected from rain. Temperatures during the experiment were 22 to 26°C during the day and 19 to 22°C at night.

Design of simulated salt and alkaline conditions

Salt and alkaline solutions were prepared with Hoagland nutrient solution. Two neutral salts were mixed in a 1:9 molar ratio ($NaCl:Na_2SO_4$), and applied to the salt stress group. Two alkaline salts were mixed in a 1:9 molar ratio ($NaHCO_3:Na_2CO_3$), and applied to the alkali stress group. Within each group, two total salt concentrations (40 and 80 mM) were applied. Therefore, in the 80 mM solution for salt stress, a mixture of 8 mM NaCl and 72 mM Na_2SO_4 would result in total ion concentrations of 152 mM Na^+ + 8 mM Cl^- + 72 mM SO_4^{2-}. In the 80 mM solution for alkali stress, a mixture of 8 mM $NaHCO_3$ and 72 mM Na_2CO_3 would result in total ion concentrations of 152 mM Na^+ + 8 mM HCO_3^- + 72 mM CO_3^{2-}. The pH ranges in the salt stress and alkali stress groups were 6.70 to 6.72 and 10.46 to 10.62, respectively.

Stress treatment

The seedlings of *C. virgata* were treated with varying salt stress (1:9 molar ratio of NaCl to Na_2SO_4; pH 6.70 to 6.72; 40, 80 mM) and alkali stress (1:9 molar ratio of $NaHCO_3$ to Na_2CO_3; pH 10.46 to 10.62; 40, 80 mM) to explore the metabolic control mechanisms of organic acid accumulation as a response to these abiotic stress

factors. When the seedlings of *C. virgata* were 3 weeks old, 15 pots with seedlings growing uniformly were selected and randomly divided into 5 sets, 3 pots per set. One set was used as a control, and the remaining 4 sets were used as various stress treatments. Each pot was considered a single replicate; therefore, there were three replicates per set. Stress treatments were performed once every day around 8:00 am, with the application of nutrient solutions containing the appropriate salts. All pots were watered thoroughly with 500 cm^3 treatment solution applied in three portions. Control plants were maintained by watering with nutrient solution. The entire treatment duration was 3 days.

Organic acid analysis

The composition and content of organic acids in shoots was analyzed and compared to determine the characteristics of organic acids accumulation in response of *C. virgata* to salt and alkali stresses. All plants were harvested in the morning after the final treatment. The plants were first washed with tap water, then with distilled water. Roots and shoots were separated. The samples were oven-dried at 80°C for 15 min, then vacuum-dried at 40°C to constant weight. Shoots were then crushed, and used for testing organic acid. Dry samples (100 mg) were treated with 10 ml deionized water at 100°C for 60 min, and the extract was used to determine the contents of organic acids. Oxalic acid was determined by ion chromatography (DX-300 ion chromatographic system; AS4A-SC ion-exchange column, CD M-II electrical conductivity detector, mobile phase: $Na_2CO_3/NaHCO_3$ = 1.7/1.8 mM; DIONEX, Sunnyvale, USA). The other organic acids were determined by ion chromatography (DX-300 ion chromatographic system; ICE-AS6 ion-exclusion column, CDM-II electrical conductivity detector, AMMS-ICE II suppressor, mobile phase: 0.4 mM heptafluorobutyric acid; DIONEX, Sunnyvale, USA).

Determination of enzyme activity

According to the analysis of organic acids, the relevant enzymes for study were selected and assayed. The main enzymes of the organic acid metabolism should include phosphoenolpyruvate carboxylase (PEPCase, EC 4.1.1.31), citrate synthase (CS, EC 4.1.3.7), aconitase, NADP-isocitrate dehydrogenase (NADP-ICDH, EC 1.1.1.42), Malate dehydrogenase (MDH, EC 1.1.1.37), isocitrate lyase (ICL, EC 4.1.3.1) and malate synthase (MS, EC 4.1.3.2). Following this, *C. virgata* plants were cultivated and treated in exactly the same way as mentioned earlier. After the final treatment, about 3 g leaves were randomly removed with scissors and cut as fresh samples.

Enzyme extraction

250 mg fresh samples were homogenized in an ice-cold pestle and mortar with 4 ml 50 mM HEPES-NaOH buffer (pH 7.5) containing 5 mM $MgCl_2$, 5 mM EDTA, 10% (v/v) glycerol, and 0.1% (v/v) Triton X-100 (Yang et al., 2004). The homogenate was then centrifuged at 15,000 *g* at 4°C for 5 min, and the supernatant was used as the enzyme sources of PEPCase, CS, aconitase, NADP-ICDH and MDH. Another 0.3 g fresh leaves were homogenized in an ice-cold 3 ml 167 mM Tris-HCl buffer (pH 7.5) containing 10 mM KCl, 1 mM EDTA and 1 mM $MgCl_2$. The homogenate was then centrifuged at 10, 000 *g* at 4°C for 5 min and the supernatant was used to measure the activities of ICL and MS (Gerhardt and Beevers, 1970).

Enzyme assay

The final volume of each assay was 1 ml. The activity of CS was spectrophotometrically measured using method of Li et al. (2000). The NADP-ICDH activity was assayed by monitoring the increase of NADPH at 340 nm for 3 min, and according to method of Yang et al. (2004). The activities of PEPCase and MDH were spectrophotometrically assayed by monitoring the decrease of NADH at 340 nm for 3 min using method of Johnson et al. (1994). For the MDH activity measurement, the reaction mixture contained 100 mM Tris–HCl buffer (pH 7.8), 1 mM EDTA, 0.25 mM NADH, 1.25 mM oxaloacetate and 25 µl crude enzyme extract diluted 20 times. The PEPCase reaction mixture contained 100 mM Tris–HCl (pH 7.5), 5 mM $MgCl_2$, 100 mM $NaHCO_3$, 1.5 mM PEP, 1 mM NADH and 2 units of MDH. The activities of MS were assayed by a DTNB method at 30°C (Hock and Beevers, 1966). The ICL assay measured the formation of glyoxylate-phenylhydrazone by following the increase of absorbance at 324 nm at 30°C (Ebel and Schwienbacher, 2006). The protein in the enzyme extract was quantified by the method of Bradford (Bradford, 1976). Each sample was repeated at least five times and the error could not exceed 5%.

Data analysis

Each result was the mean of at least three replicated treatments. Values indicate mean ± standard error (SE). Statistical analyses were performed by one-way analysis of variance (ANOVA) using the statistical program SAS. The treatment mean values within the same stress type were compared by post hoc least significant difference (LSD) test at 0.05 level.

RESULTS

Qualitative and quantitative changes of organic acids under salt and alkali stress

The analysis of organic acid composition showed that there were no changes in composition of organic acids in the shoots of *C. virgata* under salt and alkali stress compared with the control. Citrate, malate, succinate, acetate, oxalate and lactate were detected in *C. virgata* shoots (Figure 1). However, the content of total organic acids and the percentages of six organic acids to total organic acid in the shoots of *C. virgata* were significantly different between salt stress and alkali stress. The content of total organic acids increased remarkably with increasing salinity under alkali stress (Figure 1, $p<0.01$), and they increased to 2.3 and 3.3 times that of control for 40 and 80 mM alkali stress, respectively. Of these, citrate content was the greatest, with 26.2 and 44.9% of total organic acids, and increased to 4.6 and 11.3 times than that of the control in shoots (Table 1) for 40 and 80 mM alkali stress, respectively ($p<0.01$). For malate, they were 40.3 and 26.9% and increased to 2.9 and 2.8 times, respectively ($p<0.001$). In addition, the alkali stress increased the content of lactate, succinate and acetate weakly to different extents (Figure 1).

Enzyme activity responses to salt and alkali stress

The activities of CS in leaves of *C. virgata* increased significantly with increasing salinity under alkali stress

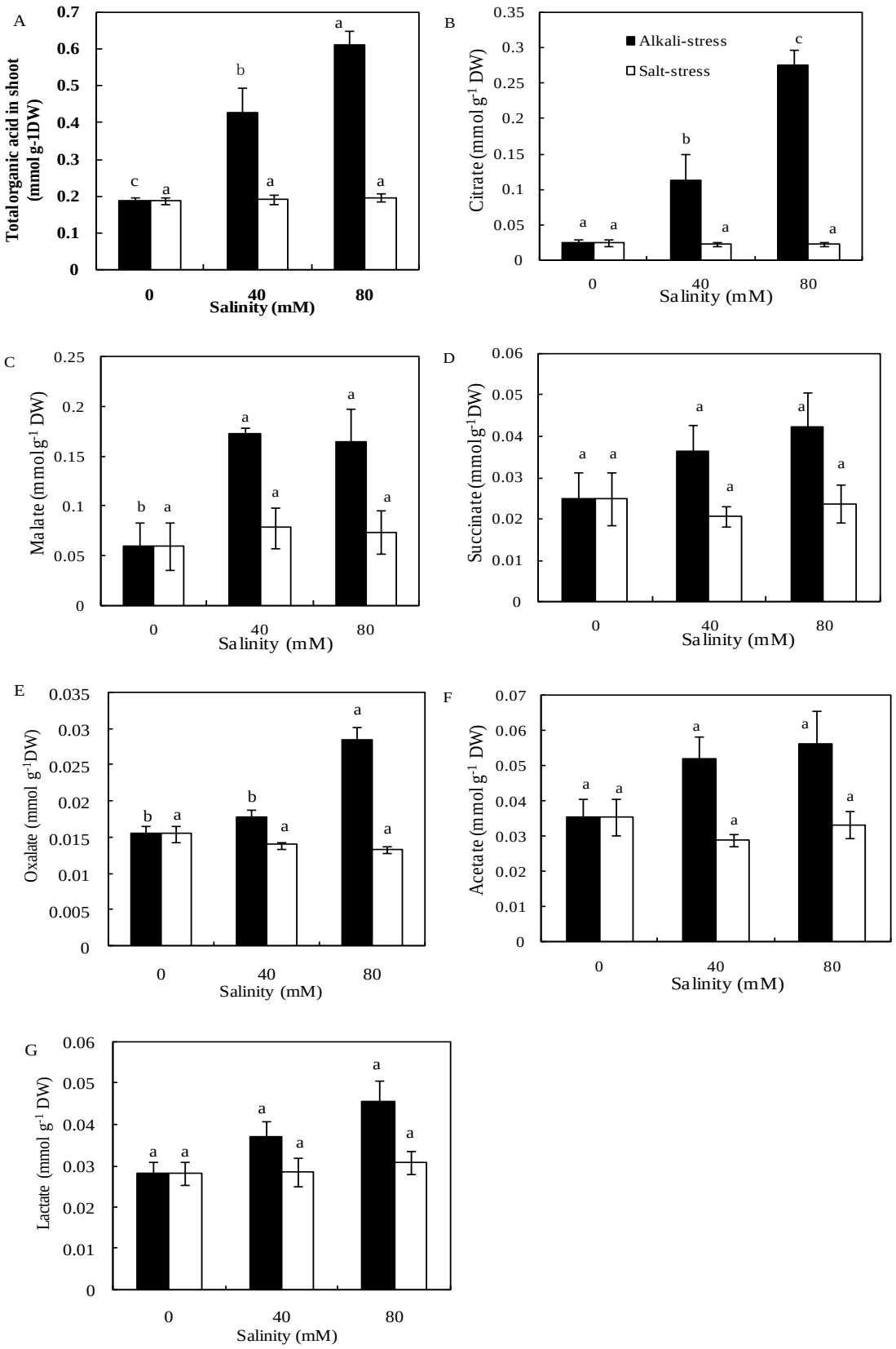

Figure 1. Effects of alkali and salt stresses on contents of organic acids in shoots of *C. virgata*. The values are means ± S.E. of three replicates. Means followed by different letters within the same stress type are significantly different at P ≤ 0.05, according to post hoc least significant difference (LSD) test.

Table 1. Percentage contribution of six organic acids to total moles of organic acid in *C. virgata* shoots under salt and alkali stresses. Percentage is calculated according to the means of three replications.

Parameter	Salinity (mM)	Citrate (%)	Malate (%)	Succinate (%)	Acetate (%)	Oxalate (%)	Lactate (%)
Control	0	13	31.6	13.2	18.9	8.3	15
Alkali stress	40	26.2	40.3	8.5	12.2	4.2	8.6
	80	44.9	26.9	6.9	9.2	4.7	7.4
Salt stress	40	11.8	40.6	10.6	15	7.2	14.8
	80	11.3	37.4	12	16.8	6.8	15.7

($p<0.01$); they increased by 10.4 and 14.9%, respectively, compared to the control under 40 and 80 mM alkali stress (Figure 1). PEPCase activity showed little change or decreased weakly. In the meantime, the activity of aconitase decreased slowly under 80 mM alkali stress, MDH activity markedly decreased, but the activity of NADP-ICDH increased significantly. However, the activities of PEPCase, CS, aconitase, NADP-ICDH and MDH in leaves of *C. virgata* were unaffected or increased weakly by exposure to 40 and 80 mM salt stress.

Under salt stress, the activity of ICL had no significant change, but its activity increased markedly under alkali stress ($p<0.0001$). Salt and alkali stress all increased MS activity, but it was greater under alkali stress ($p<0.0001$) than under salt stress ($p<0.05$); it increased to 1.51 and 1.55 times as against the control for 40 and 80 mM alkali stress, respectively, but it was greater only 1.16 and 1.17 times for 40 and 80 mM salt stress, respectively.

DISCUSSION

Accumulation of organic acids is the key physiological response for *C. virgata* during adaptation to alkali stress

Some reports have clearly demonstrated that alkali salt and salt stress are two distinct kinds of stress for plants and that the effects of alkali stress on plants are more severe than those of salt stress (Yang et al., 2008a, b, c). An explanation for the different effects of the two stresses might be their different mechanisms of action on plants. The injurious effects of salt stress may be a result of low water potentials and ion toxicities. Alkali stress consists of the same stress factors as salt stress, but the influence of high pH is added. The high pH environment surrounding the roots not only may have effect on the ion activities in the nutrient solution, but also may directly cause metal ions, such as Ca^{2+}, Mg^{2+}, Fe^{2+} and Cu^{2+}, to precipitate (Shi and Zhao, 1997), which may lead to depletion of the nutrient supply and disturbance of ion balance around the roots.

The previous studies have also indicated that accumulation of organic acids in plants was an adaptive response to the influx of sodium ions and an important mechanism to maintain stable tissue pH and ion balance for the internal environment (Yang et al., 2007; Shi et al., 2002). Our results also show that the stable tissue pH and ion balance maintained in *C. virgata* is primarily due to the significant accumulation of organic acids. Results shown in Figure 2 indicate that various organic acids and the ratio of each component, do not change much under salt stress. However, a large number of organic acids accumulated under alkali stress, especially for citrate and malate.

Although, an accumulation of organic aids in shoots is a widespread physiological response to plants under alkali stress, the characteristics of organic acid accumulation, especially the kinds of organic acids among various species, is obviously different. For instance, it was reported that the oxalate represented about 90% of total organic acids in the stems and leaves of *K. sieversiana* (Yang et al., 2007) and *S. glauca* (Yang et al., 2008c); oxalate was also the dominant accumulated component under alkali stress. However, *C. virgata* was found to predominantly accumulate citrate under alkali stress; the contents of 40 and 80 mM alkali stress treatments were greater 4.6 and 11.3 times compared with the control, respectively. The gramineous halophyte *P. tenuiflora*, which is in the same family as *C. virgata,* also mainly accumulated citrate under alkali stress (Shi et al., 2002). This may indicate that the plants of different families and genus (or even from the same family), have different metabolic control mechanism of organic acids under alkali stress.

The metabolic control regulation mechanism of organic acids under alkali stress in *C. virgata*

Organic acid metabolism exerts key roles in the plant adapting to various adversity stresses (Ryan et al., 1995; Wang et al., 2007; Ligaba et al., 2004; Rauser, 1999; Yang et al., 2007). A large amount of published data has shown the formation and transport of organic acids in plant cells, characteristics of related enzymes and the exudation of roots (Wang, 2001; López-Bucio et al., 2000; Li et al., 2000). The characteristics of organic acid

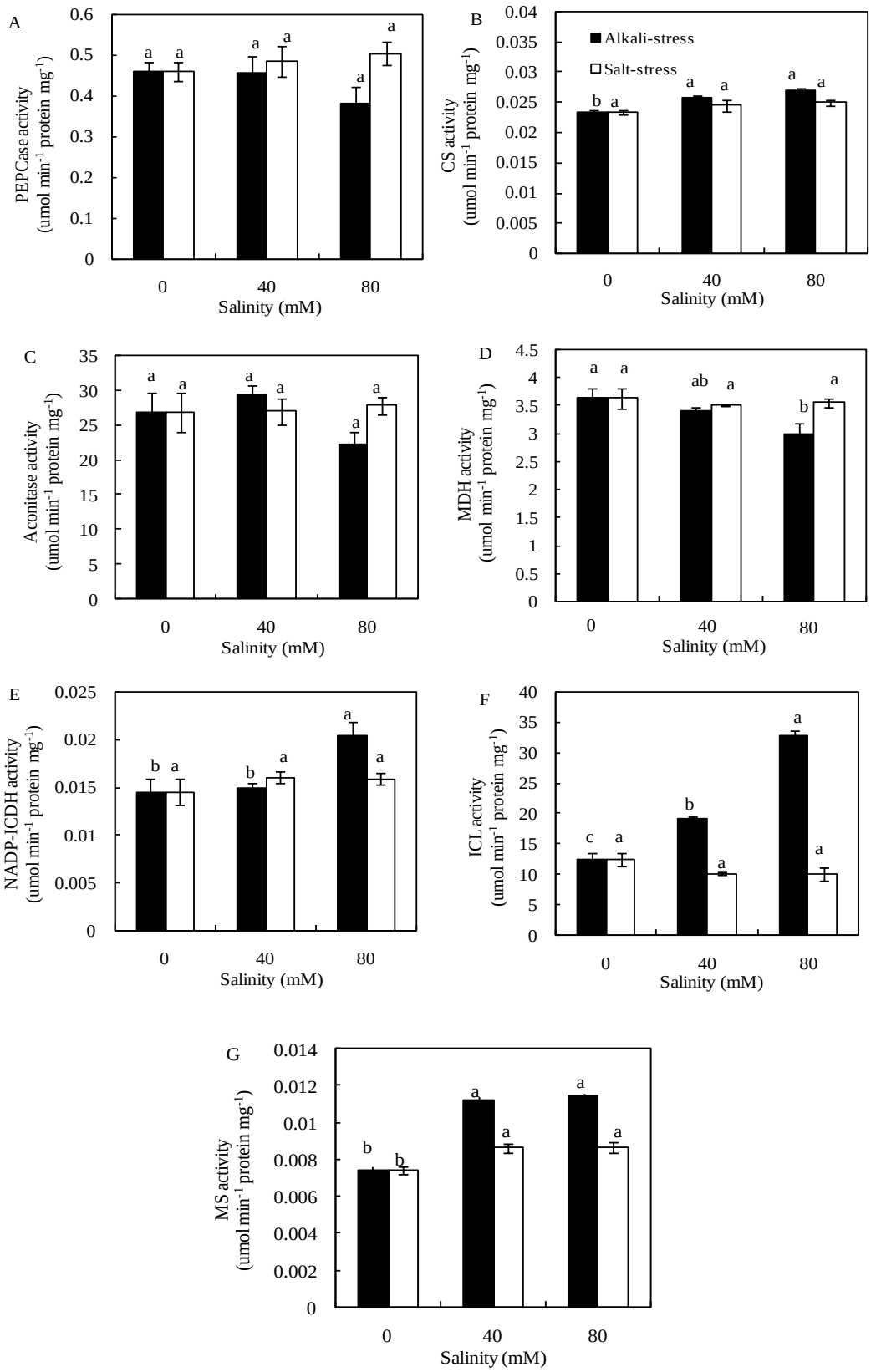

Figure 2. Effects of alkali and salt stresses on activities of key enzymes involved in organic acid metabolism in leaves of *C. virgata*. The values are means ± S.E. of three replicates. Means followed by different letters within the same stress type are significantly different at $P \leq 0.05$, according to post hoc least significant difference (LSD) test.

metabolism at the enzyme level should be revealed under alkali stress by monitoring the key enzymes that determine the rates of relevant reactions under alkali stress. Furthermore, the key genes of plant alkali tolerance would be easily identified by finding the key enzymes of plant alkali tolerance. According to the dominantly accumulated organic acids under alkali stress, citrate and malate, the activities of relevant enzymes were determined and assayed and were expected to reveal the organic acid metabolism in *C. virgata* under alkali stress.

The enzymes, such as CS, MDH, PEPCase, aconitase, and NADP-ICDH involved in synthesis or degradation of citrate, all affect the accumulation of citrate in plants. Yang et al. (2004) reported that aluminium-induced exudation of citrate from roots of *C. tora* was mainly due to the increase in CS activity and the decrease in aconitase activity, but NADP-ICDH, MDH and PEPCase were not directly involved in this physiological process. The P-stressed proteoid roots of *Lupinus albus* also largely excreted citrate, but the activities of CS, MDH and PEPCase were all increased. Meanwhile, western blot analysis also showed that the PEPCase enzyme protein was more highly expressed in –P proteoid roots compared to other tissues (Johnson et al., 1994). The organic acid metabolism is extremely complex in plants and various stress-induced metabolism control mechanisms may also be different. Our results proved this point and showed that the activities of enzymes involved in organic acid accumulation did not alter much under salt stress; however, some enzymes changed significantly under alkali stress (Figure 2).

Our results showed that the CS activity was significantly increased under alkali stress, which may be the main reason for the accumulation of citrate. In addition, the cytosolic form of NADP-ICDH is probably the major pathway for the catabolism of citrate after its transport out of mitochondria and conversion to isocitrate by aconitase in the cytosol (Delhaize et al., 2003; Gálvez et al., 1999). It had been shown that carrot cell lines with a high citrate efflux have reduced NADP-ICDH activity, along with enhanced CS activity, which is consistent with a role for the cytosolic NADP-ICDH in contributing towards the control of citrate concentrations in plant cells (Takita et al., 1999; Kihara et al., 2003). However, the NADP-ICDH activity was significantly increased under 80 mM alkali stress; although this was not conducive to the explanation of accumulated citrate, it was beneficial to interpreting the accumulation of malate simultaneously. Interestingly, alkali stress did not affect the PEPCase activity, indicating that this enzyme was not the limiting factor for the substrate of synthesizing citrate.

The experimental data showed that, although MS activity significantly increased under salt stress, ICL, NADP-ICDH, PEPCase and MDH activities showed little change; this may be one of the reasons for the unchanged malate content. However, MS activity increased significantly under 40 mM alkali stress; when the alkali stress intensity increased to 80 mM, the activities of MS and ICL increased significantly, whereas MDH activity decreased. These results indicated that the changes in these enzyme activities facilitated the accumulation of malate. However, the activities of two specific enzymes in the glyoxylate cycle, namely, MS and ICL, were significantly increased under alkali stress, which might contribute to the malate accumulation. Although, ICL and NADP-ICDH compete for the same substrate, isocitrate, the two enzymes may be expressed together. Malate accumulated sharply due to the high-level expression of glyoxylate-cycle enzymes under alkali stress. The isocitrate, citrate and oxaloacetate may be transported to glyoxysome to support the glyoxylate-cycle activity. When plants become senescent or are kept in the dark for a longer period of time, they start to degrade their endomembrane system and the glyoxylate cycle becomes important in exploiting the end product of fatty acid β-oxidation (Cornah and Smith, 2002). The malate accumulation may also be associated with lipid metabolism under alkali stress.

The organic acid accumulation response to alkali stress was a comprehensive regulated result of two or more enzymes for *C. virgata*: CS, MS and ICL might play key roles in this process. However, the regulation of enzyme activity was likely to be a complex process that occurred at different levels or at different stages, such as transcription, translation, zymoprotein assembly or modification. It could also be the result of interactions of enzyme inhibitors or activators with other regulating substances. Thus, the organic acid metabolic control mechanism at the enzyme level remains to be further studied.

Intracellular organic acid accumulation was not only related to the organic acid metabolism, but also to the organic acid transport. Organic acids synthesized in mitochondria or other parts entered into the certain sites through carriers or specific channels for storage or other specific physiological functions. Under alkali stress, organic acids were mainly transferred to the vacuole and accumulated in order to balance the positive charge and regulate intracellular pH (Yang et al., 2007; Shi et al., 2002). The transport route and efficiency are also closely related to the accumulation of organic acids, and this is worth studying further. Some research had concerned the gene expression and protein interaction in response of plants to alkali stress (Wang et al., 2015a, 2012; Gong et al., 2014; Sun et al., 2014). Metabolism regulation of organic acid should be considered in model plants such as rice and Arabidopsis, which may further facilitate the identification of gene involved in alkali tolerance.

Conflict of Interests

The authors have not declared any conflict of interests.

ACKNOWLEDGEMENTS

This study was supported by 13th Five-Year Science and Technology Project of Educational Department of Jilin Province (No. 2016195), Initial Project of Jilin Agricultural University (No. 201508), and Key Project of Science and Technology Development in Jilin Province (No. 20126033). We thank anonymous reviewer for the critical and constructive comments for further improving of the manuscript.

REFERENCES

Allakhverdiev SI, Sakamoto A, Nishiyama Y, Inaba M, Murata N (2000). Ionic and osmotic effects of NaCl-induced inactivation of photosystems I and II in *Synechococcus* sp. Plant Physiol. 123:1047-1056.

Bradford MM (1976). A rapid and sensitive method for the quantitation of microgram of proteins utilizing the principle of protein–dye-binding. Anal. Biochem. 72:248-254.

Cornah JE, Smith SM, (2002). In. Baker A, Graham IA (Eds.) Plant Peroxisomes. Kluver Academic Publishers, London, Pp. 57-101.

Cushman JC (1993). Molecular-cloning and expression of chloroplast NADP-malate dehydrogenase during crassulacean acid metabolism induction by salt stress. Photosynth. Res. 35:15-27.

Delhaize E, Ryan PR, Hocking PJ, Richardson AE (2003). Effects of altered citrate synthase and isocitrate dehydrogenase expression on nternal citrate concentrations and citrate efflux from tobacco (*Nicotiana tabacum* L.) roots. Plant Soil 248:37-144.

Delhaize E, Ryan PR, Randall PJ (1993). Aluminum tolerance in wheat (*Triticum aestivum*) II. Aluminum-stimulated excretion of malic acid from root apices. Plant Physiol. 103:695-702.

Ebel F, Schwienbacher M (2006). Analysis of the regulation, expression, and localisation of the isocitrate lyase from *Aspergillus fumigatus*, a potential target for antifungal drug development. Fungal Genet. Biol. 43:476-489.

Gerhardt BP, Beevers H (1970). Developmental studies on glyoxysomes in Ricinus endosperm. J. Cell Biol. 44:94-102.

Gong B, Zhang CJ, Li X, Wen D, Wang SS, Shi QH (2014). Identification of NaCl and $NaHCO_3$ stress responsive proteins in tomato roots using iTRAQ-based analysis. Biochem. Biophys. Res. Commun. 446:417-422.

Hock B, Beevers H (1966). Development and decline of the glyoxylate cycle enzymes in watermelon seedlings (*Citrullus vulgaris, Schrad*.). Effects of dactinomycin and cycloheximide. Z Pfanzenphysiol. 55:405-414.

Johnson JF, Allan DL, Vance CP (1994). Phosphorus stress–induced proteoid roots show altered metabolism in *Lupinus albus*. Plant Physiol. 104:657-665.

Kihara T, Ohno T, Koyama H, Takuya Sawafuji, Tetsuo Hara (2003). Characterization of NADP-isocitrate dehydrogenase expression in a carrot mutant cell line with enhanced citrate excretion. Plant Soil. 248:145-153.

Kumar RG, Shah K, Dubey RS (2000). Salinity induced behavioural changes in malate dehydrogenase and glutamate dehydrogenase activities in rice seedlings of differing salt tolerance. Plant Sci. 156:23-34.

Li XF, Ma JF, Matsumoto H (2000). Pattern of aluminum-induced secretion of organic acids differs between rye and wheat. Plant Physiol. 123:1537-1543.

Ligaba A, Shen H, Sasaki T, Yamamoto Y, Tanakamaru S, Matsumoto H (2004). The role of phosphorus in aluminum-induced citrate and malate exudation from rape (*Brassica napus*). Physiol. Plant. 120:575-584.

López-Bucio J, Nieto-Jacobo MF, Ramírez-Rodríguez V, Herrera-Estrella L (2000). Organic acid metabolism in plants: from adaptive physiology to transgenic varieties for cultivation in extreme soils. Plant Sci. 160:1-13.

Miyasaka SC, Buta JG, Howell RK, Foy CD (1991). Mechanism of aluminum tolerance in Snap beans. Plant Physiol. 96:737-743.

Popova OV, Ismailov SF, Popova TN, Dietz KJ, Golldack D (2002). Salt-induced expression of NADP-dependent isocitrate dehydrogenase and ferredoxin-dependent glutamate synthase in *Mesembryanthemum crystallinum.* Planta 215:906-913.

Rauser WE (1999). Structure and function of metal chelators produced by plants. Cell Biochem. Biophys. 31:19-48.

Ryan PR, Delhaize E, Randall PJ (1995). Characterization of Al-stimulated efflux of malate from the apices of Al-tolerant wheat roots. Planta 196:103-110.

Shi DC, Sheng YM (2005). Effect of various salt–alkaline mixed stress conditions on sunflower seedlings and analysis of their stress factors. Environ. Exp. Bot. 54:8-21.

Shi DC, Yin LJ (1993). Difference between salt (NaCl) and alkaline (Na_2CO_3) stresses on *Puccinellia tenuiflora* (Griseb.) Scribn. et Merr. plants. Acta Bot. Sin. 35:144-149.

Shi DC, Yin SJ, Yang GH, Zhao KF (2002). Citric acid accumulation in an alkali-tolerant plant *Puccinellia tenuiflora* under alkaline stress. Acta Bot. Sin. 44:537-540.

Shi DC, Zhao KF (1997). Effects of NaCl and Na_2CO_3 on growth of *Puccinellia tenuiflora* and on present state of mineral elements in nutrient solution. Acta Pratacu. Sin. 6(2):51-61.

Sun X, Yang S, Sun M, Wang X, Zhu Y (2014). A novel *Glycine soja* cysteine proteinase inhibitor GsCPI14, interacting with the calcium/calmodulin-binding receptor-like kinase GsCBRLK, regulated

Takita E, Koyama H, Hara T (1999). Organic acid metabolism in aluminum-phosphate utilizing cells of carrot (*Daucus carota* L.). Plant Cell Physiol. 40:489-495.

Wang BL, Shen JB, Zhang WH, Zhang FS, Neumann G (2007). Citrate exudation from white lupin induced by phosphorus deficiency differs from that induced by aluminum. New Phytol. 176(3):81-589.

Wang H, Ahan J, Wu Z, Han J, Shi D, Yang C (2012). Alteration of nitrogen metabolism in rice variety 'Nipponbare' induced by alkali stress. Plant Soil 355:131-147.

Wang H, Lin X, Cao S, Wu Z (2015a). Alkali tolerance in rice (*Oryza sativa* L.): growth, photosynthesis, nitrogen metabolism, and ion homeostasis. Photosynthetica 53:55-65.

Wang X, Geng S, Ma Y, Shi D, Yang C, Wang H (2015b).Growth, Photosynthesis, Solute Accumulation, and Ion Balance of Tomato Plant under Sodium- or Potassium-Salt Stress and Alkali Stress. Agron. J. 107:1-11.

Wang XL (2001). Carboxylic acid. In. Wang XL (ed) Organic Chemistry. Higher Education Press, Beijing. pp. 149-150.

Yang CH, Crowley DE (2000). Rhizosphere microbial community structure in relation to root location and plant iron nutritional status. Appl. Environ. Microbiol. 66:345-351.

Yang CW, Chong JN, Li CY, Kim CM, Shi DC, Wang DL (2007). Osmotic adjustment and ion balance traits of an alkali resistant halophyte *Kochia sieversiana* during adaptation to salt and alkali conditions. Plant Soil 294:263-276.

Yang CW, Jianaer A, Li CY, Shi DC, Wang DL (2008a). Comparison of the effects of salt-stress and alkali-stress on photosynthesis and energy storage of an alkali-resistant halophyte *Chloris virgata*. Photosynthetica 46(2):273-278.

Yang CW, Shi DC, Wang DL (2008c). Comparative effects of salt and alkali stresses on growth, osmotic adjustment and ionic balance of an alkali-resistant halophyte *Suaeda glauca* (Bge.). Plant Growth Regul. 56:179-190.

Yang CW, Wang P, Li CY, Shi DC, Wang DL (2008b). Comparison of effects of salt and alkali stresses on the growth and photosynthesis of wheat. Photosynthetica 46(1):107-114.

Yang ZM, Yang H, Wang J, Wang YS (2004). Aluminum regulation of citrate metabolism for Al-induced citrate efflux in the roots of *Cassia tora* L. Plant Sci. 166:1589-1594.

Zheng HY, Li JD (1999). Form and dynamic trait of halophyte community. In. Zheng HY, Li JD (eds) Saline plants in Songnen plain and restoration of alkaline-saline grass. Science Press, Beijing, China. pp. 137-138.

academicJournals

Vol. 15(40), pp. 2251-2258, 5 October, 2016
DOI: 10.5897/AJB2016.15490
Article Number: DC526E960856
ISSN 1684-5315

http://www.academicjournals.org/AJB

African Journal of Biotechnology

Full Length Research Paper

Comparison of four nonlinear growth models for effective exploration of growth characteristics of turbot *Scophthalmus maximus* fish strain

Xin'an Wang[1,2,3,4] and Aijun Ma[1,2,3,4]*

[1]Yellow Sea Fisheries Research Institute, Chinese Academy of Fishery Sciences, China.
[2]Key Laboratory of Sustainable Development of Marine Fisheries, Ministry of Agriculture, China.
[3]Qingdao Key Laboratory for Marine Fish Breeding and Biotechnology, Qingdao 266071, China.
[4]Laboratory for Marine Biology and Biotechnology, Qingdao National Laboratory for Marine Science and Technology, Qingdao 266071, China.

Received 24 May, 2016; Accepted 15 September, 2016

This study was conducted to compare the effectiveness for non-linear growth models designated as Chapman-Richards, Gompertz, Logistic and von Bertalanffy for selection of fast-growing fish strain of turbot *Scophthalmus maximus*. These models were compared using the goodness of fit (the coefficient of determination (R^2) and the mean square error (MSE)) and the Akaike information criterion (AIC) and the growth characteristics of turbot from 3 to 27 months of age. The results in the present study showed that R^2 was the highest in Chapman-Richards, but the lowest in von Bertalanffy model. The MSE and AIC values were the highest in Chapman-Richards followed by von Bertalanffy model, whereas Gompertz model is the lowest compared to other models. The Gompertz model had the lowest mean square error (6421.8706) and Akaike information criterion (65.1322) and *the second highest* coefficient of determination (0.9908) (*almost equal to* the first highest coefficient of determination), suggesting being the best fit model for description of turbot growth trajectories. Furthermore, the results of turbot growth characteristics explored by the Gompertz model revealed that the fast-growth time interval of turbot were (10.23, 26.78) (unit: months) and the fast-growth time interval distance was 16.55 months. The results of this study suggested that the Gompertz model could be the best fit model for description of turbot growth trajectories, whereas the deduced mathematical formulas of growth intervals could be used in determining the growth characteristics of other fish.

Key words: *Scophthalmus maximus*, nonlinear models, comparison, growth characteristics.

INTRODUCTION

Turbot *Scophthalmus maximus* (L.) is a commercial flatfish inhabiting European waters (Ruan et al., 2011). It was first introduced into China in 1992 (Ruan et al., 2011; Liang et al., 2012). However, as a result of technological

*Corresponding author. Email: maaj@ysfri.ac.cn. Tel/Fax: +86 532 85835103.

problem-solving in the large-scale artificial breeding, the commercial culture of the species has been spreading rapidly along the coast of China (Wang et al., 2015). But, due to the degeneration of germplasm, it is necessary to carry out the selective breeding (Wang et al., 2015). However, the most important economic trait considered in an aquaculture breeding program has been growth rate which determine the total harvest yield (Wang et al., 2010). In this respect, the number of research has been carried out in turbot breeding for growth under the support of Chinese Government.

The selection for rapid growth breeding is commonly evaluated using the body weight collected from one single time point (usually in commercial-size fish), that is, point evaluations. But, the genes are expressed selectively at different growth stages in specific temporal and spatial patterns (Atchley and Zhu, 1997), whereas genetic mechanism controlling quantitative traits have significant changes at various developmental periods during ontogeny *(*Atchley and Zhu, 1997*).* This scenario could lead to uncertainty in determining fish growth rates under different space-time conditions and this could suggest probably that the use of point evaluations for determining fish growth rate could not be appropriate. However, the nonlinear growth models based on general system theory could be a good approach in solving this problem*,* that is, curve evaluations (Richards, 1959). The curve evaluations defined by nonlinear growth models has definite advantages over point evaluations. This is because point evaluations are based on constant ages, constant time periods or constant weight periods, whereas non-linear growth models provides parameters that can describe the biological growth along the entire lifetime (Masso et al., 2000).

The nonlinear growth models which have been extensively used in fish are Chapman-Richards (Richards, 1959), Gompertz (Gompertz, 1825), Logistic (Richards, 1959) and von Bertalanffy (Bertalanffy, 1938) models. The characteristics of these models have been studied in detail by Fitzhugh (1976), Deniel (1990), Tsangridis and Filippousis (1994), Imai et al. (2002), Tsoularis and Wallace (2002), Katsanevakis and Maravelias (2008), Lin and Tzeng (2009), Helidoniotis et al. (2011), Baer et al. (2011), Bilgin et al. (2014), Figueiredo et al. (2014), Ansah and Frimpong (2015); Drew et al. (2015), and Lugert et al. (2016). Moreover, some relevant mathematical formulas reflecting biological growth characteristics, such as time to inflection point, weight at inflection point, instantaneous growth rate and relative growth rate were reported by various authors (Fitzhugh, 1976; France et al., 1996; Tsoularis and Wallace, 2001; Koya and Goshu, 2013). However, the mathematical formulas of different growth intervals have not been previously reported. The whole growth process of fish can be divided into slow-growing, fast-growing and asymptotic period by two extreme points (starting point and ending point), that is, slow-growing, fast-growing and asymptotic interval. In slow-growing period, the body weight increased slowly as the instantaneous growth rate is low and increased slowly. In fast-growing period, the instantaneous growth rate during the period is higher than that during both slow-growing and asymptotic period; body weight, therefore, also increase quickly. In asymptotic period, the instantaneous growth rate continues declining and reduces slowly to zero. Among, the fast-growing period, interval has important significance on the study of the growth characteristics of fish.

Various nonlinear growth models have been proposed to explain the growth pattern of individuals for a particular species (Bilgin et al., 2014). Growth pattern of turbot or other flatfish species are mainly described by von Bertalanffy model (Deniel, 1990), von Bertalanffy, Schnute, and Gompertz model (Baer et al., 2011) and logistic, Gompertz, von Bertalanffy, Kanis, and Schnute models (Lugert et al., 2016), due to goodness of fit of the data. And Chapman-Richards model encompasses Gompertz ($m \rightarrow 1$), Logistic ($m = 2$) and von Bertalanffy ($m = 2/3$) models for particular values of parameter m. So, the four nonlinear growth models including Chapman-Richards, Gompertz, Logistic and von Bertalanffy were applied to turbot to obtain reliable and suitable growth parameters to explore the growth characteristics of turbot. The objective of this study was to identify appropriate non-linear growth model which best fit for determining the growth rate and establish mathematical formulas exploring growth intervals of rapid growing turbot fish strain. It is anticipated that the identified model and deduced mathematical formula of growth intervals could help in evaluating the effects of selection in the process of turbot breeding.

MATERIALS AND METHODS

Study area

This study was carried out in China Tianyuan Aquaculture Ltd.

Source and management experimental turbot fish strain

The fast growing strain of turbot fish were obtained from China Tianyuan Aquaculture Ltd. The fifty fish were weighed using an electronic balance with a precision of 0.01 g (Table 1) at every 3-month intervals from 3 to 27 months of age. The rearing conditions of experimental fish at different stages of growth periods were same as recommended by Wang et al. (2010).

Analytical procedure

Analysis of parameters of non-linear growth models

The Chapman-Richards, Gompertz, Logistic and von Bertalanffy models were compared by fitting the data to model the relationship between weight and age. The goodness of fit was assessed by

Table 1. Mean body weight of turbot in different month of age (mean values ± standard deviations).

Month	3	6	9	12	15	18	21	24	27
Body weight (g)	2.09 ± 0.51	47.21 ± 10.68	162.02 ± 33.46	311.07 ± 60.94	619.85 ± 97.42	1001.07 ± 129.67	1203.59 ± 244.91	1784.54 ± 328.28	1865.48 ± 401.56

using the coefficient of determination (R^2) and mean square error (MSE) according to Gbangboche et al. (2008) and the lower Akaike information criterion (AIC) (Akaike, 1974). The models parameters (A, B, k and m), the R^2 and MSE were calculated using *SAS* software package (SAS 1999). The four models used in this study are as follows:

Chapman-Richards: $W_t = A(1-Be^{-kt})^{1/(1-m)}$ (Richards 1959);
Gompertz: $W_t = Ae^{-B\exp(-kt)}$ (Gompertz,1825);
Logistic: $W_t = A(1+Be^{-kt})^{-1}$ (Richards 1959);
von Bertalanffy: $W_t = A(1-Be^{-kt})^3$ (Bertalanffy, 1938).

where W_t is the body weight at time t, t is time, A is the asymptote value, B is the scale parameter, k is the intrinsic growth rate representing growth rate per capita and m is the inflection parameter, which determines the shape of the function.

AIC is a measure to help in the selection between candidate models. Using this criterion, the best model is the one with the lowest AIC results. AIC was calculated as (Bilgin et al., 2014):

AIC = $N\log(\mathrm{WSS})+2M$,

where N is the number of data points, WSS is the weighted sum of squares of residuals, and M is the number of model parameters.

Analysis for growth intervals for turbot

The growth intervals of turbot were determined by deducing the mathematical formulas of three growth intervals of the four non-linear models shown subsequently. The growth curves of the four models had inflection points and the growth processes were divided into accelerated and decelerated periods using the point of inflection. The instantaneous growth rate of the four models had two inflection points and the growth process were divided into slow, fast and asymptotic periods using these two points (starting point and ending point).

(1) Chapman-Richards: $W_t = A(1-Be^{-kt})^{1/(1-m)}$

The instantaneous growth rate ($\mathrm{d}W/\mathrm{d}t$) can be written as follows:

$\mathrm{d}W/\mathrm{d}t = kW_t/(1-m)[(A/W_t)^{1-m}-1]$

Growth acceleration ($\mathrm{d}^2W/\mathrm{d}t^2$) can be described as follows:

$\mathrm{d}^2W/\mathrm{d}t^2 = g(t)\cdot k\cdot\{m/(1-m)\cdot(W_t/A)^{m-1}\cdot[1-(W_t/A)^{1-m}]-1\}$

where $g(t) = \mathrm{d}W/\mathrm{d}t$ and $\mathrm{d}^3W/\mathrm{d}t^3 = Amk^3Be^{-kt}(1-Be^{-kt})^{m-3}[m^2(Be^{-kt})^2-(3m-1)\,Be^{-kt}+1]$

Setting $\mathrm{d}^3W/\mathrm{d}t^3 = 0$ produces the following equation:

$Amk^3Be^{-kt}(1-Be^{-kt})^{m-3}[m^2(Be^{-kt})^2-(3m-1)\,Be^{-kt}+1] = 0$

Solving this equation produces the following:

$t = \ln X/k$,

where $X_{1,2} = B(m+2\pm\sqrt{m^2+4m})/[2(m-1)]$

The rate of change in the instantaneous growth rate has two extreme values and the responding body weight W_t is as follows:

$W_t = A[1+(m-1)\,(m+2\mp\sqrt{m^2+4m})/2]^{1/(1-m)}$

The time interval distance $\triangle t$ between the two extreme values can be written as follows:

$\triangle t = t_2-t_1 = \ln[(m+2+\sqrt{m^2+4m})/(m+2-\sqrt{m^2+4m})]/k$

(2) Gompertz: $W_t = Ae^{-B\exp(-kt)}$

Instantaneous growth rate ($\mathrm{d}W/\mathrm{d}t$) based on Gompertz model can be written as follows:

$\mathrm{d}W/\mathrm{d}t = kW_t(\ln A-\ln W_t)$

Growth acceleration ($\mathrm{d}^2W/\mathrm{d}t^2$) can be written as follows:

$\mathrm{d}^2W/\mathrm{d}t^2 = Bk^2W_te^{-kt}(Be^{-kt}-1)$

$\mathrm{d}^3W/\mathrm{d}t^3 = ABk^3e^{-kt-Be^{-kt}}[Be^{-kt}-(3+\sqrt{5})/2][Be^{-kt}-(3-\sqrt{5})/2]$

Setting $\mathrm{d}^3W/\mathrm{d}t^3 = 0$ produces the following equation:

$[Be^{-kt}-(3+\sqrt{5})/2][Be^{-kt}-(3-\sqrt{5})/2] = 0$

Solving this equation produced the following:

$Be^{-kt}-(3+\sqrt{5})/2 = 0 => t_1 = -\ln[(3+\sqrt{5})/(2B)]/k => W_1 = Ae^{-(3+\sqrt{5})/2}$

$Be^{-kt}-(3-\sqrt{5})/2 = 0 => t_2 = -\ln[(3-\sqrt{5})/(2B)]/k => W_2 = Ae^{-(3-\sqrt{5})/2}$

The time interval distance $\triangle t$ between the two extreme values is written as follows:

$\triangle t = t_2-t_1 = \ln[(3+\sqrt{5})/(3-\sqrt{5})]/k$.

(3) Logistic: $W_t = A(1+Be^{-kt})^{-1}$

Instantaneous growth rate ($\mathrm{d}W/\mathrm{d}t$) based on Logistic model can be written as follows:

$\mathrm{d}W/\mathrm{d}t = kW_t(1-W_t/A)$

Growth acceleration ($\mathrm{d}^2W/\mathrm{d}t^2$) can be written as follows:

$\mathrm{d}^2W/\mathrm{d}t^2 = k^2W_t(1-W_t/A)\,(1-2W_t/A)$

$d^3W/dt^3 = ABk^2e^{-kt}[Be^{-kt}-(2+\sqrt{3})][\ Be^{-kt}-(2-\sqrt{3})]/(1+Be^{-kt})^4$

Setting $d^3W/dt^3 = 0$ produces the following equation:

$[Be^{-kt}-(2+\sqrt{3})][\ Be^{-kt}-(2-\sqrt{3})] = 0$

Solving this equation produced the following:

$Be^{-kt}-(2+\sqrt{3}) = 0 => t_1 = -\ln[(2+\sqrt{3})/B]/k => W_1 = A/(3+\sqrt{3})$

$Be^{-kt}-(2-\sqrt{3}) = 0 => t_2 = -\ln[(2-\sqrt{3})/B]/k => W_2 = A/(3-\sqrt{3})$

The time interval distance $\triangle t$ between the two extreme values is as follows:

$\triangle t = t_2-t_1 = \ln[(2+\sqrt{3})/(2-\sqrt{3})]/k.$

(4) von Bertalanffy: $W_t = A(1-Be^{-kt})^3$

Instantaneous growth rate (dW/dt) based on von Bertalanffy model can be written as follows:

$dW/dt = 3kW_t[(A/W_t)^{1/3}-1]$

Growth acceleration (d^2W/dt^2) can be written as follows:

$d^2W/dt^2 = 3ABk^2e^{-kt}(W_t/A)^{1/3}(3\ Be^{-kt}-1)$

$d^3W/dt^3 = 3ABk^3e^{-kt}[Be^{-kt}-(4+\sqrt{7})/9][\ Be^{-kt}-(4-\sqrt{7})/9]$

Setting $d^3W/dt^3 = 0$ produces the following equation:

$[Be^{-kt}-(4+\sqrt{7})/9][\ Be^{-kt}-(4-\sqrt{7})/9] = 0$

Solving this equation produces the following:

$Be^{-kt}-(4+\sqrt{7})/9 = 0 => t_1 = -\ln[(4+\sqrt{7})/(9B)]/k => W_1 = A/[1-(4+\sqrt{7})/9]^3$

$Be^{-kt}-(4-\sqrt{7})/9 = 0 => t_2 = -\ln[(4-\sqrt{7})/(9B)]/k => W_2 = A/[1-(4-\sqrt{7})/9]^3$

The time interval distance $\triangle t$ between the two extreme values can be written as follows:

$\triangle t = t_2-t_1 = \ln[(4+\sqrt{7})/(4-\sqrt{7})]/k.$

These new formulas deduced are summarized in Table 2.

RESULTS

Parameters of non-linear growth models

The model R^2, MSE, A, B, k, m and AIC of the four compared models are shown in Table 3. The results showed that all the compared models had R^2 with a narrow range of 0.11, but the R^2 values were the highest in Chapman-Richards and lowest in von Bertalanffy model compared to other models. Moreover, the results showed a wide range of MSE values among studied models but Gompertz model had the lowest, whereas Chapman-Richards model had the highest MSE value compared to their counterparts. The AIC value ranged from 65.1322 to 68.4522 and the Gompertz was ranked 1st in term of the lowest AIC value. The AIC of the four models had same change trend as MSE. The parameter 'A' values was the highest in the von Bertalanffy, but was the lowest in logistic model. The parameter 'B' value was the highest in Logistic, but the lowest in Chapman-Richards model. The parameter '*k*' value was the highest in Logistic, but the lowest in von Bertalanffy.

The growth intervals for turbot

The non-linear growth models in the present study showed different growth intervals for the turbot fish strain (Table 4). Logistic model had the longest (13.63 month), whereas the Chapman Richards model had the shortest (7.58 month) slow growth interval distance compared to the other models. The longest (22.72 month) fast growth interval distance was noted in the von Bertalanffy model, whereas the shortest (10.53 month) was revealed in the Logistic model. Moreover, the asymptotic growth interval was the longest (30.8 month) in von Bertalanffy model, but the shortest in Chapman Richards model.

DISCUSSION

As typical sigmoid growth curves, the properties of Chapman-Richards, Gompertz, Logistic and von Bertalanffy models in the past few decades have been studied in detail and some property formulas were obtained from the first and second differentials of the models, that is, the instantaneous growth rates, the relative growth rate, and the growth acceleration. All instantaneous growth rates of the four models have a vertex (maximum value). These vertexes are the inflection points of the sigmoid curves [the inflection point coordinates of Chapman-Richards, Gompertz, Logistic and von Bertalanffy is $(\ln[B/(1-m)]/k,\ Am^{1/(1-m)})$, $(\ln B/k,\ A/e)$, $(\ln B/k,\ A/2)$ and $(\ln 3B/k,\ 8A/27)$, respectively]. This indicates that the instantaneous growth rate has an inverted bell-shaped curve (Figure 1). The curve characteristics of the relative growth rates have already been reported and are always decreasing according to Minot's law (Figure 1) (Medawar, 1941). The growth accelerations of the four models all have two vertexes (a maximum and a minimum), which indicates that the growth accelerations have a transverse S-shaped curve (Figure 1). The transverse S-shaped curve of the growth acceleration shows that the two extreme points are the point of inflection of the instantaneous growth rate. In this way, the growth process can be divided into slow, fast and asymptotic periods using these two points (starting

Table 2. Properties of four nonlinear growth models (time).

Type of model	Chapman-Richards	Logistic
Slow-growth interval	$\left(0, \frac{1}{k}\ln\left[-\frac{B\left(m+2-\sqrt{m^2+4m}\right)}{2(m-1)}\right]\right)$	$\left(0, -\frac{1}{k}\ln\frac{2+\sqrt{3}}{B}\right)$
Fast-growth interval	$\left(\frac{1}{k}\ln\left[-\frac{B\left(m+2-\sqrt{m^2+4m}\right)}{2(m-1)}\right], \frac{1}{k}\ln\left[-\frac{B\left(m+2+\sqrt{m^2+4m}\right)}{2(m-1)}\right]\right)$	$\left(-\frac{1}{k}\ln\frac{2+\sqrt{3}}{B}, -\frac{1}{k}\ln\frac{2-\sqrt{3}}{B}\right)$
Asymptotic growth interval	$\left(\frac{1}{k}\ln\left[-\frac{B\left(m+2+\sqrt{m^2+4m}\right)}{2(m-1)}\right], +\infty\right)$	$\left(-\frac{1}{k}\ln\frac{2-\sqrt{3}}{B}, +\infty\right)$
Fast-growth interval distance	$\ln[(m+2+\sqrt{m^2+4m})/(m+2-\sqrt{m^2+4m})]/k$	$\ln[(2+\sqrt{3})/(2-\sqrt{3})]/k$
Type of model	**Gompertz**	**von Bertalanffy**
Slow-growth interval	$\left(0, -\frac{1}{k}\ln\frac{3+\sqrt{5}}{2B}\right)$	$\left(0, -\frac{1}{k}\ln\frac{4+\sqrt{7}}{9B}\right)$
Fast-growth interval	$\left(-\frac{1}{k}\ln\frac{3+\sqrt{5}}{2B}, -\frac{1}{k}\ln\frac{3-\sqrt{5}}{2B}\right)$	$\left(-\frac{1}{k}\ln\frac{4+\sqrt{7}}{9B}, -\frac{1}{k}\ln\frac{4-\sqrt{7}}{9B}\right)$
Asymptotic growth interval	$\left(-\frac{1}{k}\ln\frac{3-\sqrt{5}}{2B}, +\infty\right)$	$\left(-\frac{1}{k}\ln\frac{4-\sqrt{7}}{9B}, +\infty\right)$
Fast-growth interval distance	$\ln[(3+\sqrt{5})/(3-\sqrt{5})]/k$	$\ln[(4+\sqrt{7})/(4-\sqrt{7})]/k$

Table 3. The parameter values and goodness of fit of four nonlinear curve models of family.

Model	Logistic	Gompertz	von Bertalanffy	Chapman-Richards
Coefficient of determination (R^2)	0.9906	0.9908	0.9898	0.9909
Mean square error **(MSE)**	6574.1773	6421.8706	7127.1754	7436.3161
A	2156.69	2788.11	3584.70	2788.24
B	112.61	8.60	1.28	0.0013
k	0.25	0.12	0.07	0.12
m	/	/	/	0.9998
Akaike's Information Criteria (AIC)	65.3431	65.1322	66.0700	68.4522

Table 4. Properties of four nonlinear growth models for Turbot fish strain (month).

Type of model	Slow-growth interval	Fast-growth interval	Asymptotic growth interval	Fast-growth interval distance
Chapman-Richards	(0, 7.58)	(7.58, 23.62)	(23.62, 0)	16.04
Logistic	(0, 13.63)	(13.63, 24.16)	(24.16, 0)	10.53
Gompertz	(0, 10.23)	(10.23, 26.78)	(26.78, 0)	16.55
von Bertalanffy	(0, 7.86)	(7.86, 30.58)	(30.58, 0)	22.72

point and ending point). However, the property formulas from three differentials have not been previously deducted. To evaluate deeply the effects of selection of fast-growing strain of turbot, we have deducted the

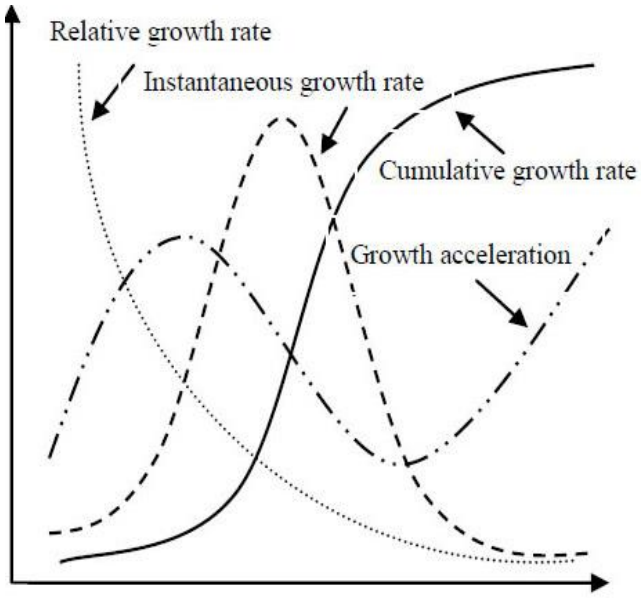

Figure 1. The curve shape characteristics of sigmoid growth curve (cumulative growth curve), instantaneous growth rate, relative growth rate and growth acceleration. The meaning and scale of coordinate axis, for the four curves, are different.

mathematical formulas of the three special growth intervals and explored the growth characteristics of turbot using the formulas.

The model selection was a daunting task, given the broad range of criteria for goodness of fit, as the coefficient of determination (R^2), the mean squares errors (MSE), the loglikelihood (lnL) values, the AIC (Akaike, 1974; Gbangboche et al., 2008), and the least average prediction error (APE) (Lambe et al., 2006; Gbangboche et al., 2008). The goodness of fit, in this study, was assessed using R^2, MSE and AIC, and the model with the higher R^2 and the lower MSE and AIC were selected as the optimal model (Akaike, 1974; Gbangboche et al., 2008). All competing models had high R^2 from 0.9898 to 0.9909, suggesting overall good fits to the data. The MSE value ranged from 6421.8706 to 7436.3161 and the Gompertz was ranked 1st according to the lowest MSE value. The AIC value ranged from 65.1322 to 68.4522 and the Gompertz was ranked 1st according to the lowest AIC value. Among the four models, although the Chapman-Richards model showed the highest R^2 (0.9909), its MSE value was also the highest (7436.3161), which indicated that the Chapman-Richards model was not the best model to describe the growth data of turbot; by contrast, the Gompertz model showed the lowest MSE (6421.8706) and AIC (65.1322) and the second highest R^2 value (0.9908) (almost equal to the first highest R^2 of the Chapman-Richards model). Hence, the Gompertz model has been considered as the best fit according to MSE, AIC and R^2 value and was optimal for the description of turbot growth trajectories. Research has shown that the Gompertz model, in fish population such as *Spicara smaris* and *Tribolodon nakamurai*, can be deemed as the best fit based on AIC lowest value (Tsangridis and Filippousis, 1994; Imai et al., 2002). The conclusion was consistent with the result of this study. Even so, it cannot be assumed that the Gompertz model could produce the goodness of fit in the other breeding farm when the environmental conditions change. Therefore, the model parameters can be routinely re-adjusted, allowing even the possibility of testing all other nonlinear models (Gbangboche et al., 2008). The growth of turbot is influenced by rearing conditions, especially water temperature. In this study, during the larval period, water temperature is 18°C and during sub-adult and adult period are 13 to15°C. In the appropriative temperature range, turbot can show a rapid growth as temperature rises. But, the growth rate of turbot will decrease when the water temperature is too high or too low, for example, the water temperature of larval period is lower than 16°C or higher than 23°C and the water temperature of sub-adult and adult period are lower than 10°C or higher 22°C. Various nonlinear growth models have been proposed to explain the growth characteristics of turbot (Baer et al., 2011; Lugert et al., 2016). Baer et al. (2011) used three different growth models, the von Bertalanffy model, the Gompertz model and the Schnute model, to analyze the growth of turbot (*Psetta maxima*) in a commercial recirculation system. The results indicate that the Schnute model was the optimal model to simulate the growth data collected. In the present study, we were unable to determine whether the Schnute model was the optimal model, because the model was not used. But, in the paper of Baer et al. (2011), the Gompertz model was more suitable to simulate the growth data than the von Bertalanffy model according to AIC and sum of squared residuals (SSE) without considering the Schnute model. The conclusion, to some extent, was consistent with our research result. Lugert et al. (2016) used five nonlinear growth functions, the logistic model, the Gompertz model, the von Bertalanffy model, the Kanis and Schnute model, to model the collected growth data in a recirculation aquaculture system (RASs). The fitting weight showed that the Gompertz model gave the best results with the lowest residual standard error (RSE) and AIC among the applied five growth models and was considered to be the best model to simulate the weight collected. The conclusion was consistent with our research findings. Furthermore, the asymptotic values A of the Gompertz model are also very similar in two studies and are more realistic in biological terms; the asymptotic value A and the intrinsic growth rate k.

The asymptotic body weight A was estimated as 2156.69 g by the logistic model and 2788.11 g by the Gompertz model and 3584.70 g by the von Bertalanffy model and 2788.24 g by the Chapman-Richards model, and correspondingly the intrinsic growth rate k of the four models was 0.25, 0.12, 0.07 and 0.12, respectively.

Obviously, the parameter *A* and *k* estimated by the Gompertz model were almost the same as the Chapman-Richards model. On the whole, the larger the asymptotic body weight *A* (mature weight), the less the intrinsic growth rate *k*, the longer it tends to take to mature. Clearly, the *A* value from the logistic model was too low (2156.69 g) and was not consistent with the breeding goal for the body weight. The *A* value from the von Bertalanffy model was the highest (3584.70 g), but its k value was the lowest (0.07) and the individual will take a longer time to mature and was not consistent with the breeding objectives since prolonging breeding generation interval. Although the *A* and *k* from the Gompertz model were almost the same as the Chapman-Richards model, the Gompertz model was considered as the most suitable growth models to simulate the present growth data according to both MSE, AIC and R^2 value and biological meaning. In addition to the asymptotic value *A* and the intrinsic growth rate *k*, the third parameter point of inflection is often used to partition the growth curve into two stages (Fitzhugh, 1976). To explore deeply the growth characteristics of turbot, we further investigated the curve property of growth models used in this paper and deducted the starting point and ending point formulas. And thus, the growth process can be divided into slow, fast and asymptotic periods using the two points (starting point and ending point) but not two stages based on point of inflection. In fact, the point of inflection, starting point and ending point of a growth curve is determined by the same parameters of the curve. In the present study, based on the optimal model selection, we have explored the growth characteristics of turbot using the Gompertz model. Three kinds of growth time intervals of the four models were quite different according to starting- and ending-point, and the corresponding fast-growth time interval distance were radically different (The fast-growth time interval distances of Chapman-Richards, Logistic, Gompertz and von Bertalanffy models were 16.04, 10.53, 16.55 and 22.72 months, respectively). In this study, the Gompertz model to was used to descript the growth trajectories of turbot based on the goodness of fit (R^2, MSE and AIC), and decided that the fast-growth time interval of turbot and the fast-growth time interval distance were (10.23, 26.78) (unit: months) and 16.55 months. The conclusion calculated by Gompertz model was more in accordant with the realistic growth characteristics of fast-growth turbot from selective breeding than by the other three models.

Conclusion

In this paper, the Gompertz model gave the best results with the lowest MSE ((6421.8706)) and AIC (65.1322) and the second highest R^2 value (0.9908) (almost equal to the first highest R^2 value) among the applied four growth models and was considered to be the best model to simulate the weight collected. On this basis, we have explored the growth characteristics of turbot using the Gompertz model selected and decided that the fast-growth time interval of turbot and the fast-growth time interval distance were (10.23, 26.78) (unit: months) and 16.55 months, respectively**.**

Conflict of interests

The authors have not declared any conflict of interests.

ACKNOWLEDGEMENTS

The authors thank the Ministry of Science and Technology of China and Ministry of Agriculture of China for grants supporting this work. This study was funded by National‘‘863’’ plan of Ministry of Science and Technology of China (2012AA10A408-8) and the earmarked fund for Modern Agro-Industry Technology Research System of Ministry of Agriculture of China (CARS-50- G01).

REFERENCES

Akaike H (1974). A new look at the statistical model identification. IEEE Trans. Automat. Contr. 19(6):716-723.

Ansah YB, Frimpong EA (2015). Using Model-Based Inference to Select a Predictive Growth Curve for Farmed Tilapia. N. Am. J. Aquac. 77(3):281-288.

Atchley WR, Zhu J (1997). Developmental quantitative genetics, conditional epigenetic variability and growth in mice. Genetics 147(2):765-776.

Baer A, Schulz C, Traulsen I, Krieter J (2011). Analysing the growth of turbot (Psetta maxima) in a commercial recirculation system with the use of three different growth models. Aquac. Int. 19:497-511.

Bertalanffy LV (1938). A quantitative theory of organic growth (Inquiries in Growth Laws II). Hum. Biol. 10(2):181-213.

Bilgin S, Taşçi B, Bal H (2014). Population dynamics of the garfish, Belone euxini (Belonidae: Belone) from the south-east Black Sea. J. Mar. Biol. Assoc. U.K. 94(8):1687-1700.

Deniel C (1990). Comparative study of growth of flatfishes on the west coast of Brittany. J. Fish Biol. 37(37):149-166.

Drew M, White WT, Harry AV, Huveneers C (2015). Age, growth and maturity of the pelagic thresher Alopias pelagicus and the scalloped hammerhead Sphyrna lewini. J. Fish Biol. 86(1):333-354.

Figueiredo C, Diogo H, Pereira JG, Higgins RM (2014). Using information-based methods to model age and growth of the silver scabbardfish, from the mid-Atlantic Ocean. Mar. Biol. Res. 11(1):86-96.

Fitzhugh HA (1976). Analysis of growth curves and strategies for altering their shape. J. Anim. Sci. 42(4):1036-1051.

France J, Dijkstra J, Dhanoa MS (1996). Growth functions and their application in animal science. Ann. Zootech. 45(Suppl):165-174.

Gbangboche AB, Glele-Kakai R, Salifou S, Albuquerque LG, Leroy PL (2008). Comparison of non-linear growth models to describe the growth curve in West African Dwarf sheep. Animal 2(7):1003-1012.

Gompertz B (1825). On the nature of the function expressive of the law of human mortality and on a new mode of determining the value of life contingencies. Philos. Trans. R. Soc. Lond.115:515-585.

Helidoniotis F, Haddon M, Tuck G, Tarbath D (2011). The relative suitability of the von Bertalanffy, Gompertz and inverse logistic models for describing growth in blacklip abalone populations (*Haliotis rubra*) in Tasmania, Australia. Fish. Res. 112(1-2):13-21.

Imai C, Sakai H, Katsura K, Honto W, Hida Y (2002). Growth model for the endangered cyprinid fish *Tribolodon nakamurai* based on otolith analyses. Fish. Sci. 68(4):843-848.

Katsanevakis S, Maravelias CD (2008). Modelling fish growth: multi-model inference as a better alternative to a priori using von Bertalanffy equation. Fish Fish. 9(2):178-187.
Koya PR, Goshu AT (2013). Generalized Mathematical Model for Biological Growths. Open J. Model. Simul. 1(4):42-53.
Lambe NR, Navajas EA, Simm G, Bunger L (2006). A genetic investigation of various growth models to describe growth of lambs of two contrasting breeds. J. Anim. Sci. 84(10):2642-2654.
Liang XF, Ma AJ, Wang XA, Li J, Huang ZH, Shang XM (2012). Morphological comparison between a selected fast-growing strain and the common cultured strain of turbot *Scophthalmus maximus*. Chin. J. Oceanol. Limnol. 30(4):563-568.
Lin YJ,Tzeng WN (2009). Modelling the growth of Japanese eel Anguilla japonica in the lower reach of the Kao-Ping River, southern Taiwan: an information theory approach. J. Fish Biol. 75(1):100-112.
Lugert V, Thaller G, Tetens J, Schulz C, Krieter J (2016). A review on fish growth calculation: multiple functions in fish production and their specific application. Rev. Aquac. 8:30-42.
Masso RJD, Silva PS, Font MT (2000). Asymptotic weight and maturing rate in mice selected for body conformation. Genet. Mol. Biol. 23(2):235-240.
Medawar PB (1941). The “laws” of biological growth. Nature 148(3765):772-774.
Richards FJ (1959). A flexible growth function for empirical use. J. Exp. Bot. 10(2):290-301.
Ruan XH, Wang WJ, Kong J, Hu JJ (2011). Isolation and analy-sis of microsatellites in the genome of turbot (*Scophthalmus maxi-mus* L.). Afr. J. Biotechnol. 10(4):507-518.
Tsangridis A, Filippousis N (1994). Analysis of two models for picarel (*Spicara smaris* L.) growth using Schnute’s micro-simplex nonlinear estimation procedure. Fish. Res. 20(2-3):181-189.
Tsoularis A, Wallace J (2002). Analysis of Logistic Growth Models. Math. Biosci. 179(1):21-55.
Wang XA, Ma AJ, Huang ZH, Zhou Z (2010). Heritability and genetic correlation of survival in turbot (*Scophthalmus maximus*). Chin. J. Oceanol. Limnol. 28(6):1200-1205.
Wang XA, Ma AJ, Ma DY (2015). Developmental quantitative genetic analysis of body weights and morphological traits in the turbot, Scophthalmus maximus. Acta Oceanol. Sin. 34(2):55-62.

academicJournals

Vol. 15(40), pp. 2259-2264, 5 October, 2016
DOI: 10.5897/AJB2016.15295
Article Number: EAC7CFB60912
ISSN 1684-5315

http://www.academicjournals.org/AJB JB

African Journal of Biotechnology

Review

Genetic determinants of antifungal resistance in *Candida* species

Danielly Beraldo dos Santos Silva*, Alexéia Barufatti Grisolia and Kelly Mari Pires de Oliveira

Faculty of Biological and Environmental Sciences at Federal University of Grande Dourados, Mato Grosso do Sul, Brazil.

Received 19 February, 2016; Accepted 21 September, 2016

In the previous decades, it has been an increase in cases of resistance to antifungal agents used in the prophylaxis and treatment of infections caused by *Candida* species. The emergence of resistance to drug classes, it is usually explained by genome alterations ranging from point mutations to gain or loss of whole chromosomes. Therefore, identify and understand into the molecular mechanisms that underlie resistance of the *Candida* spp. is important because this information can provide appropriate treatments in emergency candidemia cases. In this sense, this review have the aim of discuss about the genetic variations associated the antifungal resistance in *Candida* spp.

Key words: Antifungal agents, candidiasis, molecular characterization, mutations, overexpression.

INTRODUCTION

Candida spp. can cause several types of infections with a wide spectrum of clinical presentations, from benign skin-mucosal forms to invasive ones that compromise various human organs (Pfaller and Diekema, 2010). Prophylaxis or prolonged treatment with antifungal agents has increased the incidence of clinical isolates of *Candida* spp. that are resistant to these drugs (Sanglard et al., 2003). Although 50% of worldwide candidemia cases are caused by *C. albicans*, it has been an increase in cases with non-*albicans* species over the past 20 years (Diekema et al., 2012; Healey et al., 2016). Therefore, the identification and characterization of such isolates at the molecular level is important for understanding the spread of *Candida* spp. and the mechanisms of their resistance to antifungal agents (Silva et al., 2016).

The resistance is typically assessed by measuring drug MICs and comparing results to reference breakpoints. Reference broth microdilution testing methods and clinical breakpoint MICs for drug against *Candida* spp. have been developed by the Clinical and Laboratory Standards Institute (CLSI) and European Committee on Antimicrobial Susceptibility Testing (EUCAST) (CLSI, 2012; Leclercq et al., 2013). Also there are the methods instead employ commercial assays such as Sensititre YeastOne (SYO; Trek Diagnostics) and Etest (bioMérieux) or automated systems like the Vitek 2 (bioMérieux) antifungal testing instrument (Shields et al., 2015).

The antifungal drugs are limited to treat candidiasis. The classes of medications most commonly are polyenes

*Corresponding author. E-mail: daniellyberaldo@gmail.com Tel/Fax: +55 (067) 34102223.

(amphotericin B and nistadine), but this class use is more restricted due to nephrotoxicity; pyrimidine analogs (flucytosine); azoles (fluconazole, itraconazole, and voriconazole) and echinocandins (caspofungin, anidufungina, and micafungin). Resistance to antifungal agents may be intrinsic to an organism or may be the result of extensive drug use in the prophylaxis or treatment of fungal infections (Da Matta et al., 2007). Typically, resistance can be attributed to mutations in or increased expression of genes that encode ATP-binding cassette proteins (ABC-type proteins), enzymes that are responsible for ergosterol and glucan biosynthesis, or transcription factors (Barker and Rogers, 2006).

Antifungal drug resistance is nearly always due to fungal genome alterations ranging from point mutations to gain or loss of whole chromosomes. The challenge is to identify these mutations to provide insights into the molecular mechanisms that underlie resistance of the *Candida* spp. This review is about the genetic variations associated the antifungal resistance in *Candida* spp.

POLYENES

Amphotericin B is one of the earliest antifungals from the polyene class and is considered the reference drug for treatment of most of systemic fungal infections. Amphotericin B acts by binding to sterols in cell membranes, resulting in a leakage of cellular components and cell death. Its action spectrum includes all *Candida* spp., some species of *Aspergillus*, *Blastomyces dermatitidis*, and other fungi. This drug is not absorbed by the gastrointestinal tract and must be administered intravenously with hospital supervision (Batista et al., 1999).

Resistance mechanisms for this class of drugs have not yet been fully elucidated. However, it is believed that alterations in the steroids of the cell membrane and their phospholipid profile, protection against oxidative damage, and mutations in genes involved in ergosterol biosynthesis, especially in *ERG6*, may be related to resistance in *Candida* spp. (Perea and Patterson, 2002).

Vandeputte et al. (2008) identified a specific non-sense mutation (encoding a stop codon) in *ERG6* that resulted in a decrease in the ergosterol content of a clinical isolate of *C. glabrata* resistant to amphotericin B (Table 1). Hull et al. (2012) identified two mutations (T121V and T121I) in *ERG2* in two isolates of *C. glabrata* with decreased sensitivity to amphotericin B. Replacement of the threonine in the 121st position by valine or isoleucine affected *ERG2* function, promoting a reduction in the sensitivity of these isolates to amphotericin B (Table 1).

PYRIMIDINE ANALOGS

Flucytosine (5-fluorocytosine or 5-FC) is a pyrimidine that transforms itself within the fungal cell into 5-fluorouracil and then to 5-fluordesoxiuridine. These latter molecules behave as antimetabolites and interfere with the normal biosynthesis of nucleic acids and nucleotides vital for fungal growth. This drug is indicated for infections caused by *Cryptococcus neoformans*, *Candida* spp., *Torulopsis* spp., and *Aspergillus* (Vermes et al., 2000).

Mutations that lead to a decrease or halt in the drug's import or its intracellular conversion are often responsible for resistance to pyrimidine analogs. The most frequent mechanism of resistance is a mutation in *FUR1* (5-fluorouridine resistant 1), which encodes the enzyme responsible for the intracellular conversion of 5-fluorouracil into metabolites capable of being integrated into cytosine metabolism. A point mutation that resulted in the replacement of arginine with cysteine at the 101st position of *FUR1* was found to be associated with resistance to 5-FC in *C. albicans* by Hope et al. (2004) (Table 1).

Florent et al. (2009) demonstrated that the mutation T26C, which results in the amino acid change M19T of the FCY1 (fluorocytosine resistance 1) gene that encodes cytosine deaminase, which is responsible for the conversion of 5-FC to 5-fluorouridine monophosphate, was associated with a *C. lusitane* isolate's resistance to 5-FC.

AZOLES

The azoles have a wide spectrum of action, and so are the most commonly used drug class in the treatment of diseases caused by fungi, particularly by *Candida* spp. Ergosterol is an essential component in maintaining both the integrity and the function of the fungal plasma membrane and is the target of many antifungal agents, including the azoles. The ergosterol biosynthetic pathway converts acetic acid into ergosterol using a number of enzymes, similar to what occurs in the biosynthesis of cholesterol in mammals.

Fluconazole, voriconazole, itraconazole, and posaconazole act on the ergosterol biosynthetic pathway of the fungal membrane through inhibition of the enzyme 14α-demethylase (*Erg11p* or *14DM*), which is dependent on cytochrome P450. Thus, the conversion oflanosterol into ergosterolis prevented, increasing both the permeability and the progressive instability of the fungal cell (Barker and Rogers, 2006; Vandeputte et al., 2005).

Several studies have been conducted for the elucidation of the molecular mechanisms responsible for development of resistance to azoles in clinical isolates of *Candida* spp. Defect in DNA repair may account for accelerated emergence of various genetic changes responsible for drug resistance. The role of DNA repair in fungal pathogens, especially in the emergence of antifungal resistance, has not been explored in depth (Healey et al., 2016).

Table 1. Genes associated with antifungal resistance in clinically relevant *Candida* species.

Class of molecule	Gene name	Location of genes	Mechanism	Fungal species	Class of antifungal	References
Transport proteins of the type ABC	CDR1	Chr 3	Overexpression	*C. albicans*	Azoles	Holmes et al. (2006)
	CDR2	Chr 3	Overexpression	*C. albicans*	Azoles	
Enzyme complex in the biosynthesis of ergosterol	ERG2	Chr 1	Point mutation	*C. glabrata*	Polyenes	Hull et al. (2012)
	ERG3	Chr 1	Point mutation	*C. albicans*	Azoles	Sanglard et al. (2003)
	ERG6	Chr 3	Point mutation	*C. glabrata*	Polyenes	Vandeputte et al. (2008)
	ERG11	Chr 5	Overexpression Point mutation	*C. albicans* *C. dubliniensis* *C. glabrata* *C. krusei* *C. tropicalis*	Azoles	Carvalho et al. (2013), Eddouzi et al. (2013), Jiang et al. (2012) and Silva et al. (2016)
Enzyme complex of the glucan biosynthesis	FKS1	Chr 1	Point mutation	*C. glabrata*	Polyenes	Zimbeck et al. (2010); Naicker et al. (2016)
	FKS2	Chr R	Point mutation			
Transcription factors	UPC2	Chr 1	Unknown	*C. albicans*	Azoles	Heilmann et al. (2010)
	TAC1	Chr 5	Point mutation	*C. albicans*	Azoles	Coste et al. (2004)
	PDR1	Chr A	Point mutation	*C. glabrata*	Azoles	Tsai et al. (2010)
	MRR1	Chr 3	Point mutation	*C albicans*	Azoles	Dunkel et al. (2008)
Major facilitator superfamily	MDR1	Chr 6	Overexpression	*C. albicans,* *C. dubliniensis*	Azoles	Chau et al. (2004) and Akins (2005)
	PDH1	Chr F	Overexpression	*C. glabrata*	Azoles	Izumikawa et al. (2003)
	PDR16	Chr 1	Overexpression	*C. albicans*	Azoles	Saidane et al. (2006)
Other	FCY1	Chr 6	Point mutation	*C. lusitaniae*	Pyrimidine analogs and Azoles	Florent et al. (2009)
	FCY2	Chr 3	Point mutation	*C. lusitaniae*	Pyrimidine analogs and Azoles	Florent et al. (2009)
	FCY22	Chr 2	Point mutation	*C. albicans*	Pyrimidine analogs	Chapeland-Leclerc et al. (2005)
	FCA1	Chr 6	Point mutation	*C. albicans*	Pyrimidine analogs	Hope et al. (2004)
	FUR1	Chr5	Point mutation	*C. albicans*	Pyrimidine analogs	Hope et al. (2004)

ABC: ATP-binding cassette. MFS: Major Facilitator Superfamily; Chr R, 1, 2, 3. 5 and 6: Chromosome location based on the complete genome of *C. albicans* SC5314.Chr A and F: Location of the chromosome based on complete genome of *C. glabrata* CBS138.

Recently, Healey et al. (2016) demonstrated that a mutator phenotype caused by a mismatch repair defect is prevalent in *C. glabrata* clinical isolates. Strains carrying alterations in mismatch repair gene MSH2 exhibit a higher propensity to breakthrough antifungal treatment in vitro and are recovered at a high rate from patients. This genetic mechanism promotes the acquisition of resistance to multiple antifungals, at least partially explaining the elevated rates of triazole and multi-drug resistance associated with *C. glabrata*. The identification the MSH2 defects in infecting strains

may influence the management of patients on antifungal drug therapy.

One such mechanism involves efflux pumps that export the antifungal agent from the intracellular environment to the extracellular environment, thus reducing its intracellular concentration (Holmes et al., 2006). Studies conducted with fluconazole have demonstrated that this drug is actively transported into the extracellular environment by fungal cells in an energy-dependent manner and that most antifungal efflux is caused by the overexpression of genes that encode membrane transport proteins (Holmes et al., 2006).

Two families of efflux membrane transporters can be distinguished in yeasts according to the energy source used for extrusion of substrates (Marie and White, 2009). The genes *CDR1* and *CDR2* (*Candida* drug resistance 1 and 2) encode the ABC-type transport proteins that act as transmembrane efflux pumps, using ATP hydrolysis to transport substrates across the membrane. The expression of *CDR1* and *CDR2* is regulated by *TAC1* (Transcriptional activator of CDR genes 1). Hyper-activation of the *TAC1* transcription factor is conferred by gain-of-function mutations that consequently promote the overexpression of *CDR1* and *CDR2* (Coste et al., 2004).

In addition to *CDR1* and *CDR2*, the *MDR1* gene (Multi-drug resistance 1) is directly involved in fluconazole resistance. This gene encodes a permease protein of the *MFS* (Major facilitator superfamily) type, acting as a membrane carrier and using a proton electrochemical gradient for the transport of substrates. The expression of *MDR1* is regulated by at least three transcription factors, the most commonly described among them being the *MRR1* transcription factor (multi-drug resistance regulator 1). The hyperactivation of *MRR1* is conferred by gain-of-function mutations in *C. albicans* and *C. dubliniensis* (Table 1), leading to overexpression of *MDR1* (Schubert et al., 2008).

Changes in ergosterol biosynthesis represent another mechanism of azole resistance. This mechanism bypasses the inactivation of the sterol enzyme Δ5,6-desaturase (encoded by the gene *ERG3*) that acts just upstream of 14α-demethylase in the ergosterol biosynthesis pathway, converting 14α-metilfecoesterol into 14α-methyl-3,6-diol. As the sterol 14α-metilfecoesterolis capable of supporting fungal cell growth and 14α-methyl-3,6-diol is toxic, inactivation of the Δ5,6-desaturase sterol promotes resistance to azoles (Chau et al., 2005). Thus, isolates with changes in this enzymatic step show a selective advantage when subjected to the action of azoles (Akins, 2005).

Mutations in the *ERG11* gene of *Candida* spp. are also involved in resistance to azoles. *ERG11* is located on chromosome 5 and demonstrates significant variation in size according to the species, from 1,569 bp in *C. parapsilosis*to 2,669 bp in *C. glabrata*. Mutations in *ERG11* confer resistance to azoles by reducing the binding affinity of the drug (Barker and Rogers, 2006).

Several studies have compared *ERG11*gene sequences from isolates of different *Candida* spp. that are susceptible and resistant to azoles, *C. albicans* being the most studied species in this regard (Carvalho et al., 2013; Chau et al., 2004).

Vandeputte et al. (2005) studied isolates of *C. tropicalis* that were resistant to fluconazole, they discovered a missense mutation (Y132F) responsible for resistance that had been previously reported in *C. albicans* by Chau et al. (2004). Carvalho et al. (2013) investigated *ERG11* mutations in clinical isolates of *C. albicans*, *C. glabrata* and *C. tropicalis* that had been previously evaluated by fluconazole-susceptibility tests, identified fourteen different missense mutations, five of which had not been previously described, including a new L321F mutation identified in an isolate of *C. albicans* resistant to fluconazole.

Silva et al. (2016) identified three new synonymous mutations in the ERG11 gene in the isolates of *C. glabrata* (C108G, C423T and A1581G) and two new nonsynonymous mutations in the isolates of *C. krusei*:-A497C (Y166S) and G1570A (G524R), with dose dependent sensitivity to voriconazole. The functional consequence of these nonsynonymous mutations was predicted using evolutionary conservation scores. The Y166S mutation can affect the 14α-demethylase. This observation suggests a possible link between the mutation and dose-dependent sensitivity to voriconazole in the clinical isolate of *C. krusei*.

An increase in *ERG11* gene expression also results in resistance to antifungal agents because such an increase results in an elevated concentration of 14α-demethylase in the intracellular environment, requiring larger amounts of antifungals to inhibit enzyme activity. This mechanism has been revealed in various isolates of *C. albicans* resistant to fluconazole (Xu et al., 2015). *ERG11* gene expression is regulated by the *UPC2* (uptake control 2) transcription factor. In response to azole agents, gain-of-function mutations were identified in the *UPC2* gene, which led to hyperactivity. Such hyperactivity leads to the over-activation of*ERG11* gene expression. Over-expression of *ERG11*, in turn, significantly reduces the effect of the antifungal agent in cells, decreasing the cell's sensitivity (Heilmann et al., 2010).

ECHINOCANDINS

Echinocandins are the most recent class of antifungal agent to be introduced in clinical practice for the treatment of infections caused by fungal species, especially those of the *Candida* genus (Cappelletty and Eiselstein-Mckitrick, 2007). The three antifungal drugs in this class caspofungin, micafungin, and anidulafungin have proven effective in treating candidiasis (Chandrasekar and Sobel, 2006). These drugs inhibit β-(1,3)-D-glucansynthetase, which is composed of a

complex of proteins and polycarbohydrates and is responsible for fungal cell wall synthesis. Blocking of this enzyme causes osmotic instability, compromising the integrity of the fungal membrane and causing mortality (Morris and Villmann, 2006).

Although the use of echinocandins in treatment is recent, strains resistant to this type of drug have already been described. The drop in sensitivity to echinocandins has been found to be associated to mutations in the Fks1p and Fks2p (FK506 sensitivity protein 1 and 2) subunits of the β-1,3-glucansynthetase complex, which is necessary for the production of β-1,3 glucan, an essential component of the *Candida* cell wall (Desnos-Ollivier et al., 2008).

Specifically, mutations have been found in two regions, hot spot 1 and hot spot 2 (composed of nine and eight amino acids, respectively), which show up in both genes. These mutations in *FKS1* and *FKS2* result in an inability of the echinocandins to inhibit the production of 1, 3-β- glucan (Perlin, 2007). Mutations in hot spot 1 of *FKS1* and *FKS2* are the most prevalent among a variety of fungal species resistant to this class of drugs. Zimbeck et al. (2010) found associations between mutations in hot spot1 of both *FKS1* and *FKS2* and *C. glabrata* resistant to echinocandins (Table 1).

Mutations in the FKS2 gene were found in two *C. glabrata* isolates with echinocandin resistance mediated (Naicker et al., 2016). Both isolates were cultured from urine specimens from private-sector patients. A mutation was detected in the hotspot 1 region of the FKS2 gene where serine was replaced by phenylalanine at position 663 (S663F). Other mutation, had change from arginine to lysine at amino acid position 1377 (R1377K) was identified in the FKS2 hotspot 2 region.

Shields et al. (2015) determined the FKS mutation rates in *Candida* spp. by systematic sequencing of at-risk isolates and to determine if discrepant echinocandin susceptibility results were associated with agent-specific FKS mutations. FKS mutations were detected in 5% of sequenced isolates and 2% of isolates overall. Corresponding rates among *C. glabrata* isolates were 8 and 4%, respectively. Among *C albicans* isolates, rates were 5 and <1%, respectively. Mutations occurred exclusively with prior echinocandin exposure and were not detected in other species. Isolates with discrepant susceptibility results did not harbor FKS mutations. Mutation rates among isolates resistant to ≥2, 1, and 0 agents were 75, 13 and 0%, respectively. The authors concluded that FKS mutations were uncommon among non-*C. glabrata* species, even with prior echinocandin exposure.

CONCLUSION

Infections caused by *Candida* spp. are frequent complications of other conditions, such as pregnancy, use the medications (birth control pills, antibiotics, and steroids), Immune-suppressing diseases (including HIV), diabetes, obesity and others. Although the susceptibility of *Candida* to the currently available antifungal agents can be predicted, candidiasis infections can lead to serious health problems or cause death if left untreated. Lot of molecular mechanisms related to resistencia intrinsic or acquired *Candida* spp. to antifungals has been elucidated, however there are still many species that the mechanisms are even mysterious. In this sense, the genome sequencing of *Candida* species provides the opportunity to elucidate some of the mechanisms involved in intrinsic or acquired resistance by these yeasts. The scientific community has sought to develop strategies to understand and solve problems related to resistance, and one of these alternatives is the search for new bioactive molecules with antifungal activity based on the genetic and molecular characterization of resistant isolates, providing appropriate treatments in emergency cases that are not only socioeconomically, technologically, and industrially viable but are also based on the best specificity of new molecule activity.

Conflict of interests

The authors have not declared any conflict of interest.

ACKNOWLEDGEMENTS

This review did part of project supported by a grant from the Fundação de Apoio ao Desenvolvimento do Ensino, Ciência e Tecnologia de Mato Grosso do Sul (FUNDECT) and the Coordenação de Aperfeiçoamento de Pessoal de Nível Superior (CAPES), Mato Grosso do Sul, Brazil

REFERENCES

Akins R (2005). An update on antifungal targets and mechanisms of resistence in *Candida albicans.* Med. Mycol. 43:185:318.

Barker SKP, Rogers DP (2006). Recent insights into the mechanisms of antifungal resistance. Curr. Infect. Dis. Rep. 8:449-456.

Batista JM, Birman EG, Cury AE (1999). Suscetibilidade a antifúngicos de cepas de *Candida Albicans* isoladas de pacientes com estomatite protética. Rev.Odont. Univ. São Paulo 13(4):343-348.

Cappelletty D, Eiselstein-Mckitrick K (2007). The echinocandins. Pharmacotherapy 27:369-388.

Carvalho VO, Okay TS, Melhem MSC, Szeszs MW, Del Negro GMB (2013). The new mutation L321F in *Candida albicans* ERG11 gene may be associated with fluconazole resistance. Rev. Iberoam. Micol. 30(3):209-212.

Chandrasekar PH, Sobel JD (2006). Micafungin: a new echinocandin. Clin. Infect. Dis. 42:1171-1178.

Chapeland-Leclerc F, Bouchoux J, Goumar A, Chastin C, Villard J, Noël T (2005). Inactivation of the FCY2 gene encoding purine-cytosine permease promotes cross-resistance to flucytosine and fluconazole in *Candida lusitaniae.* Antimicrob. Agents Chemother. 49:3101-3108.

Chau AS, Mendrick CA, Sabatelli FJ, Loebenberg D, McNicholas, P (2004). Application of real-time quantitative PCR to molecular analysis of *Candida albicans* strains exhibiting reduced susceptibility

to azoles. Antimicrob. Agents Chemother. 48(6):2124-2131.
Chau AS, Gurnani M, Hawkinson R, Laverdiere M, Cacciapuoti A, McNicholas P (2005). Inactivation of sterol Delta5, 6-desaturase attenuates virulence in *Candida albicans*. Antimicrob. Agents Chemother. 49(9):3646-3651.
CLSI-Clinical and Laboratory Standards Institute (2012). Reference method for broth dilution antifungal susceptibility testing of yeasts, fourth informational supplement M27-S4, 4th ed. Clinical and Laboratory Standards Institute, Wayne, PA.
Coste AT, Karababa M, Ischer F, Bille J, Sanglard D (2004). Tac1, transcriptional activator of CDR Genes, is a new transcription factor involved in the regulation of *Candida albicans* ABC transporters. Eukaryot. Cell 3(6):1639-1652.
Desnos-Ollivier M, Ragon M, Robert V, Raoux D, Gantier JC, Domer F (2008) Debaryomyces*hansenii (Candidafamata*), a rare human fungal pathogen often misidentified as *Pichiaguilliermondii (Candida guilliermondii)*. J. Clin. Microbiol. 46:3237-3242.
Diekema D, Arbefeville S, Boyken L, Kroeger J, Pfaller M (2012) The changing epidemiology of healthcare-associated candidemia over three decades. Diagn. Microbiol. Infect. Dis. 73:45-48.
Dunkel N, Liu TT, Barker KS, Homayouni R, Morschhäuser J, Rogers PD (2008). A gain-of-function mutation in the transcription factor Upc2p causes upregulation of ergosterol biosynthesis genes and increased fluconazole resistance in a clinical *Candida albicans* Isolate. Eukaryot. Cell 7(7):1180-1190.
Eddouzi J, Parker JE, Vale-Silva LA, Coste A, Ischer F, Kelly S, Manai M, Sanglard D (2013). Molecular mechanisms of drug resistance in clinical *Candida* species isolated from Tunisian hospitals. Antimicrob. Agents Chemother. 57(7):3182-3193.
Florent M, Noël T, Robert GR, Da Silva B, Fitton-Ouhabi V, Chastin C, Papon N, Chapeland-Leclerc F (2009). Nonsense and missense mutations in FCY2 and FCY1 genes are responsible for flucytosine resistance and flucytosine-fluconazole cross-resistance in clinical isolates of *Candida lusitaniae*. Antimicrob. Agents Chemother. 53(7):2982-2990.
Healey KR, Zhao Y, Perez WB, Lockhart SR, Sobel JD, Farmakiotis D, Kontoyiannis DP, Sanglard D, Taj-Aldeen SJ, Alexander BD, Jimenez-Ortigosa C, Shor E, Perlin DS (2016). Prevalent mutator genotype identified in fungal pathogen *Candida glabrata* promotes multi-drug resistance. Nat. Commun. 7:1-10.
Heilmann CJ, Schneider S, Barker KS, Rogers PD, Morschhäuser J (2010). An A643T mutation in the transcription factor Upc2p causes constitutive ERG11 upregulation and increased fluconazole resistance in *Candida albicans.* Antimicrob Agents Chemother. 54(1):353-359.
Holmes AR, Tsao S, Ong SW, Lamping E, Niimi K, Monk BC, Niimi M, Kaneko A, Holland BR, Schmid J, Cannon RD (2006). Heterozygosity and functional allelic variation in the *Candida albicans* efflux pump genes CDR1 and CDR2. Mol. Microbiol. 62(1):170-186.
Hope WW, Tabernero L, Denning DW, Anderson MJ (2004). Molecular mechanisms of primary resistance to flucytosine in *Candida albicans.* Antimicrob. Agents Chemother. 48(11):4377-4386.
Hull CM, Bader O, Parker JE, Weig M, Gross U, Warrilow AG, Kelly DE, Kelly SL (2012). Two clinical isolates of *Candida glabrata* exhibiting reduced sensitivity to amphotericin B both harbor mutations in ERG2. Antimicrob. Agents Chemother. 56(12):6417-6421.
Izumikawa K, Kakeya H, Tsai HF, Grimberg B, Bennett JE (2003). Function of *Candida glabrata* ABC transporter gene, PDH1. Yeast 20(3):249-261.
Leclercq R, Canton R, Brown DF, Giske CG, Heisig P, MacGowan AP, Mouton JW, Nordmann P, Rodloff AC, Rossolini GM, Soussy CJ, Steinbakk M, Winstanley TG, Kahlmeter G (2013). EUCAST expert rules in antimicrobial susceptibility testing. Clin. Microbiol. Infect. 19:141-160.
Marie C, White TC (2009). Genetic basis of antifungal drug reistence. Curr. Fungal Infect. Rep. 3:123-131.
Morris MI, Villmann M (2006). Echinocandins in the management of invasive fungal infections. Am. J. Health. Syst. Pharm. 63:1693-1703.
Naicker SD, Magobo RE, Zulu TG, Maphanga TG, Luthuli N, Lowman W, Govendera NP (2016). Two echinocandin-resistant Candida glabrata FKS mutants from South Africa. Med. Mycol. Case Rep. 11:24-26.
Pfaller MA, Diekema DJ (2010). Epidemiology of invasive mycoses in North America. Crit. Rev. Microbiol. 36:1-53 .
Saidane S, Weber S, De Deken X, St-Germain G, Raymond M (2006). PDR16-mediated azole resistance in *Candida albicans*. Mol. Microbiol. 60(6):1546-1562.
Sanglard D, Ischer F, Parkinson T, Falconer D, Bille, J (2003). *Candida albicans* mutations in the ergosterol biosynthetic pathway and resistance to several antifungal agents. Antimicrob. Agents Chemother. 47(8):2404-2412.
Schubert S, Rogers PD, Morschhäuser J (2008). Gain-of-function mutations in the transcription factor MRR1 are responsible for overexpression of the MDR1 efflux pump in fluconazole-resistant *Candida dubliniensis* strains. Antimicrob. Agents Chemother. 52(12):4274-4280.
Shields RK, Nguyen MH, Press HG, Cumbie R, Driscoll E, Pasculle AW, Clancya CJ. (2015). Rate of FKS Mutations among Consecutive Candida Isolates Causing Bloodstream Infection. Antimicrob Agents Chemother. 59(12):7465-7470.
Silva DBS, Rodrigues LMC, Almeida AA, Oliveira KMP, Grisolia AB (2016). Novel point mutations in the ERG11 gene in clinical isolates of azole resistant *Candida* species. Mem. Inst. Oswaldo Cruz. 111(3):192-199.
Tsai HF, Sammons LR, Zhang X, Suffis SD, Su Q, Myers TG, Marr KA, Bennett JE (2010). Microarray and molecular analyses of the azole resistance mechanism in *Candida glabrata*oropharyngeal isolates. Antimicrob. Agents Chemother. 54(8):3308-3317.
Vandeputte P, Larcher G, Bergès T, Renier G, Chabasse D, Bouchara JP (2005). Mechanisms of azole resistance in a clinical isolate of *Candida tropicalis*. Antimicrob. Agents Chemother. 49:4608-4615.
Vandeputte P, Tronchin G, Larcher G, Ernoult E, Bergès T, Chabasse D, Bouchara JP (2008). A nonsense mutation in the erg6 gene leads to reduced susceptibility to polyenes in a clinical isolate of *Candida glabrata*. Antimicrob. Agents Chemother. 52(10):3701-3709.
Vermes A, Guchelaar HJ, Dankert J (2000). Flucytosine: a review of its pharmacology, clinical indications, pharmacokinetics, toxicity and drug interactions. J. Antimicrob. Chemother .46:171-179.
Xu Y, Sheng F, Zhao J, Chen L, Li C (2015). ERG11 mutations and expression of resistance genes in fluconazole-resistant Candida albicans isolates. Arch. Microbiol. 197(9):1087-1093.
Zimbeck AJ, Iqbal N, Ahlquist AM, Farley MM, Harrison HL, Chiller T, Lockhart SR (2010). FKS mutations and elevated echinocandinmic values among *Candida glabrata* isolates from U.S. population-based surveillance. Antimicrob. Agents Chemother. 54(12):5042-5047.

academicJournals

Vol. 15(40), pp. 2265-2271, 5 October, 2016
DOI: 10.5897/AJB2016.15598
Article Number: C9D25DB60914
ISSN 1684-5315

http://www.academicjournals.org/AJB

African Journal of Biotechnology

Full Length Research Paper

Phylogenetic relationships of the genus *Quercus* L. (Fageceae) from three different sections

Yılmaz Aykut

Department of Molecular Biology and Genetics, Faculty of Science and Arts, Uşak University, 64200 Uşak, Turkey.

Received 4 August, 2016; Accepted 21 September, 2016

In this study, the genetic diversity of 6 oak species known as *Quercus coccifera* L., *Q. robur* L., *Q. infectoria* Oliver, *Q. cerris* L., *Q. ithaburensis* subsp. *macrolepsis* (Kotschy) Hedge and Yalt. and *Q. trojana* P.B. Webb in 18 populations was screened using the randomly amplified polymorphic DNA method (RAPD). 10 RAPD primers giving the best results produced 262 total loci. The highest and lowest band sizes were between 125 and 1800 bp, respectively. The binary RAPD data was computed using the Statistica version 8.0 and Popgene 32, genetic data analysis software program. The principal component analysis and cluster analysis displayed the seperation of populations based on genetic distances. The genetic similarity and distance matrix using Popgene 32 based on Nei (1972) revealed the genetic relations between studied populations. As a result of this study, it may be expressed that genetic relationships are more similar in the species belonging to same section and especially the relationships between *Quercus cerris* and *Quercus trojana* in the section *Cerris* attracts quite attention.

Key words: *Cerris*, genetic relationships, *Quercus*, randomly amplified polymorphic DNA method (RAPD).

INTRODUCTION

Quercus L. (Oak) is a member of family Fagaceae containing very important woody plants (Jawarneh et al., 2013; Alfonso-Corrado et al., 2014). The genus has a natural distribution in the northern hemisiphere in the world with high diversity (Govaerts and Frodin, 1998; Jawarneh et al., 2013; Laakılı et al., 2016). Turkey with 18 species of oaks is an important region with high species diversity (Yaltırık, 1984; Borazan and Babaç, 2003). The classification of the species of *Quercus* by Hedge and Yaltırık (1982), two Turkish authors, has been of great contribution to the research in this field. Before the classification of Hedge and Yaltırık, many intraspecific taxa were classified as species and species concept for *Quercus* taxa was quite narrow (Borazan and Babaç, 2003). Hedge and Yaltırık reduced the total number of *Quercus* taxa from 35 to 18. However, there are still unresolved nomenclatural and typification problems today.

Hybridization has imperative impacts on the enhancement and evolution of numerous plant species (Rieseberg and Ellstrand, 1993; Rieseberg and Wendel, 1993; Arnold, 1997). Furthermore, it can be stated that hybridization behaviour between species of the genus is in high level (Burger, 1975; Van Valen, 1976). Increasing

E-mail: aykutyilmaza@gmail.com.

Table 1. The locations and populations of the six different oak species used in this study

Population number	Species	Number of sample	Provinces
Pop.1	*Q.ithaburensis*	10	Uşak üniversity/1 Eylül Campüs
Pop.2	*Q.coccifera*	10	Uşak üniversity/1 Eylül Campüs
Pop.3	*Q.robur*	10	Uşak üniversity/1 Eylül Campüs
Pop.4	*Q.trojana*	10	Uşak üniversity/1 Eylül Campüs
Pop.5	*Q.cerris*	10	Uşak üniversity/1 Eylül Campüs
Pop.6	*Q.infectoria*	10	Uşak üniversity/1 Eylül Campüs
Pop.7	*Q.infectoria*	10	The North parts of Banaz
Pop.8	*Q.trojana*	10	Over path of Uşak-Banaz
Pop.9	*Q.cerris*	10	The North parts of Banaz
Pop.10	*Q.ithaburensis*	10	Entry of Banaz
Pop.11	*Q.coccifera*	10	Sivaslı/around of Evrenli park
Pop.12	*Q.ithaburensis*	10	Sivaslı/around of Evrenli park
Pop.13	*Q.trojana*	10	Near to forest managment of Sivaslı
Pop.14	*Q.infectoria*	10	Near to forest managment of Sivaslı
Pop.15	*Q.coccifera*	10	Over path of Ulubey-Eşme
Pop.16	*Q.cerris*	10	Over path of Ulubey-Eşme
Pop.17	*Q.ithaburensis*	10	Over path of Ulubey-Eşme
Pop.18	*Q.infectoria*	10	Over path of Ulubey-Eşme
	Total	180	

evidence supports the presence of hybridization in genomic structure of different taxa that belong to oaks (Kremer et al., 2002; Petit et al., 2004). Therefore, in addition to different plant groups especially the genus *Quercus* has been used to demonstrate the presence of hybridization.

In addition to hybridization, oaks are wind-pollinated species. Generally oak species grow in mixed populations and as a result of this, hybridization is commonly observed among oak species especially in the same group or section (Bacilieri et al., 1996; Borazan and Babaç, 2003; Petit et al., 2004; Charalambos et al., 2011). Hence, taxonomy and systematic relations of the genus are debatable and not clear, despite various morphological, cytogenetic and molecular studies (Williams et al., 1990; Welsh and McClelland, 1991; Yılmaz et al., 2013). Especially multiple molecular techniques such as RAPD have been used in the analysis of hybridization and relative species (Bodenes et al., 1997).

Recently, many different studies are being conducted in order to better understand the genus *Quercus.* For example, studies are being tested on the identification of new and reliable isolation techniques, due to high phenolic content and tannins in leaf samples of *Quercus* (Pandey and Tamta, 2015). However, efforts are made towards the selection of morphological and dendrometric characters for conservation programs and the selection of provenances for reforestation schemes (Laakılı et al., 2016).

In this study, we planned to recognize each studied species and to expose relations between three different sections (*Quercus* L. (white oaks), *Cerris* Loudon (red oaks) and *Ilex* Loudon known as evergreen oaks) members by molecular analysis (RAPD). For this aim, the six species of oaks were used such as *Quercus coccifera* known as evergreen oaks, *Quercus robur* L. and *Quercus infectoria* oliver known as white oaks, *Quercus cerris* L., *Q. ithaburensis* subsp. *macrolepsis* (Kotschy) Hedge and Yalt. and *Q. trojana* P.B. Webb known as red oaks. Furthermore; this study was performed to investigate the genetic diversity of natural populations of the genus *Quercus*.

MATERIALS AND METHODS

Plant materials

Six *Quercus* species containing *Q. coccifera*, *Q. infectoria*, *Q. robur*, *Q. cerris*, *Q. ithaburensis* and *Q. trojana* belonging to three different sections were selected in Uşak, Turkey (Table 1). A representative picture belonging to Campüs region was showed in Figure 1. Study materials consist of the leaves to show variations within and among species. Leaves for statistical analysis were collected from 180 trees for 18 populations. For each population ten tree were selected and for each tree ten young and fresh leaves were collected for molecular study. After that leaf samples were stored on bags with silica gel and for further analysis they were transferred to freezer.

DNA isolation

Genomic DNA was extracted following Nucleospin Plant II Genomic DNA Isolation Kit (MN) protocol (Özbek and Kara, 2013). DNA samples extracted were controlled for the determination of quality before PCR amplification. Isolated DNA was stored in freezer at -20°C.

Figure 1. A representative picture showing the Campus area of study.

RAPD study was performed as a molecular technique (Gonzalez-Rodriguez et al., 2004; Yılmaz et al., 2013). DNA samples of species belonging to each population were amplified using 20 oligonucleotide primers. Primers were evaluated for visible bands, constancy, and unambiguity. Satisfactory results were obtained from ten of these primers which gave reproducible amplification products. RAPD primers which cause difficulty to detect band and faint were not used for amplification.

RAPD assays for DNA amplification were performed in total volume of 25 µl containing 10 ng of genomic DNA, 1x PCR buffer, 3 mM of $MgCl_2$, 0.36 µM 10-mer RAPD primer, 100 µM dATP, dCTP, dGTP, dTTP and 1.0 unit taq DNA polymerase. The thermal cycling program was obtained as follows; preliminary 94°C for 3 min, 40 cycles of 94°C for 1 min, 32°C for 1 and 72°C for 2 min. After the 40 cycle, an additional final 10 min extension at 72°C was used to complate amplification reactions. The PCR products were analysed by electrophoresis on 1.5% agarose gels with TAE buffer, visualized by ethidium bromide staining, and photographed under UV light. 100 bp plus DNA ladder (Thermo) was used to estimate the molecular weights of amplified fragments.

Data analysis

In the data analysis of PCR products, whereas presence of each band was coded as 1, absence of band was coded as 0 in all individuals. Only clear and score able bands were evaluated for molecular diversity analysis. The analysis of molecular variance was calculated using the percentage of polymorphic fragments within and among species studied.

The bivariate (1/0) data were used to estimate genetic similarity and genetic distance described by Nei (1972) using computer program Pop Gene 32. Cluster analysis (CA) and Principal component analysis (PCA) with arithmetic averages (UPGMA) were performed to show polymorphism among populations belonging to each species.

RESULTS

The surveyed RAPD primers produced 262 total bands. Molecular sizes of amplified fragments ranged from approximately 125 to 1800 bp (Table 2). During present study, a total of 262 DNA fragments were amplified in 180 individuals representing 18 populations using 10 RAPD primers sets. It is showed in Table 2 that maximum amplicons with 30 were generated by primer OPC-06; whereas OPS-09 primer amplified 23 bands. Highest band size with 1800 bp was amplified with OPS-09 primer, while lowest band size (125 bp) was produced with OPX-04. The range of polymorphism ranged from 96.2 to 100% (Table 2).

It can be observed in Table 2 that the list and sequence of primers, the size range observed in 18 populations and percentage of polymorphism for each primer.

In order to score the PCR amplification fragments, each population were run separately with 10 primers. Bands having same mobility in the length were considered as identical fragments. An example of PCR amplification profile obtained from RAPD primer OPC-09 is presented in Figure 2. The bivariate data (1/0) and dissimilarity coefficient matrices of 18 populations of 6 *Quercus* species based on the data of 10 RAPD primers were used to construct separate dendrograms using statistica version 8.0 and popgene 32 (Figures 3 and 4 and Table 3).

Cluster analysis and principal component analysis were carried out to show variations among studied species and to group of populations belonging to 6 oak species.

Table 2. Name, sequence, number of bands provided from RAPD primers and size range observed in 18 populations of the genus *Quercus.*

Primers	Sequence (5'-3')	Number of bands	Number of polymorphic bands	Size Range (bp)	Percentage of polymorphism
OPA-01	CAGGCCCTTC	29	29	200-1600	100
OPA-03	AGTCAGCCAC	27	26	150-1500	96.2
OPA-07	GAAACGGGTG	25	25	150-1500	100
OPA-13	CAGCACCCAC	24	24	150-1200	100
OPX-04	CCGCTACCGA	27	27	**125**-1600	100
OPC-06	GAACGGACTC	30	30	150-1600	100
OPU-01	ACGGACGTCA	27	26	150-1500	96.2
OPC-09	CTCACCGTCC	25	25	200-1500	100
OPS-09	TCCTGGTCCC	23	23	200-**1800**	100
OPS-20	TCTGGACGGA	25	25	150-1500	100

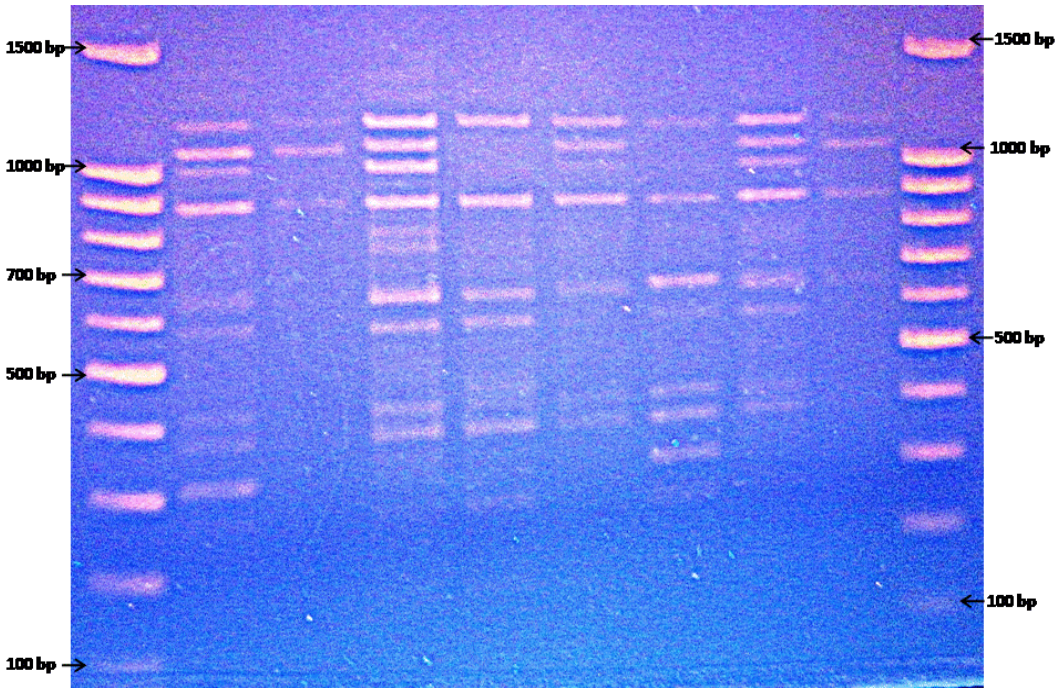

Figure 2. The representative figures of *Quercus infectoria* (Pop. 6) with OPC-09 RAPD-PCR band patterns.

Based on the analysis carried out on PCA, it can be said that the populations belonging to same species were generally observed within same group, in other words studied species were separated from each other (Figure 3).

In Figure 4, dendrogram generated by UPGMA cluster analysis of RAPD fragments indicate that the genotypes were grouped in 8 main groups (A, B, C, D, E, F, G and H).

The largest group was Group D comprising of 4 genotypes and group B and G consist of 3 genotypes each. Group C, F and H consisted of 2 genotypes. Group A and E were smallest and comprised of only 1 genotype.

The genetic similarity and genetic distance matrix derived from RAPD data using popgen 32 (Nei, 1972) are presented in Table 3. According to the results provided from Table 3, the lowest genetic distance was determined between population 4 and population 13. These are two populations belonging to *Q. trojana* species from different regions. Same results can be observed in the Figures 3 and 4 obtained from CA and PCA. The highest genetic distance was between populations 3 to 17 and populations 6 to 17 belonging to two genetically distant taxa, respectively.

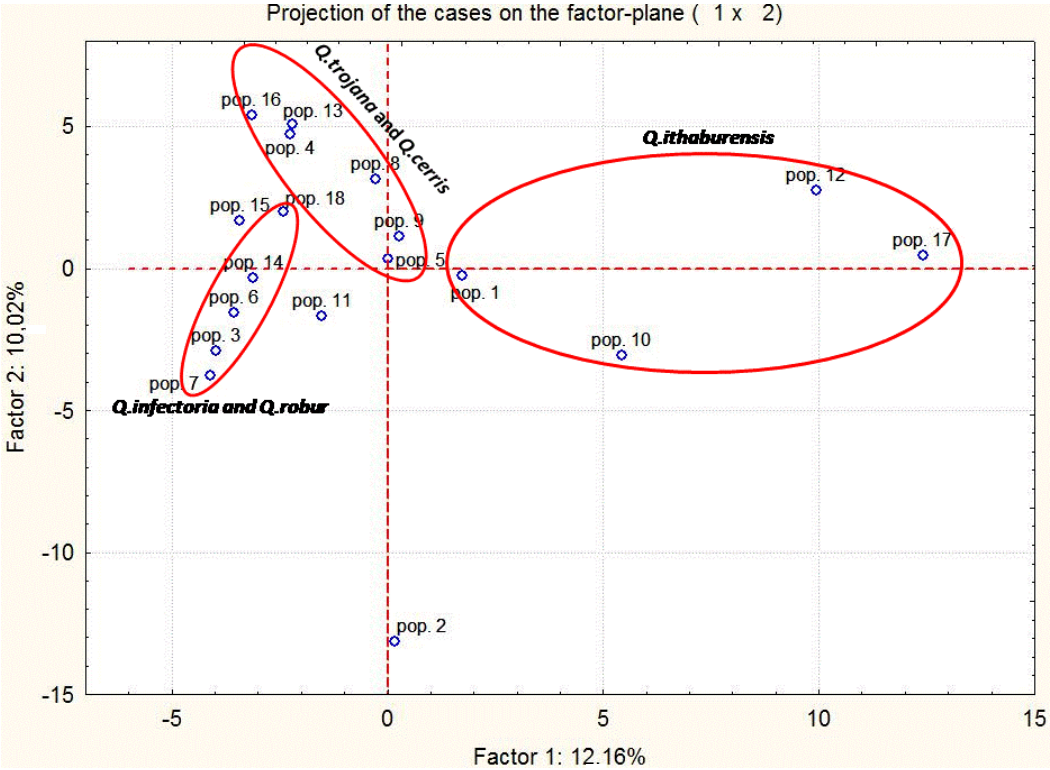

Figure 3. The resulting projection of principal component analysis.

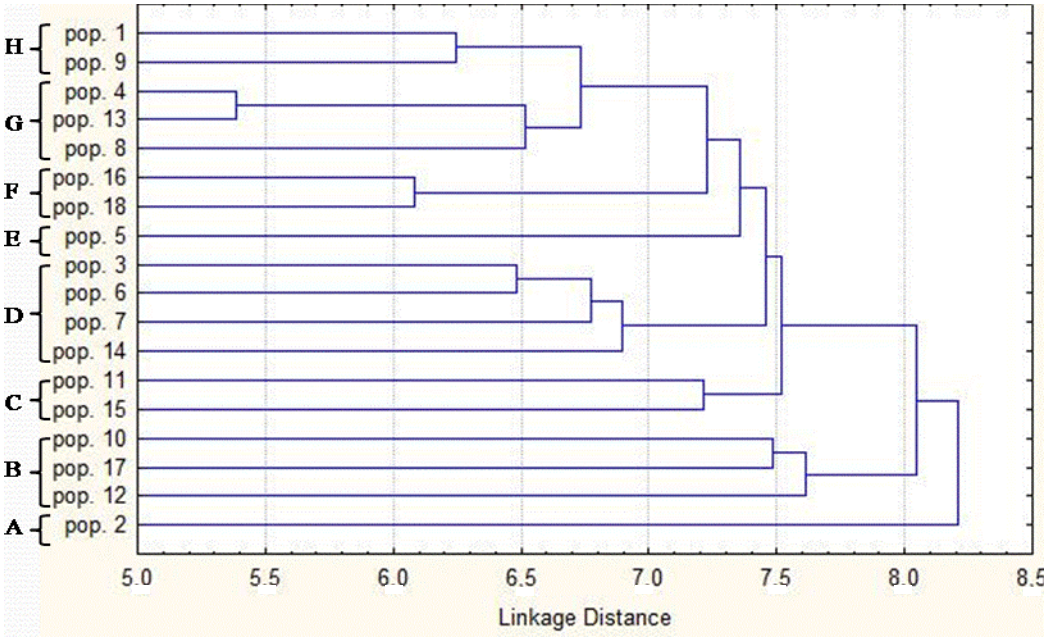

Figure 4. A dendrogram representing phylogenetic relationships between 18 *Quercus* populations.

DISCUSSION

Different DNA markers are widely used to reveal polymorphism within and among plant species (Gonzalez-Rodriguez et al., 2004; Yu et al., 2005; Coelho et al., 2006; Faltusova et al., 2011; Ardi et al., 2012). Recently,

Table 3. The compution of genetic similarity (upper diagonal) and genetic distance (below diagonal) (Nei, 1972).

Pop ID	1	2	3	4	5	6	7	8	9	10	11	12	13	14	15	16	17	18
1	****	0.993	0.981	0.965	0.992	0.984	0.976	0.982	0.984	0.986	0.986	0.974	0.975	0.984	0.961	0.960	0.961	0.982
2	0.007	****	0.980	0.948	0.974	0.981	0.980	0.969	0.974	0.983	0.982	0.959	0.957	0.976	0.955	0.941	0.936	0.967
3	0.019	0.020	****	0.977	0.972	0.992	0.979	0.989	0.994	0.984	0.980	0.982	0.944	0.984	0.969	0.971	0.923	0.981
4	0.035	0.053	0.022	****	0.980	0.982	0.970	0.984	0.992	0.962	0.964	0.955	**0.997**	0.990	0.981	0.937	0.991	0.987
5	0.007	0.025	0.028	0.019	****	0.978	0.967	0.981	0.987	0.975	0.977	0.980	0.986	0.988	0.967	0.964	0.978	0.985
6	0.015	0.018	0.007	0.017	0.021	****	0.991	0.989	0.992	0.979	0.973	0.947	0.985	0.988	0.969	0.928	0.966	0.987
7	0.023	0.020	0.020	0.029	0.032	0.008	****	0.984	0.981	0.981	0.975	0.956	0.977	0.981	0.961	0.929	0.951	0.971
8	0.018	0.030	0.011	0.015	0.018	0.010	0.016	****	0.995	0.990	0.982	0.965	0.993	0.984	0.962	0.944	0.982	0.985
9	0.015	0.026	0.005	0.007	0.013	0.007	0.018	0.005	****	0.983	0.981	0.962	0.995	0.992	0.977	0.940	0.987	0.989
10	0.013	0.016	0.015	0.037	0.025	0.020	0.019	0.010	0.016	****	0.994	0.975	0.976	0.978	0.958	0.960	0.962	0.975
11	0.014	0.018	0.019	0.036	0.023	0.027	0.024	0.017	0.018	0.005	****	0.981	0.974	0.984	0.973	0.972	0.967	0.978
12	0.025	0.041	0.056	0.046	0.019	0.053	0.044	0.035	0.038	0.024	0.018	****	0.966	0.970	0.953	0.985	0.957	0.960
13	0.025	0.043	0.018	0.002	0.013	0.014	0.022	0.006	0.004	0.024	0.025	0.034	****	0.990	0.975	0.946	0.993	0.988
14	0.015	0.023	0.015	0.009	0.011	0.011	0.018	0.015	0.007	0.021	0.015	0.030	0.009	****	0.992	0.960	0.982	0.994
15	0.038	0.045	0.031	0.018	0.032	0.030	0.039	0.038	0.023	0.042	0.027	0.047	0.024	0.007	****	0.953	0.974	0.983
16	0.039	0.066	0.029	0.008	0.021	0.034	0.050	0.018	0.012	0.038	0.033	0.043	0.006	0.017	0.026	0.945	****	0.983
17	0.040	0.060	**0.079**	0.065	0.036	0.074	0.072	0.056	0.060	0.040	0.027	0.014	0.054	0.040	0.047	****	0.056	0.961
18	0.017	0.032	0.019	0.012	0.014	0.011	0.028	0.014	0.010	0.024	0.022	0.040	0.011	0.006	0.016	0.039	0.017	****

different PCR based techniques such as amplified fragment length polymorphism (AFLP), random amplified polymorphic DNA (RAPD), restriction fragment length polymorphism (RFLP), single nucleotide polymorphism (SNP), simple sequence repeats (SSR) are used to determine the genetic variations and diversity at molecular level (Bruschi et al., 2003; Coelho et al., 2006; Franjic et al., 2006; Yılmaz et al., 2013). Despite the short-comings like problems related to reproducibility in amplification of RAPD markers, inadequacy to distinguish between heterozygotes and homo-zygotes, the RAPD method having advantages such as the high level of polymorphism and simply applicability was prefered as molecular technique to evaluate 6 oak species.

The results show that the method could reveal the genetic relationship among six species of oaks and distinguish them. Here studied species are represented by 3 different sections such as *Q. robur* and *Q. infectoria* in *Quercus* section, *Q. coccifera* in *Ilex* section and *Q. cerris*, *Q. ithaburensis* and *Q. trojana* in *Cerris* section. In this study, the molecular analysis with CA and PCA revealed a high degree of separation between studied species. According to dendrogram derived from CA, populations were grouped in 8 main groups (A, B, C, D, E, F, G and H). Generally populations of same species are localized in same group. For example, group B consists of the populations of *Q. ithaburensis*, group C from populations of *Q.coccifera*, group D from populations of *Q.infectoria* and *Q. robur*, group G from the populations of *Q. trojana*. The separation of species can be clearly observed in Figures 3 and 4.

When the dendrogram which consists of 8 main groups was investigated; it can be stated that *Q. infectoria* and *Q. robur* were observed as close species within same main group (group D) (Figures 3 and 4). These are two species belonging to section *Quercus*. Populations of *Q. coccifera* that belong to section *Ilex* showed more differences in comparison to other studied species (group A and C). Finally; the relationships among the species of the section *Cerris* draws attention, especially between *Q. cerris* and *Q. trojana*. The table of genetic similarity and distance supports this situation (Table 3).

When the distribution of populations according to dendrogram obtained from CA and PCA is

investigated, it is observed that there is more similarity in species belonging to same section and the relationship among species of section *Cerris* attracts quite attention.

As a result of this study, it may be expressed that the molecular analysis disclosed useful results in explaning genetic diversity within and among populations belonging to six species from three different section. Furthermore; study results provide quite contribution to understanding the relationships among the sections of the genus *Quercus*, as well as interactions betweeen species studied.

Conflict of Interests

The authors have not declared any conflict of interests.

ACKNOWLEDGEMENTS

The author would like to thank Uşak University Directorate of Scientific Research Projects (BAP) for providing financial support and also specially thank Mustafa Kemal Pişmiş for his great contribution to this manuscript.

REFERENCES

Alfonso-Corrado C, Clark-Tapia R, Monsalvo-Reyes A, Rosas-Osorio C, Gonzalez-Adame G, Naranjo-Luna F, Venegas-Barrera CS, Campos JE (2014). Ecological-Genetic Studies and Conservation of Endemic *Quercus sideroxyla* (Trel.) in Central Mexico. Nat. Resour. 5:442-453.

Ardi M, Rahmani F, Siami A (2012). Genetic variation among Iranian oaks (*Quercus* spp.) using random amplified polymorphic DNA (RAPD) markers. Afr. J. Biotechnol. 11:10291-10296.

Arnold ML (1997). Natural hybridization and evolution. Oxford University Press. Oxford, UK.

Bacilieri R, Ducousso A, Petit RJ, Kremer A (1996). Mating system and asymetric hybridization in a mixed stand of European oaks. Evolution 50:900-908.

Bodenes C, Joandet S, Laigret F, Kremer A (1997). Detection of genomic regions differentiating two closely related oak species *Quercus petraea* (Matt.) Liebl. and *Quercus robur* L. Heredity 78:433-444.

Borazan A, Babaç MT (2003). Morphometric leaf variation in oaks (*Quercus*) of Bolu, Turkey. Ann. Bot. Fenn. 40:233-242.

Bruschi P, Vendramin GG, Busotti F, Grossoni P (2003). Morphological and molecular diversity among Italian populations of *Quercus petraea* (Fagaceae). Ann. Bot. 91:707-716.

Burger WC (1975). The species concept in *Quercus*. Taxon 24:45-50.

Charalambos N, Filippos AA, Siegfried F, Aikaterini D (2011). Interfertile oaks in an island environment. II. Limited hybridization between *Quercus alnifolia* Poech and *Q. coccifera* L. in a mixed stand. Eur. J. Forest. Res. 130:623-635.

Coelho AC, Lima MB, Neves D, Cravador A (2006). Genetic diversity of two evergreen oaks (*Quercus suber* L. and *Quercus ilex* subsp. *rotundifolia* Lam.) in Portugal using AFLP markers. Silvae Genet. 55:105-118.

Faltusova Z, Kucera L, Ovesna J (2011). Genetic diversity of *Brassica oleracea var. capitata* gene bank accessions assessed by AFLP. Electron. J. Biotechnol. 14:4.

Franjic J, Liber Z, Skvorc Z, Idzojtic M, Sostaric R, Stancic Z (2006). Morphological and molecular differentiation of the Croation populations of *Quercus pubescens* (Fagaceae). Acta Soc. Bot. Pol. 75:123-130.

Gonzalez-Rodriguez A, Arias DM, Valencia S, Oyama K (2004). Morphological and RAPD analysis of hybridization between *Quercus affinis* and *Q. laurina* (Fagaceae), two Mexican red oaks. Am. J. Bot. 91:401-409.

Govaerts R, Frodin DG (1998). World checklist and bibliography of Fagales (Betulaceae, Corylaceae, Fagaceae and Ticodenraceae). Royal Botanic Gardens. Kew. Great Britain.

Hedge IC, Yaltırık F (1982). *Quercus* L. in Flora of Turkey. Edinburgh. 7:659-683.

Jawarneh MS, Brake MH, Muhaidat R, Migdadi HM, Lahham JN, El-Oqlah AA (2013). Characterization of *Quercus* species distributed in Jordan using morphological and molecular markers. Afr. J. Biotechnol. 12:1326-1334.

Kremer A, Dupouey JL, Deans JD, Cottrell J, Csaikl U, Finkeldey U, Espinel S, Jensen J, Kleinschmit J, Van Dam B, Ducousso A, Forrest I, de Heredia UL, Lowe AJ, Tutkova M, Munro RC, Steinhoff S, Badeau V (2002). Leaf morphological differentiation between *Quercus robur* and *Quercus petraea* is stable across western European mixed oak stands. Ann. For. Sci. 59:777-787.

Laakılı A, Belkadi B, Gaboun F, Yatrib C, Makhloufi M, El Antry S, Medraoui L, Laamarti A, Filali-Maltouf A (2016). Analysis of dendrometric diversity among natural populations of cork oak (*Quercus suber* L.) from Morocco. Turk. J. Agric. For. 40:127-135.

Nei M (1972). Genetic distance between populations. Am. Nat. 106:283-292.

Özbek Ö, Kara A (2013). Genetic variation in natural populations of *Capparis* from Turkey, as revealed by RAPD analysis. Plant Syst. Evol. 299:1911-1933.

Pandey A, Tamta S (2015). High-molecular-weight DNA extraction from six *Quercus* species of Kumaun Himalaya, India. Int. J. Adv. Res. 3:30-34.

Petit RJ, Bodenes C, Ducousso A, Roussel G, Kremer A (2004). Hybridization as a mechanism of invasion in oaks. New Phytol. 161:151-164.

Rieseberg LH, Ellstrand NC (1993). What can molecular and morphological markers tells us about plant hybridization. Crit. Rev. Plant Sci. 12:213-241.

Rieseberg LH, Wendel JF (1993). Introgression and its consequences in plants. In. R. G. Harrison [ed.], Hybrid zones and the evolutionary process. Oxford University Press. New York, USA. pp. 70-109.

Van Valen L (1976). Ecological species, multispecies, and oaks. Taxon 25:233-239.

Welsh J, McCelland M (1991). Fingerprinting genomes using PCR with arbitrary primers. Nucleic Acids Res. 18:7213-7218.

Williams JGK, Kubelik AR, Livak KJ, Rafalski JA, Tingey SV (1990). DNA polymorphisms amplified by arbitrary primers are usefull as genetic markers. Nucleic Acids Res. 18:6531-6535.

Yaltırık F (1984). Türkiye meşeleri teşhis kılavuzu. Yenilik Basımevi. İstanbul.

Yılmaz A, Uslu E, Babaç MT (2013). Molecular diversity among Turkish oaks (*Quercus*) using random amplified polymorphic DNA (RAPD) analysis. Afr. J. Biotechnol. 12:6358-6365.

Yu CY, Hu SW, Zhao HX, Guo AG, Sun GL (2005). Genetic distances revealed by morphological characters, isozymes, proteins and RAPD markers and their relationships with hybrid performance in oilseed rape (*Brassica napus* L.). Theor. Appl. Genet. 110:511-518.

academicJournals

Vol. 15(40), pp. 2272-2281, 5 October, 2016
DOI: 10.5897/AJB2016.15491
Article Number: AA5EC8060918
ISSN 1684-5315

http://www.academicjournals.org/AJB

African Journal of Biotechnology

Full Length Research Paper

Antioxidant assessment on promethazinr HCl decomposition using RP-HPLC assay method

Rasha Saad[1]*, Heyam Saad Ali[2], Babiker M. A. Elhaj[3] and Mai Al Ajaji[1]

[1]College of Pharmacy, King Saud bin Abdulaziz University for Health Sciences Ministry of National Guard Health Affairs, Riyadh, Kingdom of Saudi Arabia.
[2]Department of Pharmaceutics and Pharmacy Practice, Dubai Pharmacy College, Dubai, United Arab Emirates.
[3]Ajman University of Science and Technology, Shāriqah, United Arab Emirates.

Received 24 May, 2016; Accepted 15 September, 2016

The objective of this study was to investigate the effect of different sodium metabisulfite (SMBS) concentrations under a variety of ICH recommended test conditions. An attempt was made to test the feasibility of increasing shelf life when stored under different conditions. The promethazine hydrochloride (HCL) sample solutions used according to USP 24 and BP 1999 were prepared using different concentration of sodium metabisulfite as antioxidant. Standard solution was prepared using reference promethazine and analyses were done by employing reversed-phase high-performance liquid chromatography (RP-HPLC). The method used is efficient in acceptable resolution. The effect of different concentrations of SMBS on promethazine was investigated in promethazine HCL degradation. Chemical and physical stability was conducted in different conditions. The result shows that the drug was liable to degradation in basic pH medium condition, though the extent of degradation varied. Separation of the drug and the degradation products under various conditions was successfully achieved. The method was validated and the response was linear (r=0.9998) in the drug concentration range of 5 to 50 µg. The mean values (±RSD) of slope and intercept were 46376 (±0.006975) and 200049 (±0.4009), respectively. The recovery of the drug ranged between 98.3 and 101.16% from the mixture of degradation products. SMBS concentration influences the degradation process. Increase in concentration resulted in decrease of promethazine degradation. The developed method is simple and accurate in use for analysis of the drug and its degradation products. Antioxidant (SMBS) has important role in preventing promethazine degradation beside other factors.

Key words: Degradation, reversed-phase high-performance liquid chromatography (RP-HPLC), promethazine hydrochloride, sodium metabisulfite.

INTRODUCTION

Chemical and physical properties of promethazine HCl

Promethazine hydrochloride (HCl, Figure 1), (2RS)-(10 H-phenothiazine-10-yl) propan-2-amine hydrochloride, is a phenothiazine derivative used as a H-blocker and an antiemetic (Asghar et al., 2011). Promethazine (PROM), like other phenothiazines, is capable of both free-radical and singlet molecular oxygen photosensitization with photoallergic and phototoxic effects. The existence of light-induced free-radicals of some phenothiazines was proven by Forrest (Heyam et al., 2015). Table 1 shows

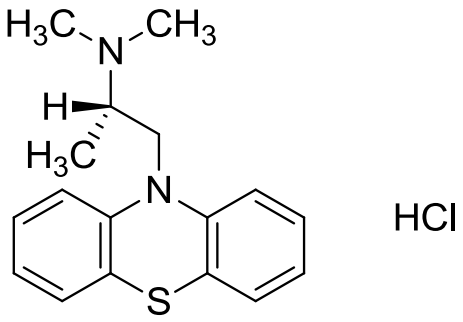

Figure 1. Chemical structures of promethazine HCl.

Table 1. Chemical and Physical properties of Promethazine HCl.

Chemical properties of promethazine hydrochloride substance	
Molecular formula	Promethazine Hydrochloride: $C_{17}H_{20}N_2S.HCl$
Molecular weight	Promethazine Hydrochloride: 320.9
Chemical names	10-[2-(Dimethylamino)propyl]-phenothiazine monohydrochloride
Physical properties of promethazine hydrochloride substance	
Colour	White or faintly yellow. On prolonged exposure to air it is slowly oxidised, becoming blue in color
State/Form	Crystalline powder
Description	-Odourless or almost odourless. -A 10% solution in water has a pH of 4.0 to 5.0 -Solubility 1 in 0.6 of water, 1 in 9 of alcohol, 1 in 2 of chloroform -Practically insoluble in ether and acetone. Melting point is about 222°C. Melting point (promethazine) is about 60°C

the chemical and physical properties of promethazine HCl.

Other characteristics

Shelf-life of the substance, which is the expiry dates of the commercially available parenteral preparation vary between 2 and 5 years. For the storage conditions, all preparations should be protected from light. Oral and parenteral preparations of the drug should be stored at a temperature of 15 to 30°C and freezing of injection should be avoided. The solutions of promethazine should be stored in tightly closed, light resistant containers (Jun et al., 2003).

Antioxidant sodium metabisulfite (SMBS)

Antioxidant plays an important positive role in the stability of promethazine. The concentration of an antioxidant is mandatory in achieving the optimum stability. Therefore, this is investigated in our study. Many antioxidants such as BHA, ascorbic acid and SMBS, and the antioxidant used in this study, all were used in parenteral solutions (Maruchin, 1979). Table 2 shows the chemical and physical properties of SMBS. The synonyms for SMBS are disodium disulfite and disodium metabisulfite (Figure 2).

Effect of antioxidant and degradation

In this case, the presence of promethazine HCl in solution formulations with some additives, like sodium metabisulfite, showed severe degradations if it has been added in insufficient concentration. This will result in insufficient drug's content uniformity, even after short

*Corresponding author. Email: sulimanr@ksau-hs.edu.sa.

Table 2. Chemical and Physical properties of Sodium Metabisulfite (SMBS).

Chemical properties of sodium metabisulfite (SMBS) substance	
Molecular formula	Sodium Metabisulfite $Na_2S_2O_5$
Molecular weight	Sodium Metabisulfite 190.1
Chemical names	Sodium pyrosulfite
Physical properties of sodium metabisulfite substance	
Colour	White to slightly yellow
State/Form	Crystalline power
Description	With an odour of sulfur dioxide. 1 g is soluble in 2 ml of water Decomposes below melting point at 150°C Density: 1.4 g/cm^3 Solubility in water, g/100 ml: 54 (good)
Other characteristics definition	Sodium pyrosulfite contains not less than95.0% of $Na_2S_2O_5$.
Use	As an antimicrobial preservative and as an anti-browning agent

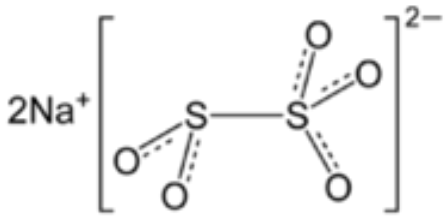

Figure 2. Chemical structures of metabisulfite.

handling periods. The drug degradation is usually accompanied by color changes or precipitation in case the pH has been changed as well, which surely will affect the product's acceptance (Qi et al., 1984).

ICH Stability requirements

Stability requirements for the world wide registrations of pharmaceutical products have undergone a dramatic change in the past few years with the advent (introduction) of the guidelines of the International Council for Harmonisation of Technical Requirements for Registration of Pharmaceuticals for Human Use (ICH). ICH has introduced a standardized approach for the development of stability data for registration through various guidelines (Heyam et al., 2015; Sane et al., 2008). From these requirements, it is necessary to develop a stability indicating assay method for these drugs to ensure the safety, quality and efficacy of these drugs. “Stable”, as used in the context of this application, means remaining in a state or condition that is suitable for administration to a patient. Formulations according to the present formulations are found to be stable when maintained at room temperature for at least 12 months and are generally stable at room temperature for 12 to 24 months. In laboratory studies, it has been found that precipitates are formed when promethazine hydrochloride solution is exposed to light and air; therefore, to be kept away from light under storage condition is mandatory. Also, it is believed that this precipitate formation could be related to change of pH and trace metals found in water. In this study, the stability of a standard promethazine HCl solution after storage at room temperature and under refrigerated conditions was monitored. In an effort to extend the shelf life of this formulation, an antioxidant, a buffering agent, or both were added to the solution; the drug stability in the modified formulations was examined (Sane et al., 2008; Stavchansky et al., 2011). Therefore, the objective of this study was to investigate the stability of promethazine HCl injectable solution using different concentrations of SMBS as antioxidant. To investigate the effect of different conditions on promethazine degradation under a variety of ICH recommended test conditions. And an attempt to test the feasibility of increasing its shelf life when stored at different conditions (Miller et al., 2010).

EXPERIMENTALS

Materials and reagents

All chemicals used were of analytical reagent grade. Promethazine reference and SMBS were provided from Julphar Company. Promethazine HCl, sodium meta-bi-sulphite, sodium EDTA (disodium edentate), glacial acetic acid, sodium acetate tri-hydrate, and water were preparation and used for injection. Promethazine

Table 3. Promethazine HCl sample formulations containing different SMBS concentrations.

Formulation composition (mg/ml)	F0	F1	F2	F3	F4
Promethazine HCl	25.4	24.8	25.06	24.9	25.5
SMBS	0.250	0.292	0.340	0.382	0.300
Disodium Edetate	0.1	0.1	0.1	0.1	0.1
Sodium acetate trihydrate	2.25	2.25	2.25	2.25	2.25
Glacial acetic acid	0.6294	0.6294	0.6294	0.6294	0.6294
Water for injection	Q.S to 1000	Q.S to 1000	Q.S to 1000	Q.S to 1000	Q.S to 1000

HCL standard, pentansulfonic acid sodium salt, glacial acetic acid, acetonitrile reversed-phase high-performance liquid chromatography (RP-HPLC) grade, and ultra-pure water were used for the assay of promethazine.

Methods

In this work, the proposed method was applied using an RP-HPLC method for the determination of PROM HCl in its injection drug formulation and is based on its oxidation by coupling with sulfanilic acid sodium (Arnao et al., 2012). Chromatographic conditions: Column, L11- (µ bondapak phenyl 125 A 10 µm 300 X 3.9 mm) (waters); Mobile phase: mixture of ion pair solution and acetonitrile in ratio 50:50 (v/v); Flow rate: 1.0 ml/min; Detection: UV 254 nm; Injection volume: 20 µl; Temperature: ambient; Diluent: 0.1% glacial acetic acid in water. Preparation of ion pair solution: Wight and transfer of 2 g of 1-Pentansulfonic acid sodium salt in 1000 ml volumetric flask, dissolve with 900 ml water, and addition of 10 ml glacial acetic acid and complete to the volume with water filtered through 0.45 µm filter paper (Jinjiang and Yongmei, 2014).

Identification of promethazine HCl

For the preparation of promethazine standard solutions, about 50 mg of promethazine HCl standard were weight and transfer accurately into a 100-ml volumetric flask, dissolve and make up to volume with diluent. 5.0 ml of the resulting solution pipetted and transferred accurately into a 100.0 ml volumetric flask, diluted to volume with diluent (this is a standard solution containing 25.0 µg/ml of promethazine HCl). For the preparation of test solution, 2.0 ml of test injection were pipetted and transferred accurately into a 100 ml volumetric flask, dilute to volume with diluent and well shake (solution A). 5.0 ml of solution A was pipetted and transferred accurately into a 100 ml volumetric flask, diluted to a volume with diluent, and well shake (this is test solution for assay containing claimed concentration about 25 µg/ml promethazine HCl) (Cano and Hernandez-Ruiz, 1998). Table 3 shows promethazine HCl sample formulations containing different SMBS concentrations.

System suitability

Make 6 replicate injection of standard solution and measure the peak area. The relative standard deviation of the replicate injection is not more than 2.0%.

RP-HPLC identification

The chromatogram of the test preparation exhibits a major peak, the retention time of which corresponds to that of the promethazine HCl peak in the chromatogram of the standard preparation (Alcolea et al., 2002; Cano et al., 2000). 20 µl of standard solution were injected separately and the solution was tested for the assay into the chromatograph. The chromatograms were recorded and the peak areas were measured. For the assay of promethazine HCl, the quantity was calculated, in mg, of promethazine HCl in each ml of injection by the formulas (Pulido et al., 2003):

$$PAt \times C \times P \times DF / PAs \times 1000$$

where Pat is the peak area of promethazine HCl in the chromatogram of test solution, Pas is the peak area of promethazine HCl in the chromatograph of the standard solution, C is the concentration of promethazine HCl (µg/ml) in the standard solution, P is the potency of promethazine HCl standard, and DF is the dilution factor (1000).

RESULTS

Promethazine HCl standard solution formulation specifications were determined initially as summarized in the Table 4. Promethazine HCl sample solution was formulated in different conditions (dark and light) at room temperature in amber glass bottles.

RP-HPLC analysis was conducted in different intervals according to ICH. The obtained chromatograms are represented in Figures 3 to 7. Figure 4 shows a typical chromatogram of promethazine HCl in standard solution. Figure 5 shows a typical chromatogram of promethazine HCl in the test solution. Figure 6 shows a typical chromatogram of promethazine HCl and its related substance, and finally, Figure 7 shows a typical chromatogram of the reference solution. The calibration curve of the chromatograms values of promethazine concentration vs. area under the curve in mAU were plotted (Figure 3).

The recovery of promethazine formulations were calculated (Table 5). The recovery calculated by dividing the added value divided by the found value in percentage.

The results of the short term physical and chemical stability studies conducted on promethazine HCl injectable solutions are shown in Tables 6 and 7, respectively. It can be observed from the results that formulations protected from light were more stable than the ones exposed to light. Formulations containing high amount of SMBS concentrations showed more stability. The samples of promethazine HCl showed an acceptable

Table 4. Specifications of reference promethazine HCl 25 mg/ml injection.

Test parameter	Specifications
Physical	
I-Description	Clear, color less solution
II-PH	Between 4.0 and 5.5
Chemical	
I-Identification	The retention time of the major peak in the chromatogram of the assay preparation corresponds to that in the chromatogram of the standard preparations, as obtained in the assay
II-Assay	25 mg/ml
Promethazine hydrochloride	Limit: Not less than 95% and not more than 110% of the labeled amount of $C_{17}H_{20}N_2S.HCl$
Sodium metabisulphite	Limit: 0.10 - 0.30 mg/ml

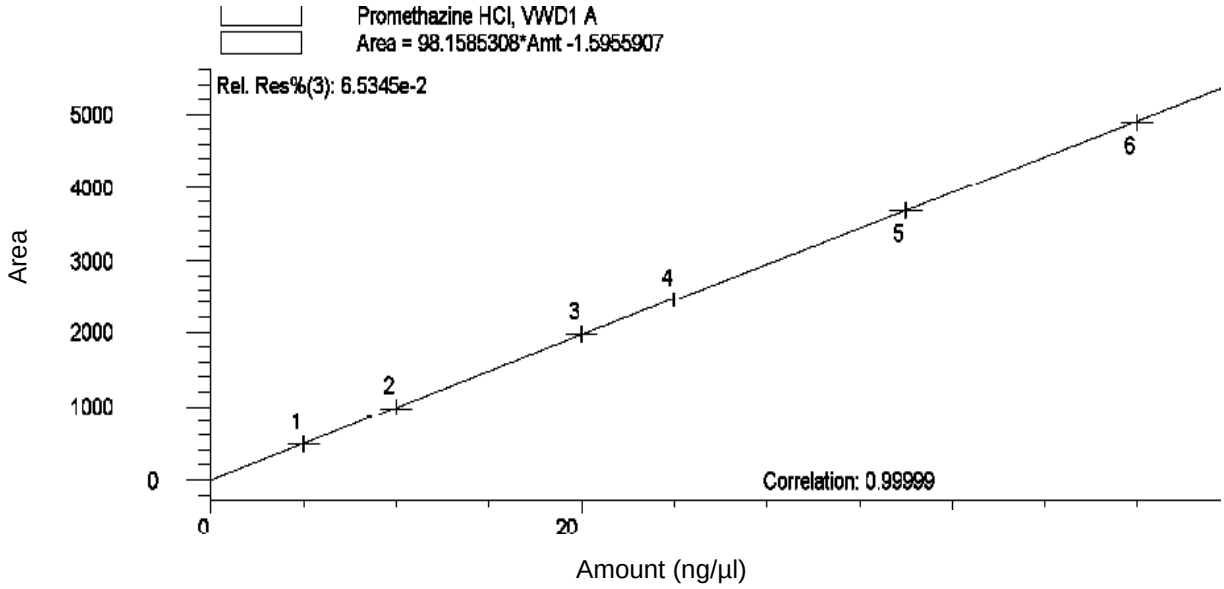

Figure 3. Calibration curve of promethazine.

physical and chemical stability of up to 3 months when stored at room temperature protected from light using all the concentrations (Nielsen et al., 2003). The addition of SMBS gave a concentration <300 mg/ml when stored and protected from light. The results showed a higher stability for all formulations after storage at room temperature protected from light compared with those stored in exposure to light.

DISCUSSION

Promethazine decomposition mechanism, rapid decomposition of promethazine HCl solution under the influence of day-light, air and trace elements in water led to the loss of an electron to yield the semi-quinone free radical (PROM●). Promethazine light + air in H_2O (PROM●) semiquinone free radical. Further degradation produces phenazathionium ion (PROM●+), (PROM●) (PROM●+), and phenazathionium ion will react with water to give the corresponding sulfoxide [PROM (S-O)], phenazathionium ion H_2O [PROM (S-O)] sulfoxide (Pietta et al., 2000).

Dimerization may occur as a result of terminating the monomers free radicals, as follows:

2 (PROM●) DimerizationPROM - PROM (2 PROM), (semiquinone free radical) (terminated dimer).

There was no color change, precipitation, or other visible sign of incompatibility at any time during the study (Borkar et al., 2009). Promethazine hydrochloride and

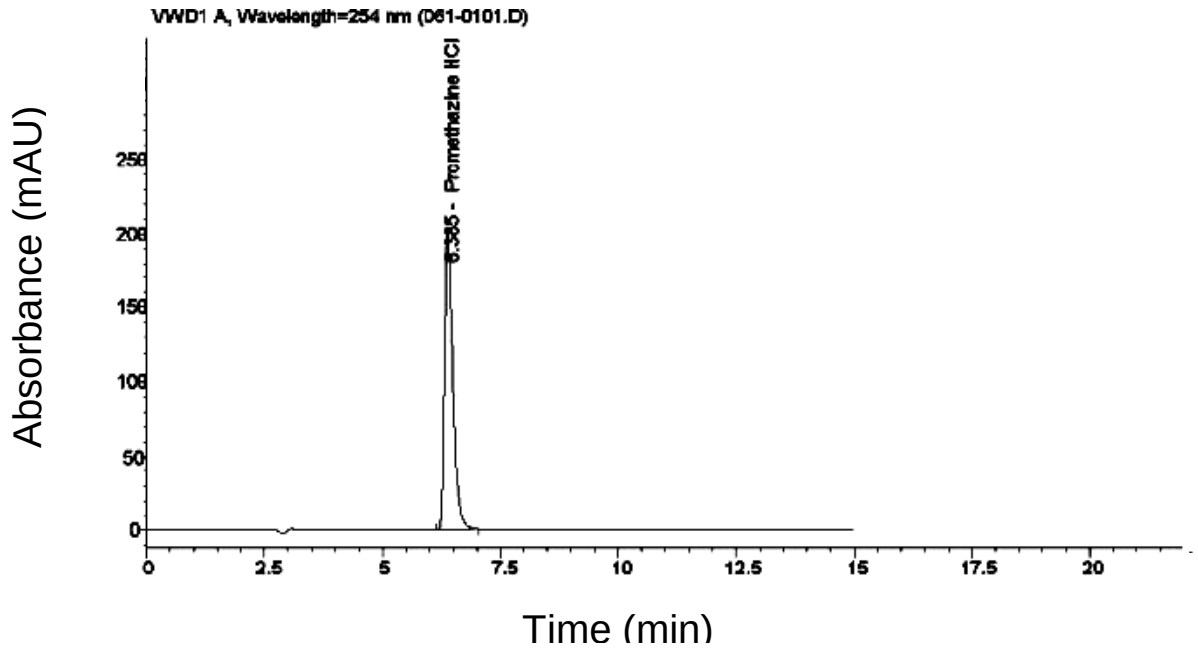

Figure 4. Typical chromatogram of promethazine HCl in standard solution.

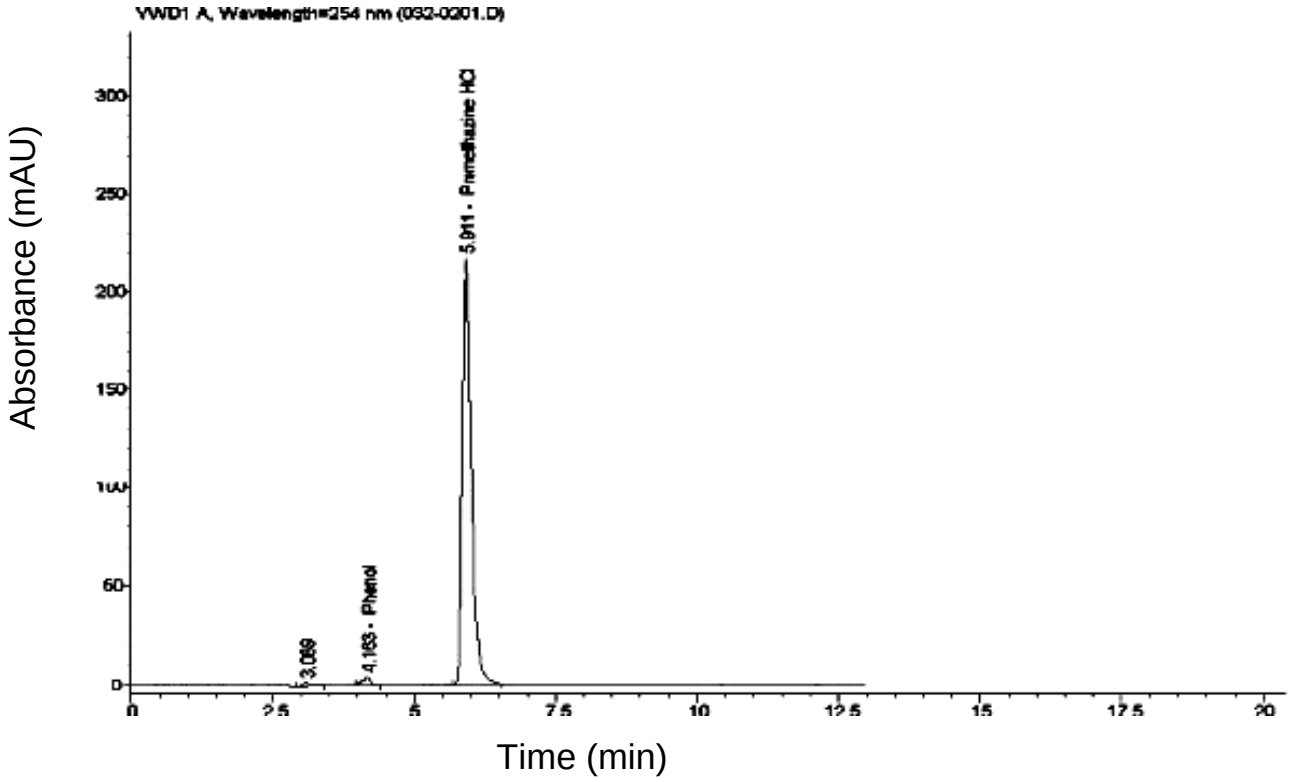

Figure 5. Typical chromatogram of promethazine HCl in test solution.

SMBS remained stable under all study conditions (Table 4). The stability of PROM in water is mediated by the rate of acid/base hydrolysis (Cao et al., 1998). The rate of degradation of PROM hydrochloride has been reduced

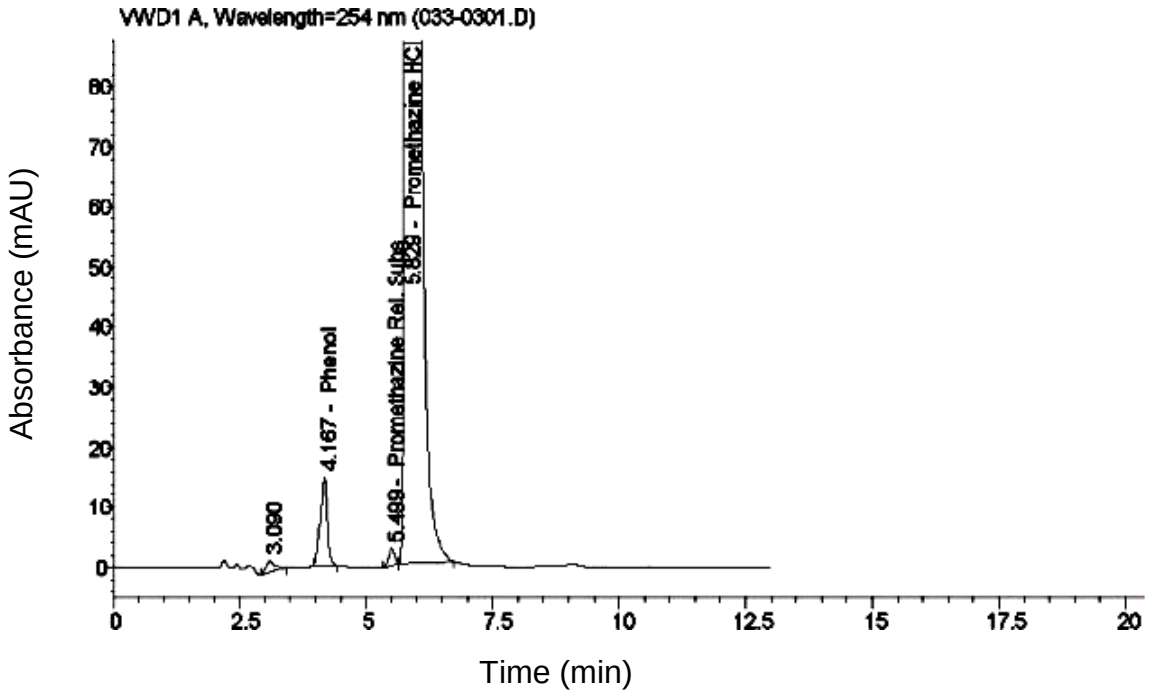

Figure 6. Typical chromatogram of promethazine HCl and its related substance.

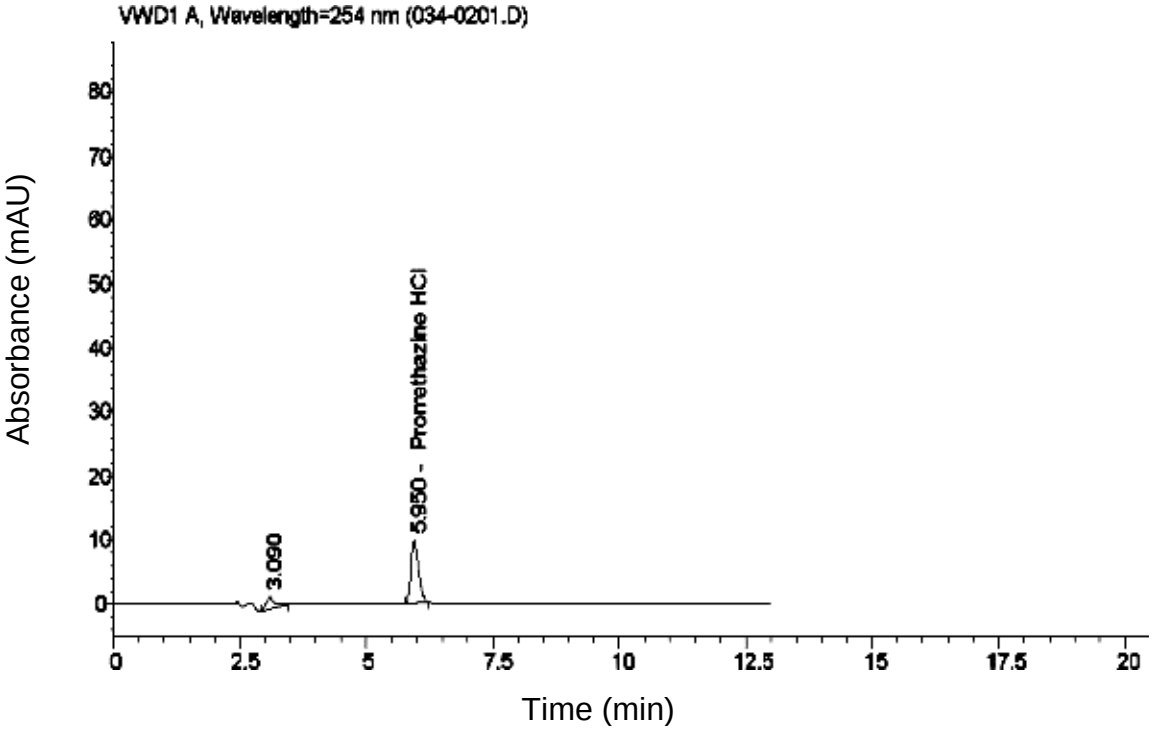

Figure 7. Typical chromatogram of the reference solution.

by the use of acetate as a buffer, maintaining the pH as close to 5.0 as possible, minimizing the hydrolysis reaction if the buffer used. The result of this study showed that the drug was liable to degradation in all

Table 5. % Recovery of promethazine formulations.

Parameter	Added* (µg)	Found (µg)	Recovery (%)
F0	25.4	24.9	98.03
F1	24.8	24.7	99.55
F2	25.06	24.8	98.96
F3	24.9	24.8	99.59
F4	25.5	25.4	99.60

Masses of standard promethazine hydrochloride added in formulations (F0 to F4).

Table 6. Physical stability of promethazine HCl solutions for three month in dark and light exposure.

Parameter	pH			Appearance		
	1st Month	2nd Month	3rd Month	1st Month	2nd Month	3rd Month
F0						
Light	4.6	4.8	.4.8	NC	NC	NC
Dark	4.5	4.5	4.6	NC	NC	NC
F1						
Light	4.6	4.8	4,9	NC	NC	NC
Dark	4.8	4.8	4.9	NC	NC	NC
F2						
Light	5.1	5.1	4.9	NC	NC	NC
Dark	4.8	4.7	4.6	NC	NC	NC
F3						
Light	4.6	4.8	4,9	NC	NC	NC
Dark	4.8	4.8	4.9	NC	NC	NC
F4						
Light	4.8	4.8	4.9	NC	Precipitate	Precipitate
Dark	5.1	5.1	4.9	NC	NC	NC

NC: No color change; D: darkening (solution); DS: slight darkening in color.

Table 7. Chemical stability of promethazine HCl 25 mg/ml formulations[a] stored in light and dark **c**onditions.

Storage condition at room temperature	Actual initial promethazine concentration (mg/ml)	SD % Initial concentration remaining		
		Mean ± 1st Month	Mean ± 2nd Month	Mean ± 3rd Month
F0				
Light	24.7 ± 0.003	99.5 ± 0.4	97.5 ± 0.2	94.5 ± 0.2
Dark	24.7 ± 0.004	101.0 ± 1.1	100.6 ± 1.1	99.8 ± 1.2
F1				
Light	24.8 ± 0.005	95.6 ± 0.3	94.5 ± 0.2	93.3 ± 0.5
Dark	24.7 ± 0.003	99.5 ± 0.4	98.6 ± 0.3	98.6 ± 0.2
F2				
Light	24.9± 0.004	98.9 ± 8.9	97.9 ± 7.8	96.9 ± 5.8
Dark	24.7 ± 0.005	99.9 ± 0.8	99.5 ± 0.6	98.5 ± 0.6

Table 7. Contd.

F3				
Light	24.9 ± 0.003	99.9 ± 0.8	98.5 ± 0.6	97.5 ± 0.5
Dark	24.8± 0.004	100.6 ± 0.3	100.5 ± 1.2	99.8 ± 1.2
F4				
Light	25.4± 0.004	96.9 ± 8.9	93.9 ± 7.8	90.9 ± 5.8
Dark	24.7 ± 0.005	99.9 ± 0.8	98.5 ± 0.6	975 ± 0.6

[a]Mean ± SD calculated from triplicate assays on single samples from each container. Samples were either protected from light by using aluminum foil or exposed to fluorescent light.

condition, though the extent of degradation varied (Awika et al., 2003). The promethazine HCl was found to be more liable to decompositions in alkaline solution than in acidic solution and neutral condition. Degradation of promethazine HCl in neutral solution was observed relatively after long hour of refluxing indicating that the drug is relatively stable in neutral condition (Rasha et al., 2014).

Conclusion

This method was specific to the drug and also selective to degradation products. The developed method is simple accurate, precise, specific and selective and rugged and thus it can be used for analysis of the drug and its degradation products. Antioxidant (SMBS) has important role in preventing promethazine degradation. Samples of promethazine HCl contained an acceptable drug concentration for up to three months when stored at room temperature protected from light (Leclercq et al., 2000). The addition of SMBS at a concentration of 0.29 to 0.38% w/v to the promethazine formulations increased the suspension's shelf life at room temperature when stored protected from light (Bonilla et al., 1999).

Conflict of Interests

The authors have not declared any conflict of interests.

REFERENCES

Alcolea JF, Cano A, Acosta M, Arnao MB (2002). Hydrophilic and lipophilic antioxidant activities of grapes. Nahrung 46:353-356.

Arnao MB, Cano A, Hernandez-Ruiz J, Garcia-Canovas F, Acosta M (2012). Inhibition by L-ascorbic acid and other antioxidants of the 2.2′-azino-bis(3-ethylbenzthiazoline-6-sulfonic acid) oxidation catalyzed by peroxidase: a new approach for determining total antioxidant status of foods. Anal. Biochem. 35:255-261.

Asghar MN, Khan IU, Bano N (2011). *In vitro* antioxidant and radical-scavenging capacities of Citrullus colocynthes (L) and Artemisia absinthium extracts using promethazine hydrochloride radical cation and contemporary assays. Food Sci. Technol. Int. 17(5):481-494.

Awika JM, Rooney LW, Wu X, Prior RL, Cisneros Zevallos L (2003). Screening methods to measure antioxidant activity of sorghum (Sorghum bicolor) and sorghum products. J. Agric. Food Chem. 51:6657-6662.

Bonilla F, Mayen M, Merida J and Medina M. (1999). Extraction of phenolic compounds from red grape marc for use as food lipid antioxidants. Food Chem., 66:209–215.

Borkar DD, Godse VP, Bafana YS, Bhosale AV (2009). Simultaneous Estimation of Paracetamol and Promethazine Hydrochloride in Pharmaceutical Formulations by a RP-RP-HPLC Method. Int. J. ChemTech Res. CODEN (USA) 2(3):667-670.

Cano A, Acosta M, Arnao MB (2000), A method to measure antioxidant activity in organic media: application to lipophilic vitamins. Redox Rep. 5:365-370.

Cano A, Hernandez-Ruiz J (1998). Garcia-Canovas, F.; Acosta, M. An end-point method for estimation of the total antioxidant activity in plant material. Phytochem. Anal. 9:196-202.

Cao G; Russell RM, Lischner N, Prior RL (1998). Serum antioxidant capacity is increased by consumption of strawberries, spinach, red wine or vitamin C in elderly women. J. Nutr. 128:2383-2390.

Heyam A, Rasha S, Babiker EH (2015). Prevention of Cap-Locking of Syrup Product by Treating the Manufacturing Process with Citric Acid Monohydrate. Int. J. Pharm. Chem. 5(6):218-226.

Jinjiang L, Yongmei W (2014). Lubricants in Pharmaceutical Solid Dosage Forms. Lubricants 2:21-43.

Jun Z, Zhimie Q, Han D, Chunhai F, Genxi L, Noaki M (2003). Sensing Phenothiazine Drugs at a Gold Electrode comodified with DNA and Nanoparticles. J. Anal. Sci. 19:653-657.

Leclercq C, Arcella D, Turrini A. (2000). Estimates of the theoretical maximum daily intake of erythorbic acid, gallates, butylated hydroxyanisole (BHA) and butylated hydroxytoluene (BHT) in Italy: a stepwise approach. Food Chem. Toxicol, 38:1075–1084.

Maruchin JE (1979). The Forrest chlorpromazine free radical, CPZ I in (Phenothiazines and Structurally Related Drugs: Basic and Clinical Studies), Usdin, E; Eckert, H & Forrest, IS (Eds.), Phenothiazines and Related Drugs, held in Zurich-Switzerland, Sep. 9-13, Elsevier/North-Holland, New York, 1980. pp. 41-44.

Miller NJ, Sampson J, Candeias LP, Bramley PM, RiceEvans CA (2010). Antioxidant activities of carotenes and xanthophylls. FEBS Lett. 384:240-242.

Nielsen ILF, Haren GR, Magnussen EL, Dragsted LO, Rasmussen SE (2003). Quantification of anthocyanins in commercial black currant juices by simple high-performance liquid chromatography. Investigation of their pH stability and antioxidative potency. J. Agric. Food Chem. 51:5861-5866.

Pietta P, Simonetti P, Gardana C, Mauri P (2000). Trolox equivalent antioxidant capacity (TEAC) of Ginkgo biloba flavonol and Camellia sinensis catechin metabolites. J. Pharm. Biomed. Anal. 23:223-226.

Pulido R, Hernandez-Garcia M, Saura-Calixto F (2003). Contribution of beverages to the intake of lipophilic and hydrophilic antioxidants in the Spanish diet. Eur. J. Clin. Nutr. 57:1275-1282.

Qi F, Shao Y, Gao N, Zhan J, Liu Y, Song Y, Zhou JG (1984). Chromatographic Determination of Chlorpromazine in Human Serum. J. Yaoxue. Tngbao. 19(10):37-40.

Rasha S, Tan P, Jiyauddin K, Li W, Sadia S, Junainah AH, Eddy Y,

Fadli A (2014). Phytochemical Screening and Antioxidant Activity of Different Parts From Five Malaysian Herbs. Experiment 19(2):1336-1347.

Sane RT, Surve SR, Gangrade MG, Bapt VV, Chonkar NL. (2008). Simultaneous Gas Chromatographic Estimation of Combined Dosages. I. Amitriptyline Hydrochloride With Chlordiazepoxide.II. Methocarbol With Ibuprofen. II. Paracetamol With Diclofenac Sodium IV. Paracetamol with Promethazine Hydrochloride. J. Indian Drugs 30(2):66-72.

Stavchansky S, Wallace JE, Chue M, Wu P (2011). Gas Liquid Chromatographic Determination of Promethazine Hydrochloride in Polyoxyethylene Glycol Suppositories Using the Hall's Electrolytic Conductivity Detector. J. Anal. Lett. 15(B16):1361-1372.

African Journal of Biotechnology

Related Journals Published by Academic Journals

- *Biotechnology and Molecular Biology Reviews*
- *African Journal of Microbiology Research*
- *African Journal of Biochemistry Research*
- *African Journal of Environmental Science and Technology*
- *African Journal of Food Science*
- *African Journal of Plant Science*
- *Journal of Bioinformatics and Sequence Analysis*
- *International Journal of Biodiversity and Conservation*

academicJournals